

---

Theses and Dissertations

---

Fall 2012

## Local and regional interactions between air quality and climate in New Delhi: a sector based analysis

Pallavi Marrapu  
*University of Iowa*

Follow this and additional works at: <https://ir.uiowa.edu/etd>

 Part of the [Chemical Engineering Commons](#)

Copyright © 2012 Pallavi Marrapu

This dissertation is available at Iowa Research Online: <https://ir.uiowa.edu/etd/3497>

---

### Recommended Citation

Marrapu, Pallavi. "Local and regional interactions between air quality and climate in New Delhi: a sector based analysis." PhD (Doctor of Philosophy) thesis, University of Iowa, 2012.  
<https://doi.org/10.17077/etd.l87oi8p0>

---

Follow this and additional works at: <https://ir.uiowa.edu/etd>

 Part of the [Chemical Engineering Commons](#)

LOCAL AND REGIONAL INTERACTIONS BETWEEN AIR QUALITY AND  
CLIMATE IN NEW DELHI- A SECTOR BASED ANALYSIS

by  
Pallavi Marrapu

An Abstract

Of a thesis submitted in partial fulfillment  
of the requirements for the Doctor of Philosophy degree  
in Chemical and Biochemical Engineering  
in the Graduate College of  
The University of Iowa

December 2012

Thesis Supervisor: Professor Gregory R. Carmichael

## ABSTRACT

Deteriorating air quality is one of the major problems faced worldwide and in particular in Asia. The world's most polluted megacities are located in Asia highlighting the urgent need for efforts to improve the air quality. New Delhi (India), one of the world's most polluted cities, was the host of the Common Wealth Games during the period of 4-14 October 2010. This high profile event provided a good opportunity to accelerate efforts to improve air quality. Computational advances now allow air quality forecast models to fully couple the meteorology with chemical constituents within a unified modeling system that allows two-way interactions. The WRF-Chem model is used to simulate air quality in New Delhi.

The thesis focuses on evaluating air quality and meteorology feedbacks. Four nested domains ranging from South Asia, Northern India, NCR Delhi and Delhi city at 45km, 15km, 5km and 1.67km resolution for a period of 20day (26<sup>th</sup>sep-15<sup>th</sup>oct, 2010) are used in the study. The predicted mean surface concentrations of various pollutants show similar spatial distributions with peak values in the middle of the domain reflecting the traffic and population patterns in the city. Along with these activities, construction dust and industrial emissions contribute to high levels of criteria pollutants. The study evaluates the WRF-Chem capabilities using a new emission inventory developed over Delhi at a fine resolution of 1.67km and evaluating the results with observational data from 11 monitoring sties placed at various Game venues.

The contribution of emission sectors including transportation, power, industry, and domestic to pollutant concentrations at targeted regions are studied and the results show that transportation and domestic sector are the major contributors to the pollution levels in Delhi, followed by industry. Apart from these sectors, emissions outside of Delhi contribute 20-50% to surface concentrations depending on the species. This indicates that pollution control efforts should take a regional perspective.

Air quality projections in Delhi for 2030 are investigated. The **Greenhouse Gas and Air Pollution Interactions and Synergies (GAINS)** model is used to generate a 2030 future emission scenario for Delhi using projections of air quality control measures and energy demands. Net reductions in CO concentrations by 50%, and increases of 140% and 40% in BC and NO<sub>x</sub> concentrations, respectively, are predicted. The net changes in concentration are associated with increases in transport and industry sectors. The domestic sector still has a significant contribution to air pollutant levels.

The air quality levels show a profound effect under this scenario on the environment and human health. The increase in pollution from 2010 to 2030 is predicted to cause an increase in surface temperature by ~0.65K. These increasing pollution levels also show effects on the radiative forcing. The high aerosols loading i.e. BC, PM<sub>2.5</sub> and PM<sub>10</sub> levels show strong influence on the short and longwave fluxes causing strong surface dimming and strong atmosphere heating due to BC. These results indicate transport and domestic sectors should be targeted for air quality and climate mitigations.

Abstract Approved: \_\_\_\_\_  
Thesis Supervisor

\_\_\_\_\_  
Title and Department

\_\_\_\_\_  
Date

LOCAL AND REGIONAL INTERACTIONS BETWEEN AIR QUALITY AND  
CLIMATE IN NEW DELHI- A SECTOR BASED ANALYSIS

by  
Pallavi Marrapu

A thesis submitted in partial fulfillment  
of the requirements for the Doctor of Philosophy degree  
in Chemical and Biochemical Engineering  
in the Graduate College of  
The University of Iowa

December 2012

Thesis Supervisor: Professor Gregory R. Carmichael

Copyright by  
PALLAVI MARRAPU  
2012  
All Rights Reserved

Graduate College  
The University of Iowa  
Iowa City, Iowa

CERTIFICATE OF APPROVAL

---

PH.D. THESIS

---

This is to certify that the Ph.D. thesis of

Pallavi Marrapu

has been approved by the Examining Committee  
for the thesis requirement for the Doctor of Philosophy  
degree in Chemical and Biochemical Engineering at the December 2012  
graduation.

Thesis Committee: \_\_\_\_\_  
Gregory R. Carmichael, Thesis Supervisor

\_\_\_\_\_  
Jerald L. Schnoor

\_\_\_\_\_  
Charles O. Stanier

\_\_\_\_\_  
David W. Murhammer

\_\_\_\_\_  
Scott Spak

To My Family and Friends

## ACKNOWLEDGMENTS

I would like to acknowledge all the people who guided and helped me through thick and thin of my journey to PhD. Here with I take this opportunity to extend my gratitude to my advisor Dr. Gregory R. Carmichael for his constant support at all times of my research. I thank Dr Jerald L. Schnoor, Dr. Charles O. Stanier, Dr. David W. Murhammer and Dr. Scott Spak for serving on the committee and valuable suggestions to shape my thesis better.

I would like to thank Dr.Yafang Cheng, for helping me at various stages of research. I also want to thank my colleagues at CGRER Aditsuda Jamroensan, Pablo Saide, Sarika Kulkarni for their valuable suggestions when ever needed.

I would like to thank all my roommates Swathi Kode, Hema Achanta and Aruna Tumuluri for being very supportive and making life in Iowa City a memorable experience.

Special mention goes to my family back in India who provided me emotional support at all times. I would like to thank my parents for all their encouragement.

## TABLE OF CONTENTS

LIST OF TABLES .....	vi
LIST OF FIGURES .....	vii
LIST OF ABBREVIATIONS.....	x
CHAPTER 1 INTRODUCTION .....	1
1.1 Motivation and Importance of Work .....	1
1.2 Objectives of the Proposed Research .....	5
1.3 Approach.....	6
1.4 History of WRF-Chem .....	7
1.5 Overview of the WRF-Chem Model .....	8
1.6 Physical and Chemical Processes in WRF-Chem .....	10
1.6.1 Transport Processes .....	10
1.6.2 Dry Deposition .....	11
1.6.3 Gas-Phase chemistry and Aerosol module .....	11
1.6.4 Photolysis Rates.....	12
1.6.5 Radiation.....	12
1.7 Emissions .....	15
1.7.1 Anthropogenic Emissions.....	15
1.7.2 Emission Preprocessor (EPRES) model.....	19
1.8 Model of Emissions of Gases and Aerosols from Nature (MEGAN) .....	25
1.9 Meteorology Data .....	27
1.10 Initial and Boundary conditions.....	27
1.11 Thesis organization.....	29
CHAPTER 2 SECTORAL CONTRIBUTIONS TO BLACK CARBON AND OTHER CRITERIA POLLUTANTS IN DELHI AND THEIR TOWWAY INTERACTIONS WITH METEOROLOGY .....	30
2.1 Introduction.....	30
2.2 Approach.....	32
2.3 Results and Discussion .....	36
2.3.1 Meteorology .....	36
2.3.2 Spatial distributions of air pollutants in Delhi.....	41
2.3.3 Comparison of Observed and Modeled Concentrations.....	44
2.3.4 Sector Contribution .....	49
2.3.5 Evaluation of Emissions .....	55
2.3.6 Importance of Feedbacks.....	56
2.4 Summary.....	63
CHAPTER 3 FUTURE EMISSION SCENARIO USING THE GREENHOUSE GAS AND AIR POLLUTION INTERACTIONS AND SYNERGIES (GAINS) MODEL .....	
3.1 Introduction.....	65
3.2 Description of the Greenhouse Gas and Air Pollution Interactions and Synergies (GAINS) 2030 Scenario.....	68

3.3 Results and Discussion .....	76
3.4 Summary.....	86
CHAPTER 4 RADIATIVE FORCING OVER DELHI.....	87
4.1 Introduction.....	87
4.2 Results and Discussion .....	90
4.3 Summary.....	101
CHAPTER 5 CONCLUSION AND FUTURE WORK.....	103
5.1 Conclusion.....	103
5.2 Future study .....	105
APPENDIX.....	107
REFERENCES .....	112

## LIST OF TABLES

Table 1.1 Important input settings of the WRF-Chem model. ....	13
Table 1.2 Percent Anthropogenic Emissions Contribution from Various Sectors to Delhi from Delhi Emission Inventory. ....	19
Table 2.1 Comparison of predicted meteorological parameters with observations at the surface monitoring sites. ....	41
Table 2.2 Comparison of 20-day mean observed and predicted concentrations of various species at all monitoring sites with NO <sub>x</sub> reduction to one third of its emissions. ....	46
Table 2.3 Comparison of 20-day mean observed and predicted concentrations of various species at all monitoring sites NO <sub>x</sub> reduced by factor of 3. ....	47
Table 3.1 Baseline projection of fuel consumption for India (PJ/yr). ....	69
Table 3.2 Emission control measures assumed in the baseline projection. ....	71
Table 3.3 Emissions Comparison from Delhi 2010 to GAINS 2030. ....	72
Table A1 Statistical analysis of various air quality species for the period of 20 days at different monitoring stations with NO <sub>x</sub> one third emissions. ....	107
Table A2 Statistical analysis of various air quality species for the period of 20 days at different monitoring stations with full NO <sub>x</sub> emissions. ....	109
Table A3 Statistical analysis of various meteorological parameters for the period of 20 days at different monitoring stations. ....	111

## LIST OF FIGURES

Figure 1.1 Population exposure to PM <sub>2.5</sub> levels greater than the WHO annual guideline of 10µg/m <sup>3</sup> and Heating effect due BC. ....	4
Figure 1.2 Flow chart of the WRF-Chem model. ....	9
Figure 1.3 Nested model domains used in the Commonwealth Games forecasts and analysis. ....	14
Figure 1.4 Carbonmonoxide emission distribution from three domains. ....	17
Figure 1.5 Emission distributions of BC, CO, NO <sub>x</sub> , PM <sub>2.5</sub> and SO <sub>2</sub> units over Delhi. ....	22
Figure 1.6 Sector contributions of Black Carbon emissions (%) over Delhi. ....	24
Figure 1. 7 Base isoprene emissions from MEGAN. ....	26
Figure 1.8 Flow chart of MACC model. ....	29
Figure 2.1 Locations of the monitoring stations for the Commonwealth Games. ....	33
Figure 2.2 20-day mean spatial distribution of criteria pollutants over South Asia , Northern India and NCR Delhi. ....	35
Figure 2.3 20-day mean surface winds at 5:30am, 11:30am, 5:30pm and 11:30pm(LT). ....	38
Figure 2.4 Wind rose plot of hourly winds at two monitoring stations a) Dhyanchand Stadium and b) Talkotaroe Stadium from the WRF-Chem model for the entire period. ....	39
Figure 2.5 20-day mean temperature at 2m over Delhi. ....	40
Figure 2.6 20-day mean PBLH at 2:30pm and 2:30am of the day. ....	40
Figure 2.7 Spatial distributions of calculated 20 Day mean concentrations of criteria pollutants over Delhi. For ozone daytime means (9:30am – 6:30pm) are shown. ....	43
Figure2.8 Comparison of the distributions of observed and modeled hourly concentrations using data from all sites with lower (25%), median (50%) and upper quartile (75%). ....	45
Figure 2. 9 Mean diurnal variation in boundary layer height, emissions and BC concentrations from model and observations at the Dhyanchand Stadium site. ....	48
Figure 2.10 Percent contribution of each species to total PM <sub>2.5</sub> at Dhyanchand Stadium. ....	49

Figure 2.11 Spatial distributions of pollutants from various sectors to period mean surface concentrations.....	51
Figure 2.12 Diurnal variation in the sector contribution (in %) to period mean surface concentrations of different pollutants at the Dhayan chand monitoring station. ....	53
Figure 2.13 20-day mean contributions of pollutants from outside source. ....	54
Figure 2.14 Comparison of correlations between different species for all the sites combined based on observations and modeled concentrations.....	56
Figure 2.15 Spatial distribution of BC, CO, PM <sub>2.5</sub> and PM <sub>10</sub> over Delhi difference between with and without feedbacks. ....	58
Figure 2.16 Wind profiles over Delhi domain without feedbacks effect at four different time steps of a day.....	59
Figure 2.17 Wind rose plot of hourly winds at two monitoring stations a) Dhyanchand Stadium and b) Talkotaroe Stadium from the WRF-Chem model for the entire period without feedbacks. ....	60
Figure 2.18 Change in PBL height due to the aerosol feedbacks and without feedbacks over Delhi.....	61
Figure 2.19 Effect of feedbacks and without feedbacks from aerosol on Temperature at 2m from surface, Relative humidity and their net change. ....	62
Figure 3.1 GAINS Model Framework adopted to estimate the baseline emission scenario. ....	70
Figure 3.2 GAINS Emissions Model Domain overlapped with total domain choose for research.....	73
Figure 3.3 Daily average GAINS 2030 emissions from each species over Delhi for the year 2030.....	75
Figure 3.4 Daily average net change in the emissions from 2010 to 2030 over Delhi.....	77
Figure 3.5 Daily average spatial distribution of BC emission from different sectors for the year 2030. ....	78
Figure 3.6 20-day Mean spatial distribution of pollutants over Delhi from GAINS 2030 emission scenario. ....	79
Figure 3.7 20 –day mean net percent change in pollutant concentrations over Delhi from the period 2010 to 2030.....	80
Figure 3.8 Spatial Distribution of pollutants from various sectors from GAINS 2030 emissions.....	82

Figure 3.9 20-day mean net change in pollutants concentrations from 2030 to 2010 across various sectors over Delhi.....	84
Figure 3.10 Net increase in surface temperature (K) over Delhi from 2010 to 2030. ....	85
Figure 4.1 Anthropogenic radiative forcing components for the year 2005 from IPCC report. ....	89
Figure 4.2 20-day mean fluxes over Delhi from 2010 emission inventory. Top left shortwave, top right total longwave reaching the surface. Bottom parts show outgoing shortwave and longwave radiation at the top of the atmosphere. ....	91
Figure 4.3 20-day mean day time downward shortwave flux ( $W m^{-2}$ ) from various sectors and surface dimming from total anthropogenic emission over Delhi 2010.....	92
Figure 4.4 20-day mean day time anthropogenic atmospheric radiative forcing from various sectors-2010. ....	94
Figure 4.5 20-day mean day time downward shortwave fluxes from various sectors over Delhi-2030. ....	96
Figure 4.6 20-day mean day time anthropogenic atmospheric radiative forcing from various sectors in the year 2030.....	97
Figure 4.7 20-day mean day time net change in anthropogenic radiative forcing from various sectors year 2010 to 2030.....	98
Figure 4.8 20-day mean net surface dimming from different sectors and total dimming from anthropogenic emissions from the year 2010 to 2030. ....	99
Figure 4.9 20-day spatial mean averages of radiation effects at surface, in and top of the atmosphere for the year 2010 and 2030.....	100

## LIST OF ABBREVIATIONS

AERONET	Aerosol Robotic NETwork
AFWA	Air Force Weather Agency
AOD	Aerosol Optical Depth
ARWpost	Advanced Research WRF post-processing
BC	Black Carbon
CBMZ	Carbon-Bond Mechanism version Z
CH <sub>4</sub>	Methane
CNG	Compressed Natural Gas
CO	Carbon monoxide
CO <sub>2</sub>	Carbon dioxide
CWG	CommonWealth Games
ECMWF	European Center for Medium-range Weather Forecasts
EES	East –East- South
EPRES	Emission Preprocessor Model
EURO	European emission standards
FAA	Federal Aviation Administration
FNL	Final Analysis
FSL	Forecast Systems Laboratory
GAINS	Greenhouse Gas and Air pollution Interactions and Synergies
GIS	Geographical Information System
GrADS	Grid Analysis and Display System
IGCC	Integrated coal Gasification Combined Cycle
IGI	Indira Gandhi International Airport
IGP	Indo Gangetic plain
IIASA	International Institute for Applied Systems Analysis
IITM	Indian Institute of Tropical Meteorology
INTEX-B	Intercontinental Chemical Transport Experiment B
IPCC	Intergovernmental panel on Climate Change

ISC	Indira Gandhi Sports Complex
JSC	Jawaharlal Nehru Sports Complex
MACC	Monitoring Atmospheric Composition and Climate
MDS	M. Dhyanchand National Stadium
MEGAN	Model of Emissions of gases and Aerosols
MODIS	Moderate Resolution Imaging Spectroradiometer
MOSAIC	Model for Simulating Aerosol Interactions and Chemistry
MOZART	Model for Ozone and Related Chemical Tracers
MSL	Mean Sea Level
NASA	National Aeronautics and Space Administration
NCAR	National Oceanic and Atmospheric Administration
NCEP	National Centers for Environmental Prediction
NMVOC	Non Methane Volatile Organic Compound
NNW	North-North-West
NO <sub>2</sub>	Nitrogen dioxide
NO <sub>x</sub>	Oxides of nitrogen
O <sub>3</sub>	Ozone
OC	Organic mass
OLR	Outgoing Longwave Radiation
PBLH	Planetary Boundary Layer Height
PM	Particulate Matter
SAPRAC	State-wide Air Pollution Research Center
SO <sub>2</sub>	Sulfur dioxide
SO <sub>x</sub>	Oxides of sulfur
TERI	The Energy and Resources Institute
TG	Talkotaroo Garden
TSC	Thyagaraj Sports Complex
UD	University of Delhi
USGS	United State Geological Survey
VOC	Volatile Organic Compound
WRF-Chem	Weather Research and Forecasting /Chemistry

YSC

Yamuna Sports Complex

YSU

Yonsei University scheme

## CHAPTER 1 INTRODUCTION

### 1.1 Motivation and Importance of Work

Criteria Air Pollutants are the air pollutants with Indian National Ambient Air Quality Standards that define allowable concentrations of these substances in ambient air. There are two kinds of air pollutants: primary pollutants are substances directly emitted from a process i.e., Carbon monoxide, sulfur oxides, nitrogen oxides and black carbon; and secondary pollutants which are not emitted directly, but rather form in air when primary pollutants react (e.g. ozone). The better management of criteria pollutants requires enhanced understanding of the sources of pollution and the various processes, including deposition, chemical reactions, that influence the concentrations. The study of criteria air pollutants is very important as they have serious socioeconomic, environmental, health and welfare impacts. Criteria air contaminants also have profound effects on climate.

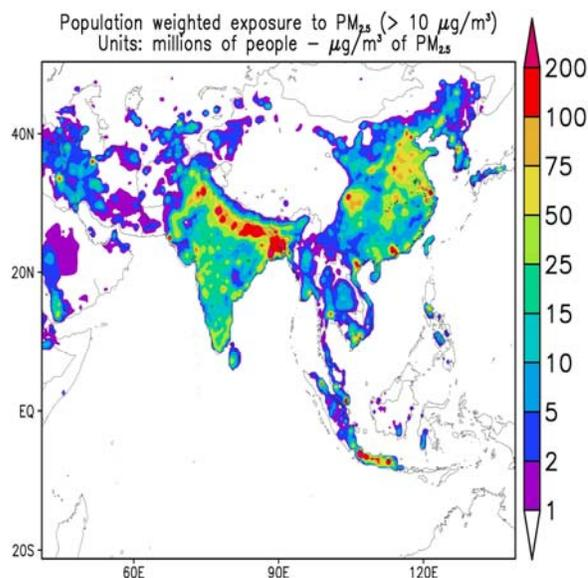
**Health Impacts:** Criteria air pollutants show serious impact on cardiovascular and respiratory problems. Carbon monoxide can cause harmful health effects by reducing oxygen delivery to the body's organs (like the heart and brain) and tissues (Buka et al., 2006). CO also contributes to the formation of ground level ozone, which also can trigger serious respiratory problems. Current scientific evidence links short-term SO<sub>2</sub> and NO<sub>2</sub> exposures, ranging from 5 minutes to 24 hours, with adverse respiratory effects including bronchoconstriction, airway inflammation in healthy people and increased respiratory symptoms in people with asthma (Buka et al., 2006). Studies also show a connection between short-term exposure and increased visits to emergency departments and hospital

admissions for respiratory illnesses, particularly in at-risk populations including children, the elderly, and asthmatics. NO<sub>2</sub> exposures near roadways are of particular concern for susceptible individuals, including people with asthma, children, and the elderly (Drimal et al., 2010). NO<sub>x</sub> and SO<sub>x</sub> react with ammonia, moisture, and other compounds to form small particles. These small particles can penetrate deeply into sensitive parts of the lungs and can cause or worsen respiratory disease, such as emphysema and bronchitis, and can aggravate existing heart disease, leading to increased hospital admissions and premature deaths (Viney et al., 2001). Control measures that reduce SO<sub>2</sub> can generally be expected to reduce people's exposures to all gaseous SO<sub>x</sub>. This may have the important co-benefit of reducing the formation of fine sulfate particles. Black Carbon another important primary pollutant considered hazardous to the lungs and general health when the particles are less than five micrometers in diameter, as such particles are not filtered out by the upper respiratory tract. Ozone is formed when NO<sub>x</sub> and Volatile Organic Compounds (VOCs) react in the presence of heat and sunlight. Children, the elderly, people with lung diseases, and people who work or exercise outside are at risk for adverse effects from ozone including reduction in lung function and increased respiratory symptoms and damage vegetation (Novaes et al., 2010). Emission control measures leading to reductions in NO<sub>2</sub> can generally reduce population exposures to all gaseous NO<sub>x</sub>. This may have the important co-benefit of reducing the formation of ozone and fine particles.

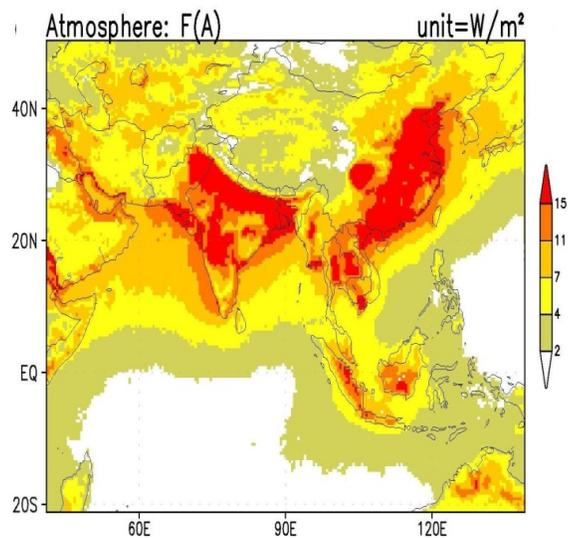
**Climate Change:** Criteria air pollutants also have an effect on climate change. Particles can affect the climate in two different ways. The direct effect is when the particles scatter and absorb solar and infrared radiation in the atmosphere. The result of the scattering of sunlight caused by particles is an increase in the amount of light

reflected back into space, which results in a decrease in the amount of solar radiation that reaches the surface. Thus cooling the atmosphere. Particles that absorb radiation (e.g., BC) heat the atmosphere and thus add to the global warming. The indirect effect of particles is more complex and more difficult to assess. The addition of PM into the atmosphere can cause water in the atmosphere to condense on to the particles (Slanina, 2010). Changes in the atmospheric aerosol number concentration can change cloud properties. More particles results in more, but smaller droplets in the clouds, which increases the cloud albedo. In addition to increasing the albedo, this effect tends to decrease the chance of heavy precipitation. If precipitation is suppressed, this results in excess water remaining in the atmosphere.

Previous studies focused on Asia air quality have provided valuable information about the health and climate impact due to air pollution. The two panels in Figure 1.1 adapted from Carmichael et al. 2009 and Chung et al., 2010 show the population exposure to PM<sub>2.5</sub> levels greater than the WHO annual guideline of 10µg/m<sup>3</sup> and the atmospheric heating effect due to BC. The Indo Gangetic plain (IGP) has high exposure to pollution when compared to other locations in South Asia. IGP is densely populated and has fertile lands. Therefore, in a way these regions contribute to high levels of pollution to atmosphere and exposure rates. On the other hand, concentrations of black carbon in Asia can be so high that heating due to the absorption of incoming solar light can more than offset the cooling by reflection of solar light. According to the IPCC, the warming effect of all the green house gases together is 2.5 watt-m<sup>-2</sup>, while the cooling effect of aerosols would be 0.7 watt-m<sup>-2</sup> (IPCC,2007). The right panel shows the four-year average heating effect from BC.



Carmichael et al., 2009



Chung et al., 2010

Figure 1.1 Population exposure to  $PM_{2.5}$  levels greater than the WHO annual guideline of  $10 \mu g/m^3$  and Heating effect due BC.

Air quality models are used to study the pollution distributions results from a given emission inventory. The past decade has witnessed rapid advances in the computational capabilities, which in turn have led to great improvements in the air quality modeling options. One such improvement is fully coupled air quality models that provide a direct interface between meteorology and chemistry, which is described later in section. This research study will implement this version of air quality model for obtaining better predictions of pollutant concentrations. Rapid industrialization and urbanization over the past few decades has led to high levels of outdoor pollution throughout the world. Previous literature has provided insights about the deteriorating air quality and high exposure levels in Asia as shown in Figure 1.1. In this research, we plan to focus on India as the study area. Delhi ( $28^{\circ}35'N$ ,  $77^{\circ}12'E$ , 217m MSL) is the capital city of India and the largest metropolis by area and the second largest by population in India. It is the

eighth largest metropolis in the world by population with more than 18 million inhabitants. Delhi hosted the Common Wealth Games (CWG) in October 2010. This high profile event provided an opportunity to intensely study air quality levels in the city during this period. To support the CWG air pollution monitoring was enhanced, and air quality forecasting efforts were initiated. The forecasting was the first of its kind in Delhi; therefore, this can be extended to other megacities in India in future. This study served as a pilot study for future expansions.

### 1.2 Objectives of the Proposed Research

There is a great need for improving air quality predictions and to investigate the feedbacks between air quality and weather and climate. To accomplish this air quality modeling is an important tool for predicting pollutant levels with better accuracy to devise effective mitigation strategies for effective air quality management and to assess the air quality impacts on health and welfare. The main objectives of this research are:

- Evaluate the role of aerosol feedbacks in air quality models to better understand the interactions among meteorology, chemistry, and aerosols in the atmosphere;
- Understand the contribution of various emission sectors including transportation, power, industry, and domestic to pollutant concentrations and radiative forcing in targeted regions;
- Evaluate the performance of the WRF-Chem model framework in South Asia;
- Simulate the pollutant distributions for the GAINS 2030 future emissions scenario and
- Study the radiative forcing effects due to increasing levels of air pollution.

### 1.3 Approach

To accomplish these research goals, the fully coupled online WRF-Chem model was used. The simulation and prediction of air quality involves both meteorology and chemical processes. The commonly used approach, termed as “offline” model, requires initially running a meteorological model independently of the chemical transport model. The output from the meteorological model is then used to drive the transport in the air quality model. Offline models are frequently used in ensembles and operational forecasting, inverse modeling and sensitivity simulation. Separating the meteorology and chemistry can lead to a loss of important information on feedbacks between chemistry and meteorology. Analysis of the wind velocity power spectrum and chemical profiles indicate that the offline simulations are susceptible to large errors in the vertical mass distribution (Grell et al., 2004).

Recent advances in air quality models have developed “online” models that treat the meteorology and chemistry together. In an “online” modeling system, chemistry is integrated simultaneously with the meteorology, allowing the feedback at each model time step both from meteorology to chemistry and chemistry to meteorology. The online models are increasingly used for applications in which the feedbacks are very much important and help in better understanding the influence of air quality on regional climate and weather (Grell et al., 2004).

While online coupled models enable a full range of feedbacks among major components and processes, the degree of coupling in these models varies substantially from slightly-coupled to moderately- or significantly-, or fully-coupled. Depending on the coupled components or processes, these online models are generally grouped into

four main categories: online meteorology and pollutant transport; online meteorology and pollutant transport and chemistry; online pollutant feedbacks to heating rates to drive meteorology; and online pollutant feedbacks to photolysis to drive photochemistry (Zhang, 2008).

A fully coupled online model, the Weather Research and Forecasting/ Chemistry (WRF-Chem) model, has recently been developed. The air quality component of the model is fully consistent with the meteorological component; both components use the same transport scheme, the same grid and the same physics scheme for the sub grid scale transport (Grell et al., 2005). WRF-Chem has several advantages when compared to many offline models. They are: meteorology and chemistry are run at the same time resolution; reduced storage requirements; feedbacks run with higher time resolution; and faster total computational time. There are certain disadvantages with these online models. One such disadvantage is in operational weather forecasting, where a longer computational time is required to produce the meteorological forecast with an online air quality prediction.

#### 1.4 History of WRF-Chem

The Weather Research and Forecasting model is a next generation mesoscale numerical weather prediction system designed to serve both operational and atmospheric research needs developed collaboratively by several agencies. (<http://www.wrf-model.org>). The effort to develop WRF has been a collaborative partnership, principally among the National Center for Atmospheric Research (NCAR), the National Oceanic and Atmospheric Administration (NOAA), the National Centers for Environmental Prediction (NCEP), the Forecast Systems Laboratory (FSL), the Air Force Weather Agency

(AFWA), the Naval Research Laboratory, Oklahoma University, and the Federal Aviation Administration (FAA) (Geng et al., 2007).

The WRF model is a fully compressible and Euler non hydrostatic model and includes several options of dynamic cores and physical parameterization so that it can be used to simulate atmospheric processes over a wide range of spatial and temporal scales (Fast et al., 2006). It calculates winds, potential perturbation potential temperatures, geopotential and surface pressure of dry air. WRF-Chem is a version of WRF that also simulates trace gases and particulates simultaneously with the meteorological fields using the mass and scalar conserving flux form of the governing equations and a terrain following mass vertical coordinate system (Fast et al., 2006).

### 1.5 Overview of the WRF-Chem Model

The model simulates the emission, transport, mixing, and chemical transformation of trace gases and aerosols simultaneously with the meteorology. The model can be employed for investigation of regional-scale air quality, field program analysis, and cloud-scale interactions between clouds and chemistry. The main process of WRF-Chem consists of three sub programs as illustrated in Figure 1.2 :

- 1) Standard initialization
- 2) WRF-Chem model
- 3) Visualization of data.

Figure 1.2 shows the simplified version of the WRF-Chem flow chart.

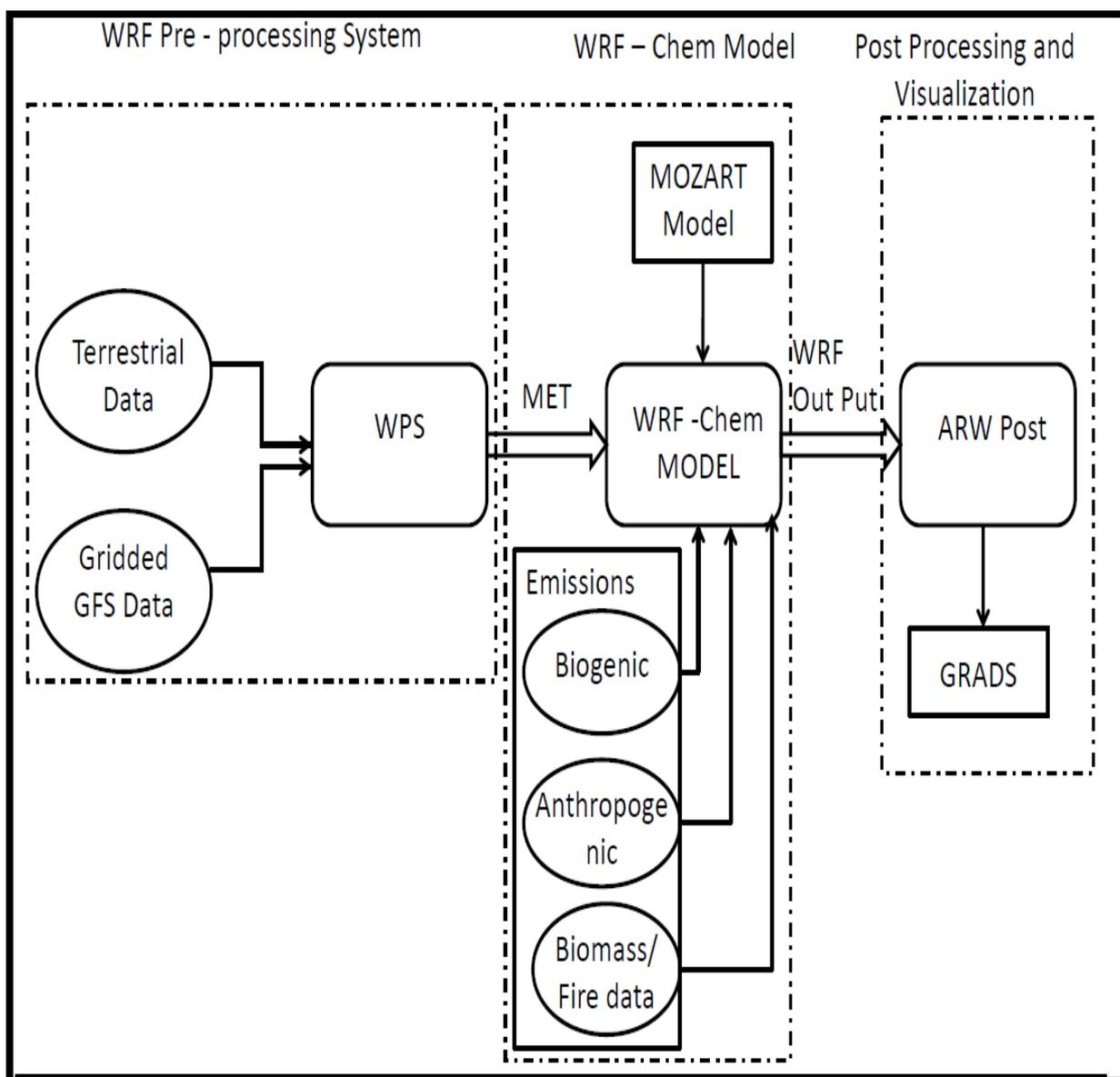


Figure 1.2 Flow chart of the WRF-Chem model.

The default settings include the United State Geological Survey (USGS) Terrestrial data and gridded GFS data are used as the main input parameters to the WRF-Preprocessing system. The meteorological output from WPS is fed as input for the WRF-Chem model along with the Model of Emissions of gases and Aerosols from Nature (MEGAN), the Moderate Resolution Imaging Spectroradiometer (MODIS) fire data, and the Intercontinental Chemical Transport Experiment B (INTEX-B) anthropogenic emissions. The Model for Ozone and Related Chemical Tracers (MOZART) is an offline global chemical transport model for the troposphere and is used to produce boundary conditions to the WRF-Chem model. The final sub program, called visualization, plays a vital role to observe the output. The Advanced Research WRF post-processing (ARWpost) along with Grid Analysis and Display System (GrADS) were utilized to serve this purpose.

### 1.6 Physical and Chemical Processes in WRF-Chem

The WRF-Chem model considers various physical and chemical processes such as transport, deposition, emission, photolysis, and radiation. These are described below. In this research the settings used are summarized in Table 1.1.

#### 1.6.1 Transport Processes

The model uses Runge Kutta 2nd and 3rd order time integration schemes. The transport is done using different boundary layer schemes. For this study, the Yonsei University scheme (YSU) was used. This is a Non-local-K scheme with explicit entrainment layer and parabolic K profile in unstable mixed layer.

### 1.6.2 Dry Deposition

The flux of trace gases and particles from atmosphere to surface is calculated by multiplying concentrations in the lowest model layer by spatially and temporally varying deposition velocity, which in turn, is the sum of three characteristic resistances i.e., aerodynamic resistance, sub layer resistance, and surface resistance. The surface resistance parameterization developed by Wesely (1989) is used. In this parameterization, the surface resistance is derived from soil and plant surface resistances. The properties of the plants are determined by land-use data and the season. The surface resistance also depends on the diffusion coefficient, the reactivity, and water solubility of the reactive trace gas.

The dry deposition of sulfate is described differently. In the case of simulations without calculating aerosols explicitly, sulfate is assumed present in the form of aerosol particles and its deposition is described according to Erisman et al. (1994).

The deposition velocity,  $v_{dk}$ , for the  $k$ th moment of a polydisperse aerosol is given by

$$v_{dk} = (r_a + r_{dk} + r_a * r_{dk} * v_{Gk})^{-1} + v_{Gk} \quad (1)$$

where  $r_a$  is the surface resistance,  $v_{Gk}$  is the polydisperse settling velocity, and  $r_{dk}$  is the Brownian diffusivity.

### 1.6.3 Gas-Phase chemistry and Aerosol

#### module

WRF-Chem supports several different chemical mechanisms. In this research, the Carbon-Bond Mechanism version Z (CBMZ) coupled with Model for Simulating aerosol Interactions and Chemistry (MOSAIC) was used. CBMZ has 156 -237 reactions among

52-77 chemical species and MOSAIC with 4 aerosol bins uses sectional size distribution, treats major aerosol species, including sulfate, methanesulfonate, nitrate, chloride, carbonate, ammonium, sodium, calcium, black carbon (BC), primary organic mass (OC) and liquid water.

#### 1.6.4 Photolysis Rates

Photolysis frequencies for the 21 photochemical reactions of gas phase chemistry model are calculated at each grid point according to Madronich (1987). The photolysis frequency of the gas  $i$ ,  $J_i$  is given by the integral of the product of the actinic flux  $I_A(\lambda)$ , the absorption cross sections  $\sigma(\lambda)$ , and the quantum yields  $\Phi(\lambda)$  over the wavelength  $\lambda$ :

$$J_i = \int^{\lambda} I_A(T, \lambda) \sigma_i(\lambda) \Phi_i(\lambda) d\lambda \quad (2)$$

Radiative transfer model by Wiscombe is used for calculation of actinic flux that is based on the delta-Eddington technique. The Radiative transfer model accounts for absorption by  $O_2$  and  $O_3$ , Rayleigh scattering and scattering and absorption by aerosol particles and clouds.

#### 1.6.5 Radiation

The radiation schemes provide atmospheric heating due to the radiative flux divergence and surface downward long and short wave radiation for the ground heat budget. Longwave radiation includes infrared or thermal radiation absorbed and emitted

by gases and surfaces. Shortwave radiation includes visible and surrounding wavelengths that make up the solar spectrum.

Table 1.1 Important input settings of the WRF-Chem model.

Feature	Option	Description
Microphysics	Lin et al. scheme	Sophisticated scheme with ice, snow, and graupel processes.
Longwave Radiation	Rapid Radiative Transfer Model (RRTM)	Accounts for multiple bands , trace gases, and microphysics
Shortwave Radiation	Goddard shortwave	Two-stream multi-band scheme with ozone from climatology and cloud effects.
Surface Layer	MM5 similarity	Based on Monin-Obukhov with Carlson-Boland viscous sub-layer and standard similarity functions from look-up tables.
Anthropogenic Emissions	Delhi Inventory & INTEX-B	Delhi inventory at 1.67 km resolution Intercontinental Chemical Transport Experiment B (INTEX-B) data at 0.5 °*0.5 ° resolution (Zhang et al.,2009).
Biogenic Emissions	MEGAN	MEGAN Model of Emissions of Gases and Aerosols from Nature , biogenic emissions online based upon the weather , land use data.
Boundary Conditions	MACC	Monitoring Atmospheric Composition & Climate, a global 3-D chemical transport model driven by offline meteorological fields.

# Asia

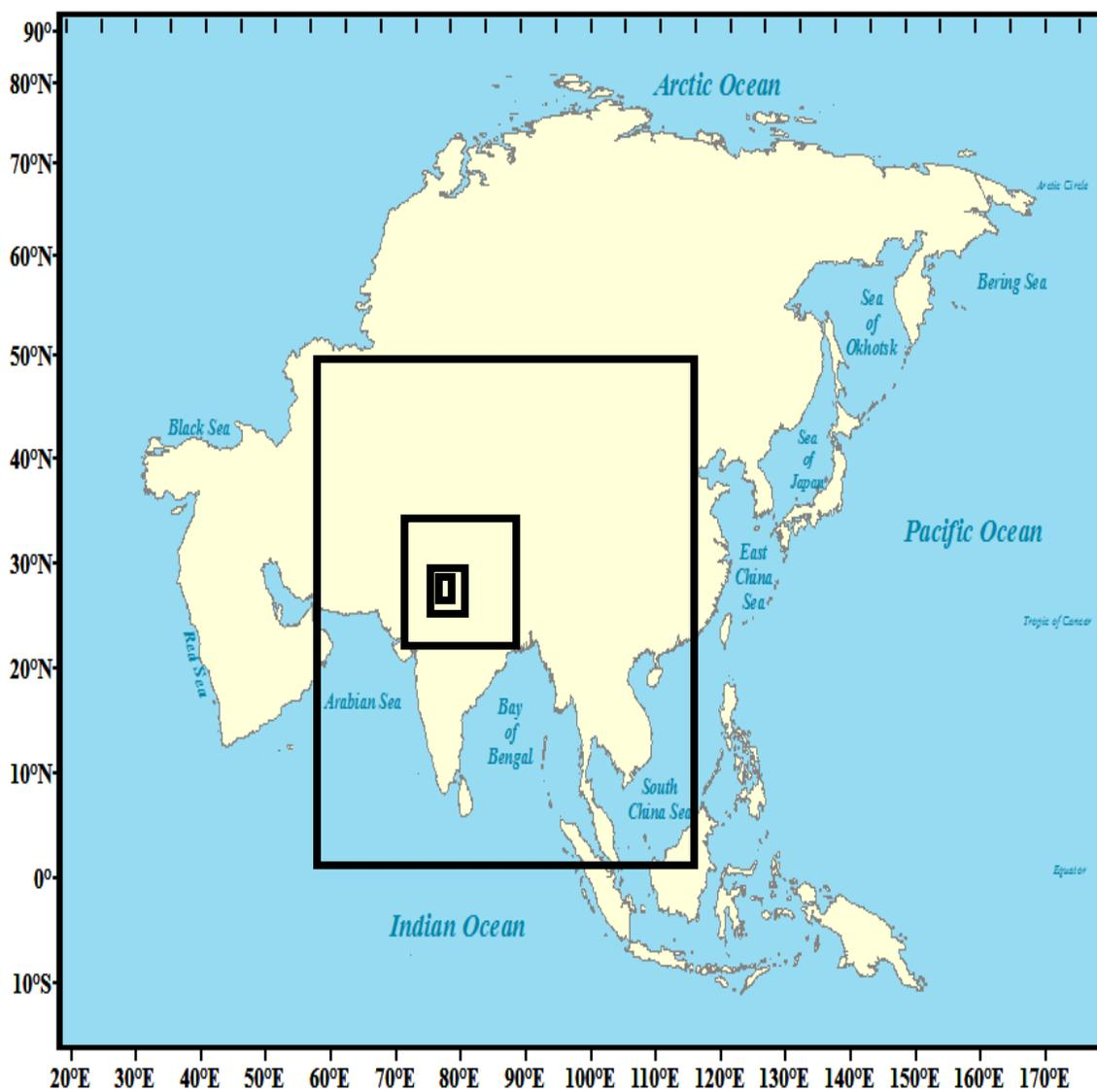


Figure 1.3 Nested model domains used in the Commonwealth Games forecasts and analysis.

## 1.7 Emissions

Various sources of pollutants include anthropogenic and biomass burning. This study focuses on estimating the contribution from various sources. Inventory studies indicate that transportation and point sources are largely responsible for criteria air pollutants release in the city (Kandlikar , 2007).

### 1.7.1 Anthropogenic Emissions

Carbon Monoxide (CO) is a criteria pollutant with a lifetime of several months in the atmosphere. It is emitted from various natural and anthropogenic sources. CO is produced by fossil fuel combustion, by biomass burning, and by oxidation of anthropogenic hydrocarbons (Aneja et al., 2001). Approximately 30 % of CO comes from natural sources such as oxidation of methane and natural hydrocarbons from ocean emissions, and from vegetation (Aneja et al., 2001). Sulfur dioxide and nitrogen dioxide are produced mainly from anthropogenic sources. Sulfur and nitrogen emissions have lifetimes in the atmosphere ranging from days to ~ 1 week. The growth in shipping industry in Asia is now an important source. Point sources such as thermal power plants and ~ 129,000 manufacturing units in Delhi contribute to SO<sub>2</sub> and CO emissions.

Black carbon (BC) is a pollutant formed through the incomplete combustion of fossil fuels, biofuel, and biomass. BC strongly absorbs visible light making it an important contributor to radiative forcing of the atmosphere and contributes to green house warming, as it couples with strong absorption of light over wide spectral range

(Beegum et al., 2009). Black carbon stays in the atmosphere for only several days to a week or so.

The primary air pollutants can also act as precursors to secondary pollutants i.e., Ozone. Ozone is a primary concern in the present day.  $\text{NO}_x$ , CO and VOC are the main precursors for ozone formation (Ghude et al., 2009). Along with health problems, ozone has serious impact on vegetation (Ghude et al., 2009) and is a green house gas. Delhi is in the Indo Gangetic plain (IGP) which is a very fertile land in India. Therefore, increased ozone levels may reduce the crop yield to a certain extent.

The four major emission sectors considered in this study are transportation, power, industry (manufacturing, refineries, and small-scale industries), and domestic. Delhi city constitutes slightly more than 1 % of the India population, and accounts for around 17 % of the nations motor vehicles, with an annual growth rate of 20% that directly affect the levels of pollution in the city (Mohan et al., 2006). Combustion of transportation fuel produces significant amounts of CO, BC,  $\text{SO}_2$  and  $\text{NO}_2$  in Delhi. Elevated ambient temperatures in Delhi, and the high volatility of gasoline enhances the potential for evaporative emissions rich in reactive hydrocarbons, which participate in the formation of ground-level ozone causing loss of crop yield in the Indo Gangetic plain (Badami, 2005).

Delhi has five thermal power plants out of which three are situated within the city. It also has many other manufacturing facilities, and cement plants. These are the major sulfur emission sources in Delhi. Extensive usage of wood and charcoal stoves is still prevalent in slums and in the out skirts of Delhi, for cooking practices. IGP is one of the

densely populated areas with high fertile lands. High levels of BC (19 %) occur in association with large coal consumption for domestic purpose (Sahu et al., 2008).

For this study, the INTEX-B emission inventory is used. This Inventory was developed in support of NASA's INTEX-B mission with reference year 2006 at a grid resolution of 0.5 degree. The inventory covers anthropogenic emissions from Power, Industry, Residential (Domestic), and Transportation. Emissions of SO<sub>2</sub>, NO<sub>x</sub>, CO, VOC, PM<sub>10</sub>, PM<sub>2.5</sub>, BC and OC from the four sectors in units of Ton/year per grid are used as input for the pollutant concentration calculation in the WRF-Chem model. VOC has 30 lumped species that are needed for the SAPRC 99 Mechanism. For the VOC species sector information is further split into power plants, industry, residential biofuel, residential fossil fuel, residential non-combustion, and transportation. Figure 1.4 shows a sample of mapped INTEX-B CO emissions over the three domains. The emissions were calculated from 0.5° to 45km, 15 km and 5km subsequently, using linear interpolation techniques.

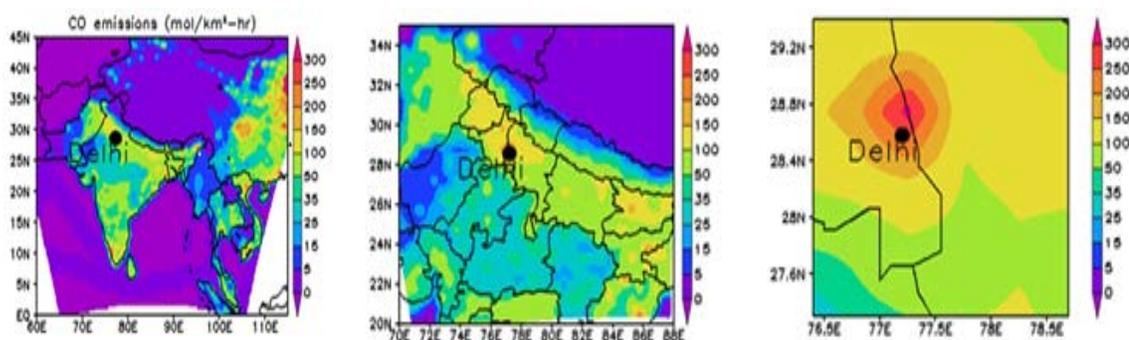


Figure 1.4 Carbonmonoxide emission distribution from three domains.

In the fine resolution (i.e. 5km) the emission distribution in Delhi is clearly visible. Emissions are one of the most crucial and sensitive area of air quality modeling and results are highly dependent on the emission data provided as input to model. Therefore, new inventories were prepared at finer resolution for Delhi as a part of the CWG action. The first component is collection of source activity data on a very high resolution. Some data are available from different ministries like the type of industries, production capacities, population of developed and under developed localities, number of registered vehicles, volume of petrol and diesel consumption per day, etc. Some activity data needed to be collected by involving various voluntary or independent service organizations who could practically count the number of various vehicular types passing through different sensitive areas /road /junctions. The second component was to construct the finely gridded emission inventory  $1.67*1.67 \text{ km}^2$  resolution using the above activity data and available emission factors using the GIS based statistical model developed at IITM, Pune.

Table 1.2 Percent Anthropogenic Emissions Contribution from Various Sectors to Delhi from Delhi Emission Inventory.

		Percent Contribution From each Anthropogenic Sector			
Species	Tonnes/Day	Transportation	Power	Industry	Domestic
SO <sub>2</sub>	81	12.9%	48.7%	25.2%	13.2%
NO <sub>x</sub>	598.5	69.4%	13.2%	4.5%	12.9%
CO	1320.3	43.7%	0.2%	4.0%	52.0%
PM <sub>10</sub>	344.8	86.8%	7.9%	4.6%	0.8%
PM <sub>2.5</sub>	128.6	52.6%	9.9%	15.3%	22.2%
BC	36.9	58.9%	3.0%	6.6%	31.5%
OC	35.1	30.5%	5.6%	10.6%	53.3%
NMOC	852.4	58.4%	1.2%	5.2%	35.3%

Table 1.2 shows the total emissions per day and the percent contribution of emissions from different sectors to Delhi. Transportation and Domestic sectors are major sources of CO, BC, and OC emissions. The power sector contributes significantly to SO<sub>2</sub> and NO<sub>x</sub> emissions (~49 % and ~13% respectively). Industries contribute ~25 % to SO<sub>2</sub>. The domestic sector is a large emissions source of BC ~32% and OC ~53%. The transportation sector plays a vital role in particulate matter emissions over Delhi.

### 1.7.2 Emission Preprocessor (EPRES) model

The spatial distribution of emissions was based on roadways, locations of power plants, plants, slums and major industries using various Delhi data sets (Sahu et.al, 2011). The emissions were transferred into the WRF-Chem modeling system using the Emission

Preprocessor Model (EPRES). The Emission Preprocessor Model (EPRES), generates the inter-media binary emission data (wrfem\_00z\_d0\* and wrfem\_12z\_d0\*) needed by the WRF-Chem model. It was designed by Dr. M. Lin (Center for Sustainability and the Global Environment at University of Wisconsin-Madison) and modified by Dr. Y.F.Cheng (CGRER at the University of Iowa). Wrfem\_00z\_d0\* and wrfem\_12z\_d0\* can be then converted by convert\_emis.exe of WRF-Chem to generate the anthropogenic emission for WRF-Chem simulations. EPRES does two things, first mapping the SAPRC 99 speciation to CBM-Z and second horizontally interpolating the emission inventory into projected model grids. When interpolating the emissions, EPRES reads in the already projected grids from the WPS/WRF output (such as geo\_em.d0\*.nc, met\_em\_date.d0\*.nc, or wrfout\_date.d0\*, which contain XLAT and XLONG), and then utilizes the I/O API mass conservative interpolation subroutine to interpolate the emission into model grids. All the interpolated species were converted into WRF-Chem required units. After wards, the mapped emissions were distributed into two vertical layers i.e. 70% emissions were distributed at surface and 30% uniformly distributed to the grids up to ~1000m (grids 2-6 in this application). Diurnal profiles were also applied. The diurnal variability of BC emissions are shown in Figure 2. 9, and exhibits two peaks, one in early morning and the second in early evening associated with both traffic and cooking activities. Seasonal variation and longitude (local time) dependent diurnal variations were applied. The EPRES model can also be used to generate emission data for SAPRC99 and CBM-4 chemical mechanisms for both WRF-Chem and CMAQ models to utilize global emissions.

Figure 1.5 shows the emissions distribution over Delhi using the EPRES model for the Delhi Inventory. From emissions distribution patterns it is evident that central regions of Delhi are high contributors of anthropogenic emission. Total CO emissions from Delhi city are mainly from transportation and domestic sources, as incomplete combustion is the major reason behind these high levels of CO emissions from the city. Particulate matter concentrations exceed the National Ambient Air Quality levels in Delhi. The main reason is the increase in vehicular count in the city during the past decade. Construction dust is the main source for these high levels of Particular matter. Geographically city is surrounded by industrially developed cities such as Gurgoan and Noida. Many cement industries and brick kilns are situated in and around Delhi city adding to the increasing particulate emissions to the City.

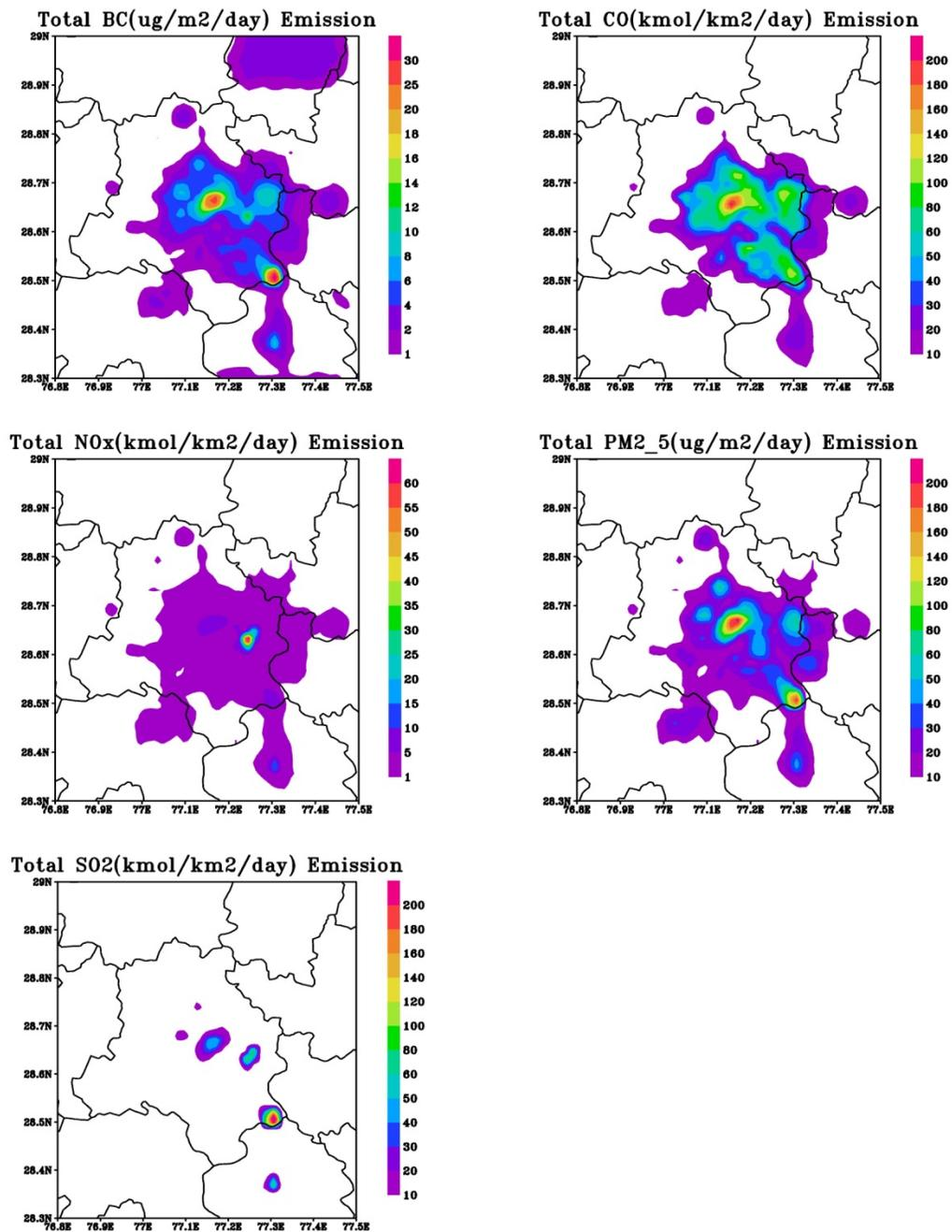


Figure 1.5 Emission distributions of BC, CO, NO<sub>x</sub>, PM<sub>2.5</sub> and SO<sub>2</sub> units over Delhi.

Extensive usage of wood and charcoal stoves for cooking is still prevalent in slums and in the out skirts of Delhi. High levels of BC emissions (19% of total) occur in association with large coal consumption for domestic purpose (Sahu et al., 2008). The sectoral distributions of the BC emissions are shown in . These show clearly the locations of the power plants, industrial clusters, the distributions of slums and the major transportation networks. The INTEX-B emissions were used over the outer three domains. Biogenic emissions were calculated hourly on-line using MEGAN. The dust emissions were turned off during the run time of the model, since the post monsoon period is a period with insignificant dust impacts on Delhi.

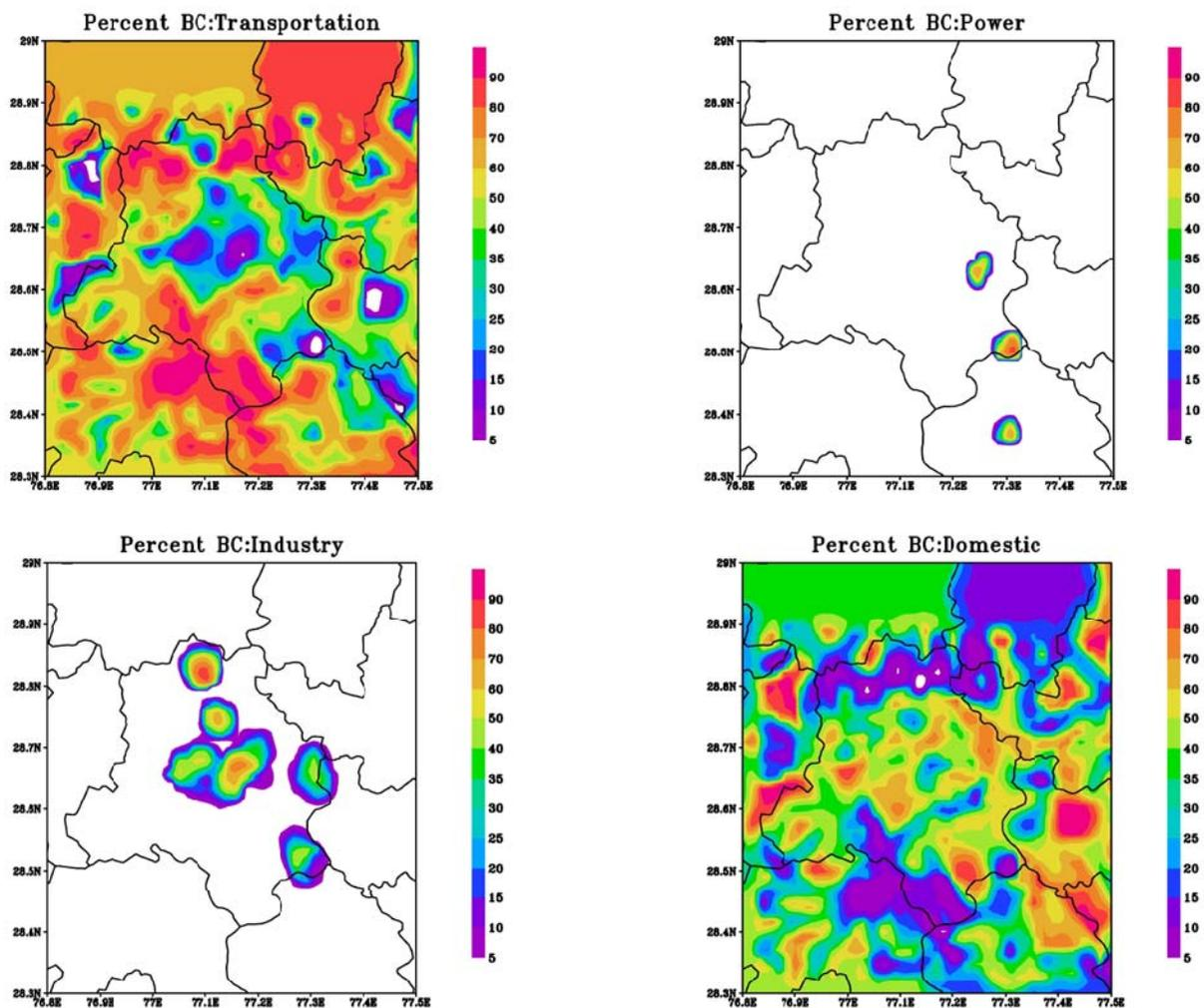


Figure 1.6 Sector contributions of Black Carbon emissions (%) over Delhi.

### 1.8 Model of Emissions of Gases and Aerosols from Nature

#### (MEGAN)

Biogenic emissions were estimated using the Model of Emissions of Gases and Aerosols from Nature (MEGAN). These biogenic emissions are calculated online based upon weather and land use data. The net emission rates of isoprene and other biogenic trace gases and aerosols from terrestrial ecosystems into the above canopy atmosphere at a specific location and time (Guenther et al., 2006) are given by

$$\text{Emission} = [\epsilon][\gamma][\rho] \quad (3)$$

where  $\epsilon$  ( $\text{mgm}^{-2}\text{h}^{-1}$ ) is an emission factor that represents the emission of a compound into the canopy at standard conditions,  $\gamma$  (normalized ratio) is an emission activity factor that accounts for emission changes due to deviations from standard conditions and  $\rho$  (normalized ratio) is a factor that accounts for production and loss within plant canopies.

Figure 1.7 show the base isoprene emissions from MEGAN, serves as input emission for the online computation. The amount of isoprene emitted from plants dominates the biosphere–atmosphere hydrocarbon exchange. The emission of isoprene from plants affects atmospheric chemistry as isoprene reacts very rapidly with hydroxyl radicals in the atmosphere making hydro peroxides that can enhance ozone formation. Aerosol formation in the atmosphere may also be influenced by biogenic isoprene.

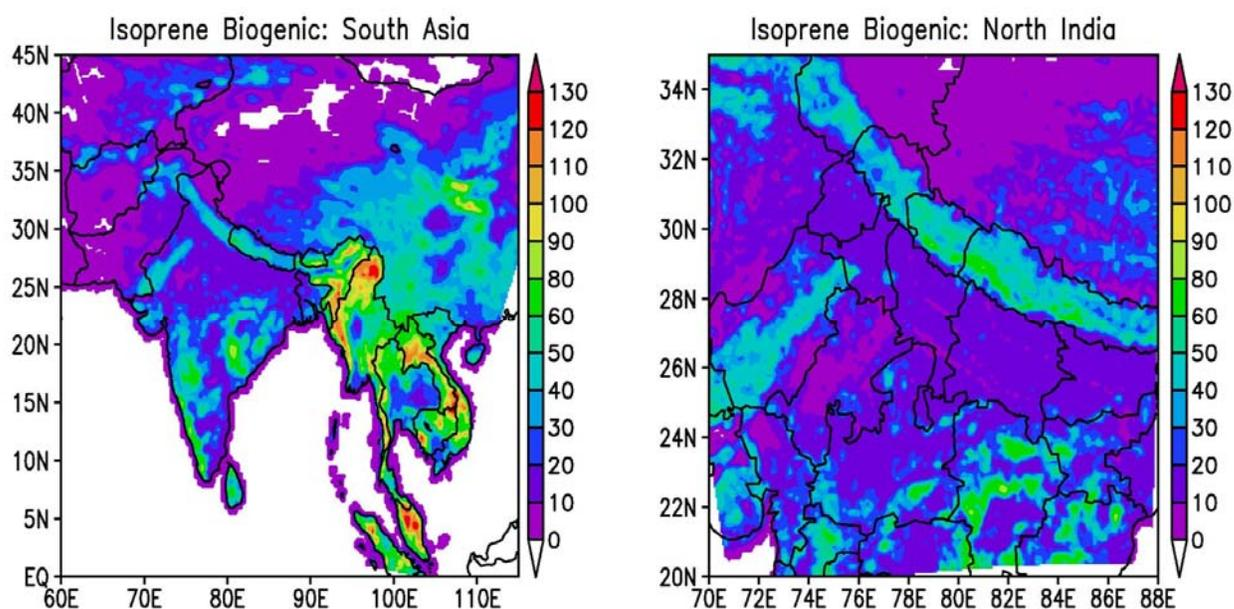


Figure 1.7 Base isoprene emissions from MEGAN.

High levels  $\sim 90$ - $110$  moles/km<sup>2</sup>-hr of isoprene are observed in North East India. Indo Gangetic plain has vast fertile agricultural land which lead to production of isoprene during certain seasons. The figure shows the emissions in the month of October, where the crops are almost in the harvesting period, therefore we could not see high levels of isoprene in the IGP. Dust emissions were turned off during the run time of the model

because the post monsoon is a stable period hence the dust emissions are small in the forecast results.

Finally, the anthropogenic and biogenic emissions were fed into the model employing the respective preprocessing tools. The generated binary files from different emissions were converted to WRF-Chem readable format using `convert_emiss.exe` program. The meteorological data from WPS program acts as important weather input to the model. WRF-Chem is an online model, therefore all the weather data, and emissions files are input into model at one time. The detailed description of model is shown in Figure 1.2.

### 1.9 Meteorology Data

Final Analyses (FNL) from National Centers for Environmental Prediction (NCEP) Global Analyses at 1\*1 degree resolution was used as meteorology input data. The output from analysis is for every 6 hours with 26 pressure levels ranging from 1000 pa to 10hpa. The data is available from National Center for Atmospheric Research (NCAR) archive site in grib format. Weather Preprocessing System (WPS) subroutine `ungrib`'s the data into readable format. Further, the `ungrib` data was processed using `metgrid` option into netCDF format which acts as meteorology input variable for WRF-Chem model.

### 1.10 Initial and Boundary conditions

The WRF-Chem model requires initial and boundary conditions for simulations. To achieve better meteorology predictions we ran the model for 5 days with 2 days of spin up time. Chemistry variables require the model to run continuously so

concentrations can be built-up. In order to accomplish that, we overwrite the chemistry variables on the newly generated wrf input conditions. Therefore by doing this we avoid the biases from the meteorology and in-turn reduce the chemistry biases. Another important input condition required is the boundary. Long range transport plays a vital role on pollutant concentrations along with emissions within the region. Therefore, to consider the influence outside the regions, boundary conditions from global model was used. The European Centre for Medium-range Weather Forecasts (ECMWF) model MACC (Monitoring Atmospheric Composition and Climate) operates and improves data-analysis and modeling systems for a range of atmospheric constituents that are important for climate, air quality and surface solar radiation.

MACC has input from various sources such as satellite, in-situ data and many other emissions related data sets. Missing satellite data is substituted with in-situ measurements of atmospheric composition. This framework provides a range of atmospheric constituents that are important for climate, air quality and surface solar radiation. This global model works as boundary conditions for regional models. MACC has forecast and reanalysis data for various reactive gases and aerosols. MACC provides 72Hr forecast for every 3hrs.

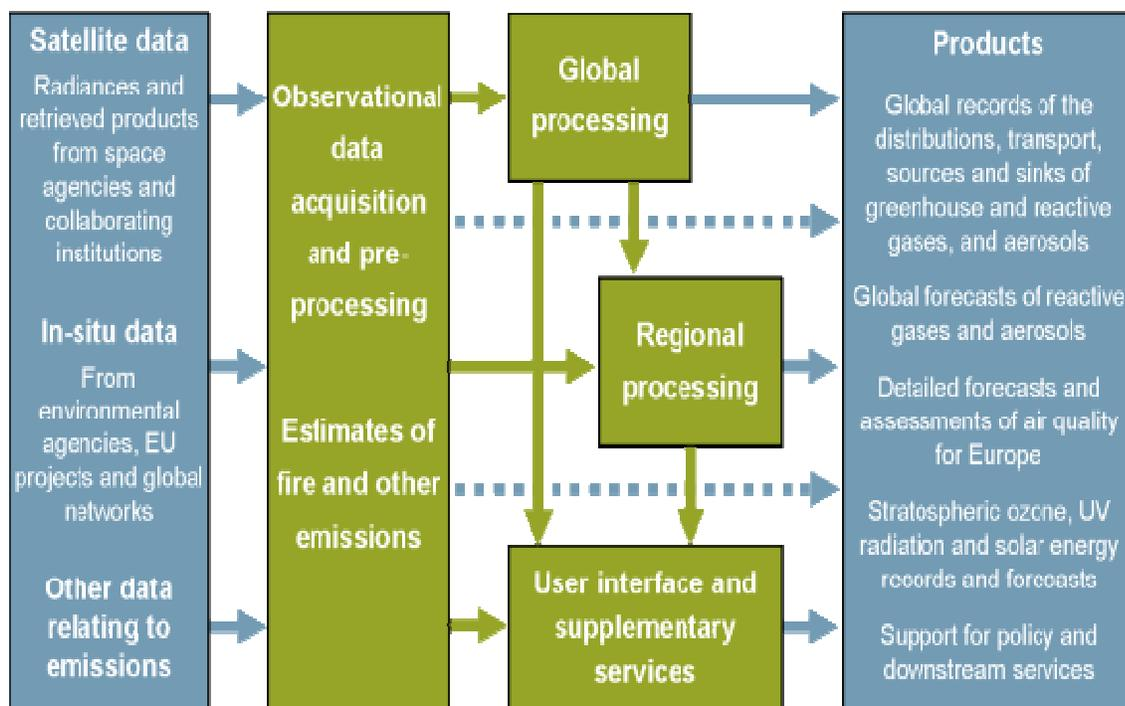


Figure 1.8 Flow chart of MACC model.

### 1.11 Thesis organization

Further details and results of this research are presented in the following chapters.

In Chapter 2 deals with sectoral contributions to black carbon and other criteria pollutants over Delhi. Chapter 3 focuses on emission projection studies using GAINS -2030 scenarios. Effects of short lived climate forcing agents on radiative forcing from with and without feedbacks are addressed in Chapter 4. Finally in Chapter 5 a summary and discussion of further research needs are discussed.

## CHAPTER 2 SECTORAL CONTRIBUTIONS TO BLACK CARBON AND OTHER CRITERIA POLLUTANTS IN DELHI AND THEIR TWOWAY INTERACTIONS WITH METEOROLOGY

### 2.1 Introduction

Rapid industrialization and urbanization over the past few decades have led to high levels of outdoor pollution throughout the world. This is particularly true in the megacities of Asia, where high concentrations of aerosols and other criteria pollutants have large impacts on the health and welfare of citizens. Small ambient particles can penetrate deeply into sensitive parts of the lungs and can cause or worsen respiratory disease, such as emphysema and bronchitis, and can aggravate existing heart disease, leading to increased hospital admissions and premature death (Agarwal et. al., 2006). These particles and other short-lived radiative forcing agents such as ozone also impact incoming solar radiation and impact weather and climate. According to the IPCC (IPCC, 2007) the warming effect of all the greenhouse gases together is 2.5 watt-m<sup>-2</sup>, while the cooling effect of aerosols is 0.7 watt-m<sup>-2</sup>. The high levels of black carbon (BC) in Asia are of particular interest, because of its dual role in impacting human health and in acting like a greenhouse gas and causing warming of the atmosphere. Ramanathan and Carmichael estimate that BC is the second most important warming agent (behind CO<sub>2</sub>) (Ramanathan and Carmichael, 2008). For these reasons there is currently mounting interest in developing strategies that will both reduce the levels of air pollutants and reduce global warming. These strategies often develop first in megacities in Asia where

air quality and energy policies respond to the rapid needs associated with the widespread urbanization. Effective management of air quality requires enhanced understanding of the sources of pollution and their effects on human health and climate.

In this chapter the analysis of BC and other pollutants in Delhi (28°35'N, 77°12'E, 217m MSL), the capital city of India and the largest city by area and the second largest by population in India are presented. It is the eighth largest megacity in the world with more than 18 million inhabitants. Delhi hosted the Commonwealth Games (CWG), a multi sport event involving 73 countries, in October 2010. This high profile event provided an opportunity to accelerate efforts to improve air quality. To support the CWG air pollution monitoring was enhanced, a new emissions inventory was developed and air quality forecasting efforts were initiated. In this chapter the WRF-Chem model is used to simulate the air quality during the GWG and evaluate its performance by comparing the predicted meteorology and concentrations of BC and other criteria pollutants with observations. The spatial patterns of BC, CO, SO<sub>2</sub>, NO<sub>2</sub>, and O<sub>3</sub> over Delhi and estimate the contributions from specific source sectors (Transportation, Power, Industrial, and Domestic) are presented and discussed. Sector information is needed in order to guide the development of effective pollution reduction measures. The emission estimates are evaluated by analyzing observed and predicted species ratios. The two-way interactions between the criteria pollutants and the meteorology are also discussed.

## 2.2 Approach

WRF-Chem version 3.1.1 is employed to perform air quality analyses over South Asia. To facilitate improved and comprehensive air quality predictions a nesting option is used over the chosen domain, which provides better representation of spatial distribution of pollutant concentrations. The coarse domain covers the South Asia from 50 E to 120 E and 0 N to 55 N at a horizontal resolution of 45km with 131x131 grid cells. The next domain, which acts as parent to the third domain focuses on the northern regions of India; i.e. stretched over the Indo Gangetic plain at a resolution of 15km with 127x127 grid cells. The finest domains cover the Delhi region in particular at a resolution of 5km with 55x55 grid cells and 1.67km with 75x70 grid cells. Figure 1.3 shows the domain details of the model.

Ten new automatic air pollution and meteorology monitoring stations were installed for the Commonwealth Games and are placed at different venues across the city i.e., Commonwealth Games Village (CWG), IITM Delhi (IITM), Yamuna Sports Complex (YSC), Indira Gandhi Sports Complex (ISC), M.Dhyanchand National Stadium(MDS), Jawaharlal Nehru Sports Complex (JSC), Thyagaraj Sports Complex (TSC), University of Delhi(UD), IGI-Airport(IGI) and finally Talkotaroo Garden (TG) as shown in Figure 2.1. The air quality parameters i.e., Black Carbon (BC) , Carbon Monoxide(CO), Nitric Oxide (NO), Nitrogen Dioxide (NO<sub>2</sub>), Ozone(O<sub>3</sub>), PM<sub>2.5</sub> and PM<sub>10</sub> were measured at hourly interval over span of two weeks from 26<sup>th</sup> Sept, 2010 to 15<sup>th</sup> Oct, 2010. Similar to the air quality species, meteorology species i.e., wind speed (m/sec), wind direction (deg), temperature (°C), relative humidity (%) were measured.

The WRF-Chem model was run for the period 26Sep -16Oct 2010. The analysis in this chapter focuses exclusively on the Delhi region (the inner-most grid).

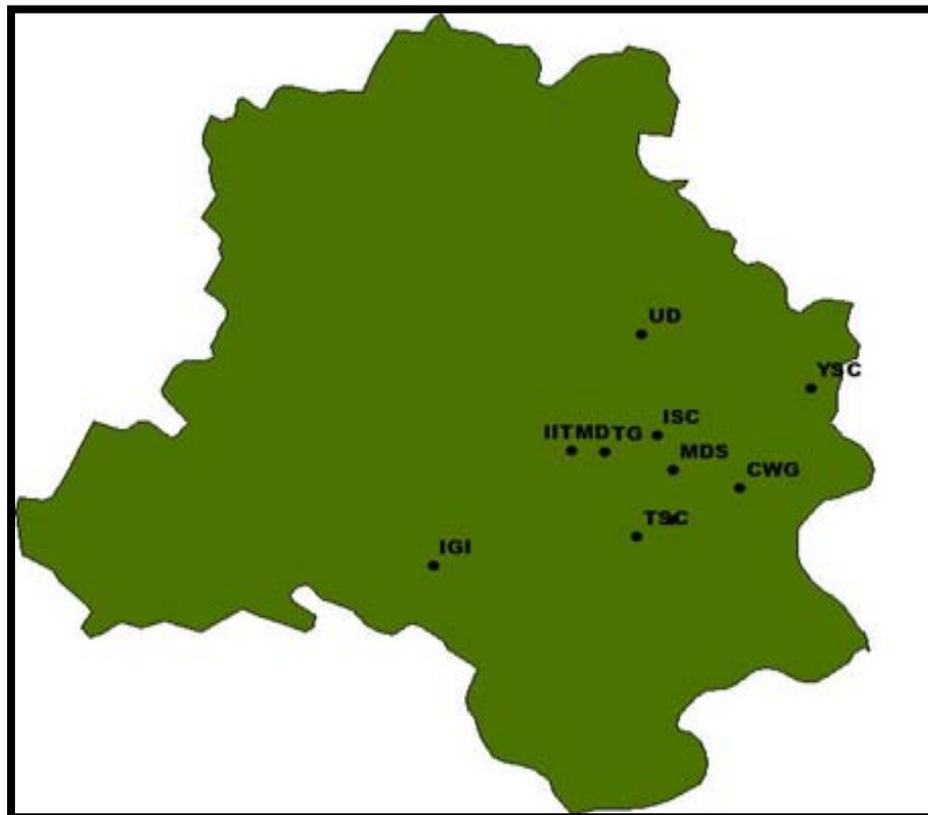


Figure 2.1 Locations of the monitoring stations for the Commonwealth Games.

Table 1.1 summarizes the input settings for the WRF-Chem model employed in this study.

Figure 2.2 show the spatial distribution of pollutants BC ( $\mu\text{g}/\text{m}^3$ ) and CO (ppbv) over three domains South Asia, Northern India and NCR Delhi. It is a 20day mean distribution pattern. CO concentrations over all regions, in particular high concentrations ( $>700$  ppbv) are observed in the Indo Gangetic plain (IGP). High CO concentrations are observed over Delhi, this is because we overlapped New Delhi emissions onto each

domain. The main reason for these high levels of CO over Delhi could be due to increase in levels of vehicular count and fuel usage. Black Carbon has much distributed pattern over third domain as lot of residential pockets are located around. This resulted in use of high cooking fuel and modes of fuel usage such as transportation and opening burning.

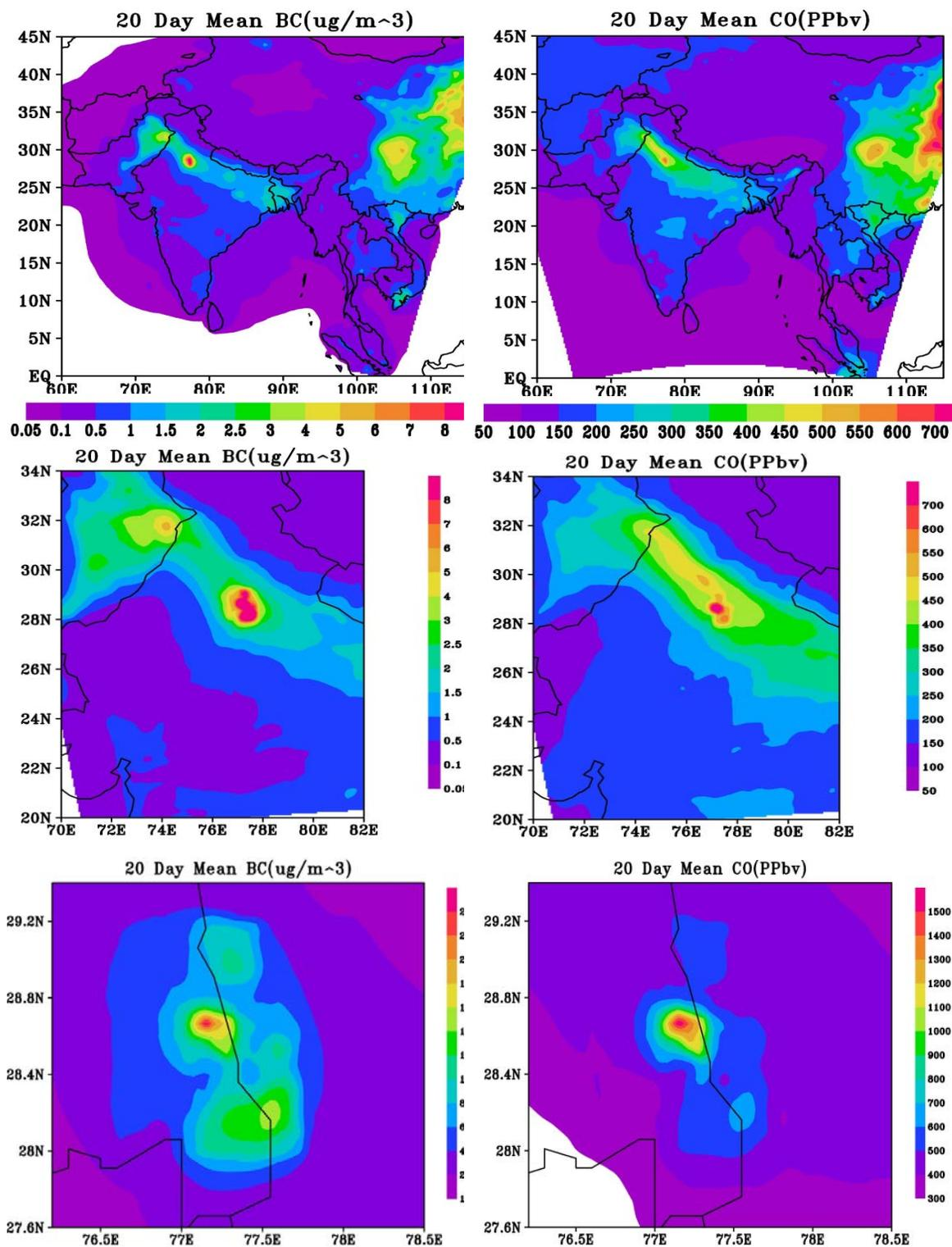


Figure 2.2 20-day mean spatial distribution of criteria pollutants over South Asia , Northern India and NCR Delhi.

## 2.3 Results and Discussion

### 2.3.1 Meteorology

Source control strategies will help to reduce the air pollution, but the reduction for fixed source strength is directly a function of the meteorological conditions and their variation in time and space over the area of interest. Meteorological parameters affecting transport, diffusion, transformation, and removal processes are functions of both time and space. Transport of pollutants and their resulting concentrations depend on meteorological parameters such as temperature, wind speed, and direction, atmospheric stability and the movement of the pressure systems. Four seasons occur in India: Winter (December – early April); Summer (April – June); Monsoon (June –September); and Post monsoon (October – early December). Concentrations vary seasonally in India in the following order: winter>post-monsoon>pre-monsoon>monsoon. In addition to the seasonal change, in many locations there is diurnal change in wind flow, which may be even more marked. It is usual that the night hours are periods of stability. Because of the effects of negative buoyancy and the increased energy required for the vertical motions, pollutants disperse slowly and may be confined in relatively small volumes. The concurrent light, variable wind may even result in return flow of material across the original source. In contrast, the day time winds are apt to be more turbulent, of higher speeds and the vertical motions are enhanced, so that the maximum dilution of materials occurs on clear, sunny days. In addition to the variation of wind flow in the horizontal and with time, there is usually a marked difference in wind flow in the vertical. Before or shortly after sunset, the air near the ground cools rapidly and a stable lapse rate begins to

form. The inversion increases with time in intensity and in depth during the night, reaching a maximum between midnight and the time of minimum surface temperatures. During this period, contaminants are effectively trapped within or below the inversion layer with little or no vertical dispersion.

The Common Wealth Games was held during the post monsoon season. This season is climatologically a very stable season. There are certain difficulties with this period. As mentioned in the previous section the IGP is a very fertile land, and October and November months are harvest season, therefore accounting for large crop residue burning. In addition the festival of lights, (Diwali) increase local pollution levels (Badarinath et al., 2009). It is necessary to understand the complexity of the seasonal variation during this period. The general situation in India is that in mid September the monsoon has shifted from the Southwest Monsoon to the Northeast monsoon. This brings in air masses from Northern and Northeast parts of the country (Ghude et al., 2009). Meteorological parameters affecting transport, diffusion, transformation, and removal processes are functions of both time and space. Transport of pollutants and their resulting concentrations depend on meteorological parameters such as temperature, wind speed, and direction, relative humidity.

Figure 2.3 shows the 20-day mean daily variation in wind flow in Delhi calculated using the WRF-Chem model. Period mean flows at 5:30 am, 11:30 am, 5:30 pm, and 11:30 pm are shown. The winds are generally low and from the NNW. During the daytime the NNW winds dominate, and after sunset there is a shift in the direction of the wind flow. Further insights into the flow fields are shown in the wind rose plots for two of the monitoring (Figure 2.4). The winds are most frequently from the NNW and low (<

3 m/s). Winds from the EES tend to be less frequent but of higher speeds. Each color on the plot corresponds to particular wind speed range. Dotted circles are drawn at 2% intervals starting from 2 % -12% corresponds to the frequency of the winds from that direction.

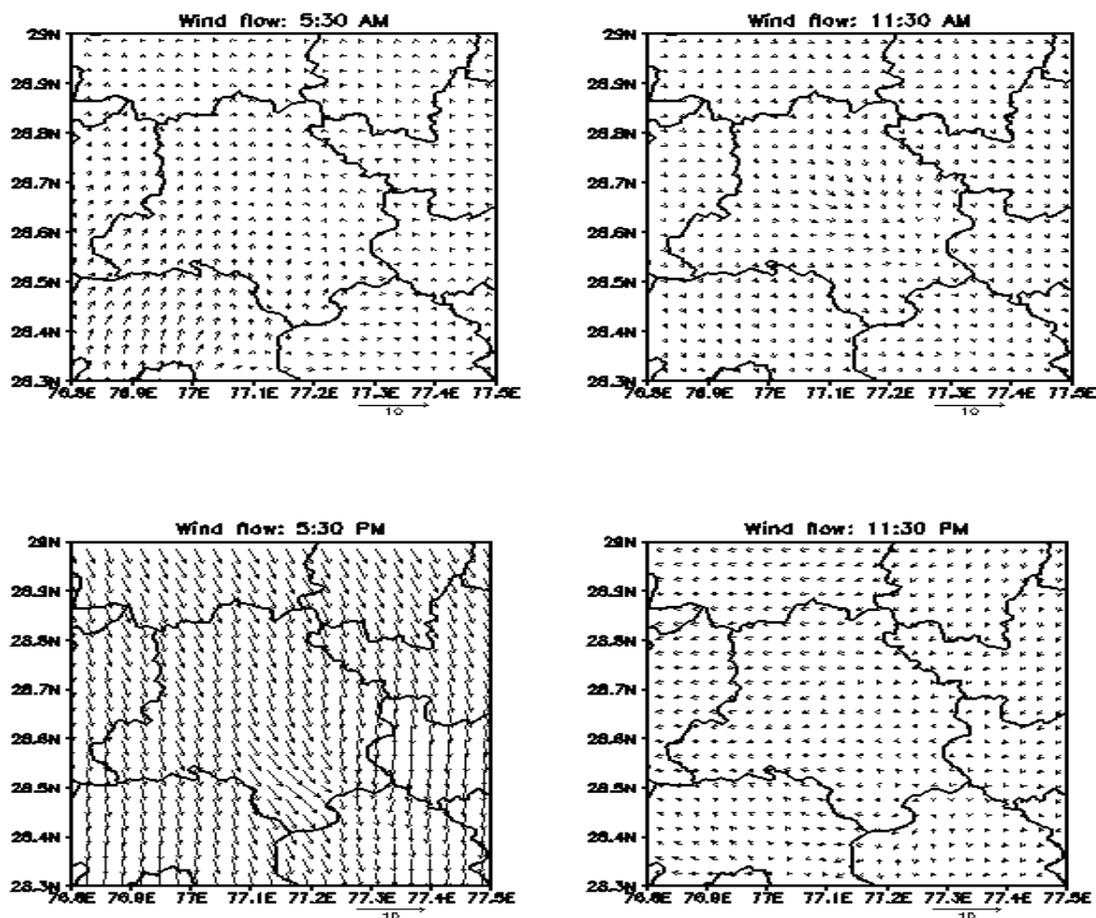


Figure 2.3 20-day mean surface winds at 5:30am, 11:30am, 5:30pm and 11:30pm(LT).

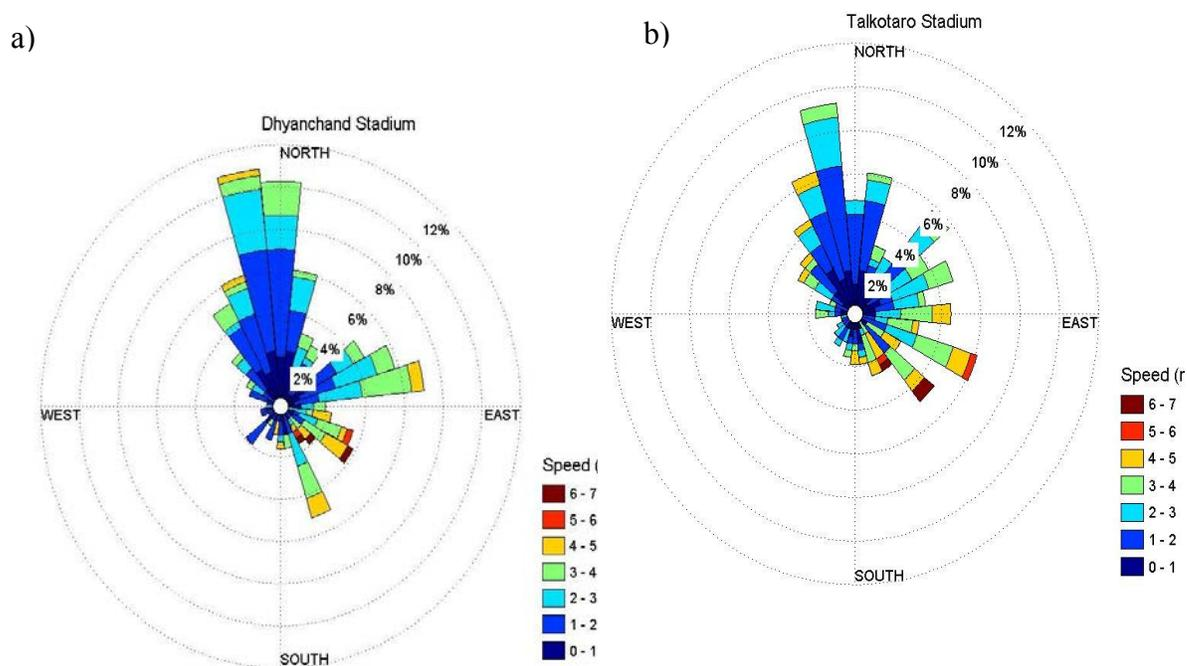


Figure 2.4 Wind rose plot of hourly winds at two monitoring stations a) Dhyanchand Stadium and b) Talkotaroo Stadium from the WRF-Chem model for the entire period.

The 20-day mean temperatures at 2m above surface are shown in Figure 2.5. The predicted temperature levels when all emissions are considered range from 27°C -30°C, which is in the normal range during the post monsoon season. High temperatures are located at the center of the city and reflect the urban heat island of Delhi. The mean pbl height during afternoon and nighttime are shown in Figure 2.6. They are highest over Delhi with afternoon values >2100m and low at night (<~60m).

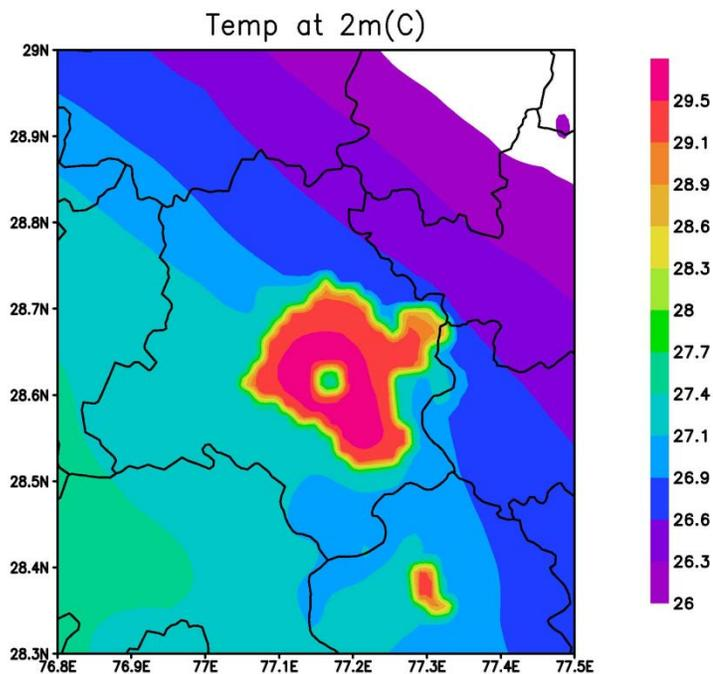


Figure 2.5 20-day mean temperature at 2m over Delhi.

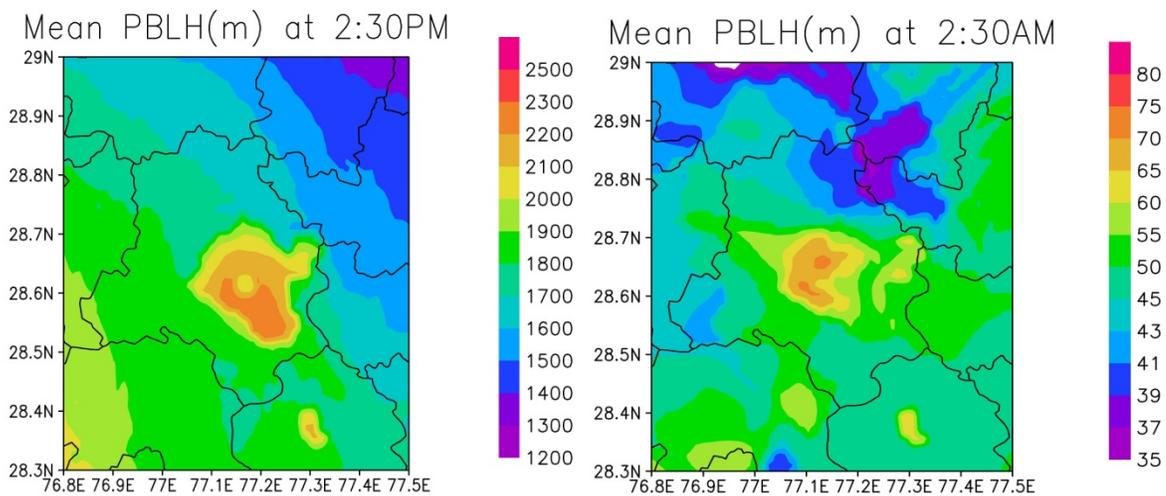


Figure 2.6 20-day mean PBLH at 2:30pm and 2:30am of the day.

The predicted meteorology is compared with surface observations at surface monitoring stations. The statistics of the comparison are shown in Table 2.1. The model has a dry bias (under predicts RH), slightly under predicts peak day time temperatures by 1-2 degrees (~5%), and is biased high in wind speed. The model captures the low wind speeds, but the observations often are less than 1 m/s, which the model estimates at 1-3 m/s.

Table 2.1 Comparison of predicted meteorological parameters with observations at the surface monitoring sites.

	<b>Temp(°C)</b>	<b>Wind speed(m sec<sup>-1</sup>)</b>	<b>RH (%)</b>
<b>Mean-Obs</b>	<b>29.0</b>	<b>1.3</b>	<b>53.5</b>
<b>Mean-Model</b>	<b>28.7</b>	<b>2.2</b>	<b>45.8</b>
<b>Bias Error</b>	<b>7.7</b>	<b>1.3</b>	<b>7.0</b>
<b>RMSE(hr avg)</b>	<b>13.6</b>	<b>2.9</b>	<b>33.9</b>
<b>R(hr avg)</b>	<b>0.9</b>	<b>0.5</b>	<b>0.7</b>

### 2.3.2 Spatial distributions of air pollutants in Delhi

The predicted period mean surface concentrations of various pollutants are shown in Figure 2.7. The primary species show similar spatial distributions with peak values in the middle of domain reflecting the traffic and population patterns in the city. Black carbon concentrations exceed 25 $\mu\text{g}/\text{m}^3$  at residential regions with the main sources being traffic and wood and charcoal burning for cooking practices. Delhi city is comprised of

mixed classes of population; therefore the fuel type used is based on economic class and this plays a vital role in BC emissions. Delhi is a densely populated city has approximately 4 million on road vehicles and the number increases at a rate of ~10 percent per year (Mohan et al., 2006). As a result of this and the large amounts of construction and industrial activity  $PM_{2.5}$  and  $PM_{10}$  levels are very high, 220-350  $\mu g/m^3$  and 350-550  $\mu g/m^3$ , respectively, over the city and exceed the National Ambient Air Quality standards. Ozone levels are also elevated in the city resulting from the growing transport emissions. The day time 20-day mean values show peak ozone levels are as high as 100 ppbv.

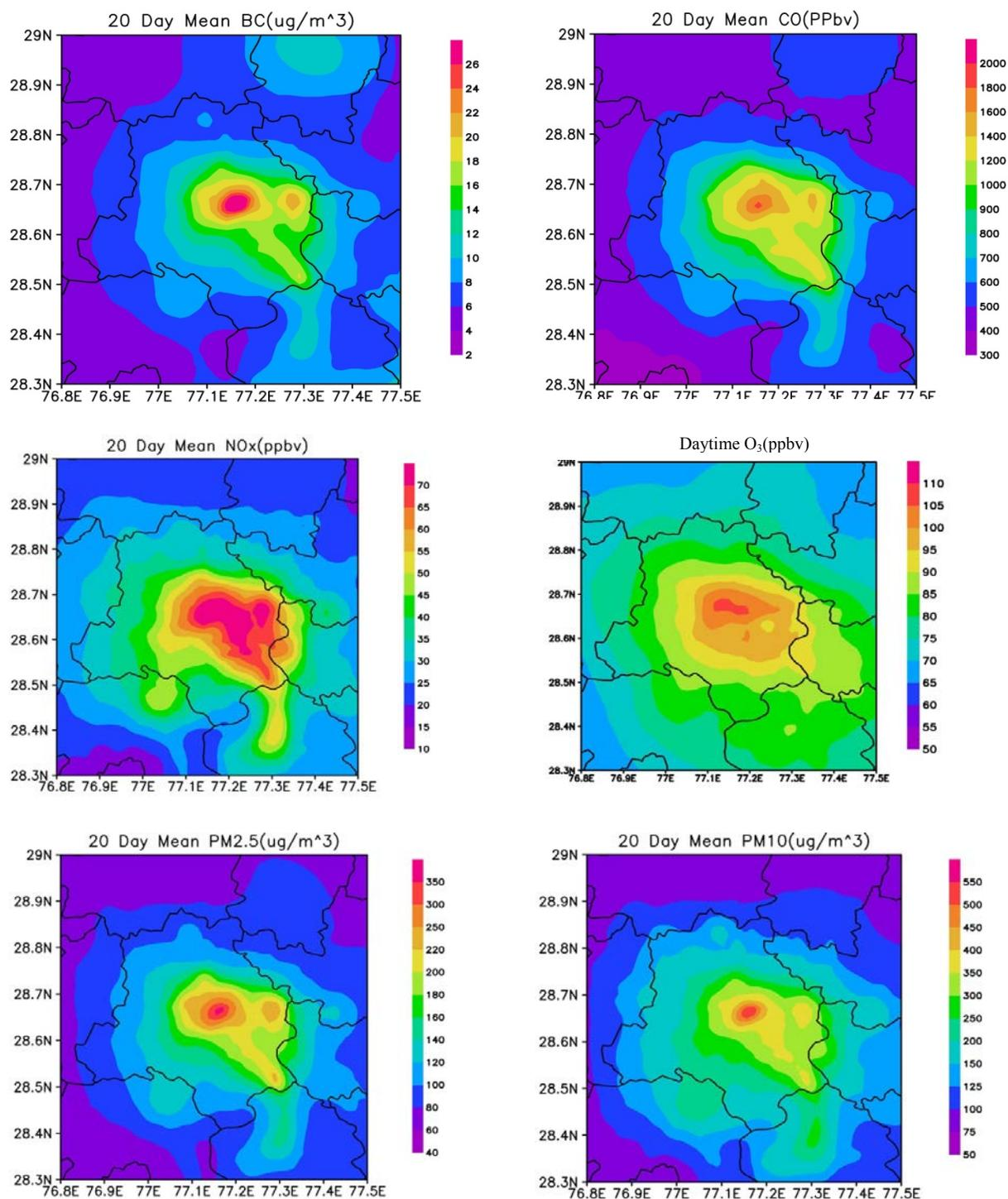


Figure 2.7 Spatial distributions of calculated 20 Day mean concentrations of criteria pollutants over Delhi. For ozone daytime means (9:30am – 6:30pm) are shown.

### 2.3.3 Comparison of Observed and Modeled Concentrations

Concentrations from all the stations were combined and their distributions are compared with the predicted distributions for each species in

. In general the aerosol quantities BC, PM<sub>2.5</sub> and PM<sub>10</sub> are pretty well predicted, showing similar variability across the monitoring sites and similar frequency distributions. All three show a high bias, with the largest for PM<sub>2.5</sub> and PM<sub>10</sub>. CO predictions have a negative bias. For the base emissions case NO<sub>x</sub> values were significantly over-predicted and the ozone distribution was very different than the observations as shown in Figure 2.8a. We also performed a sensitivity simulation where the NO<sub>x</sub> emissions were reduced to 1/3 of their original values. Those results are shown in Figure 2.8b. The NO<sub>x</sub> predictions are closer to the observations and the ozone distribution more closely fits the observed distribution, but now with a high bias. The emissions evaluation will be discussed in more detail in section 2.3.5. Statistics for the comparisons are presented in Table 2.2. The model performance was evaluated by comparison with observations. Analysis of all species at the individual sites was presented in Appendix Table A1 and Table A2

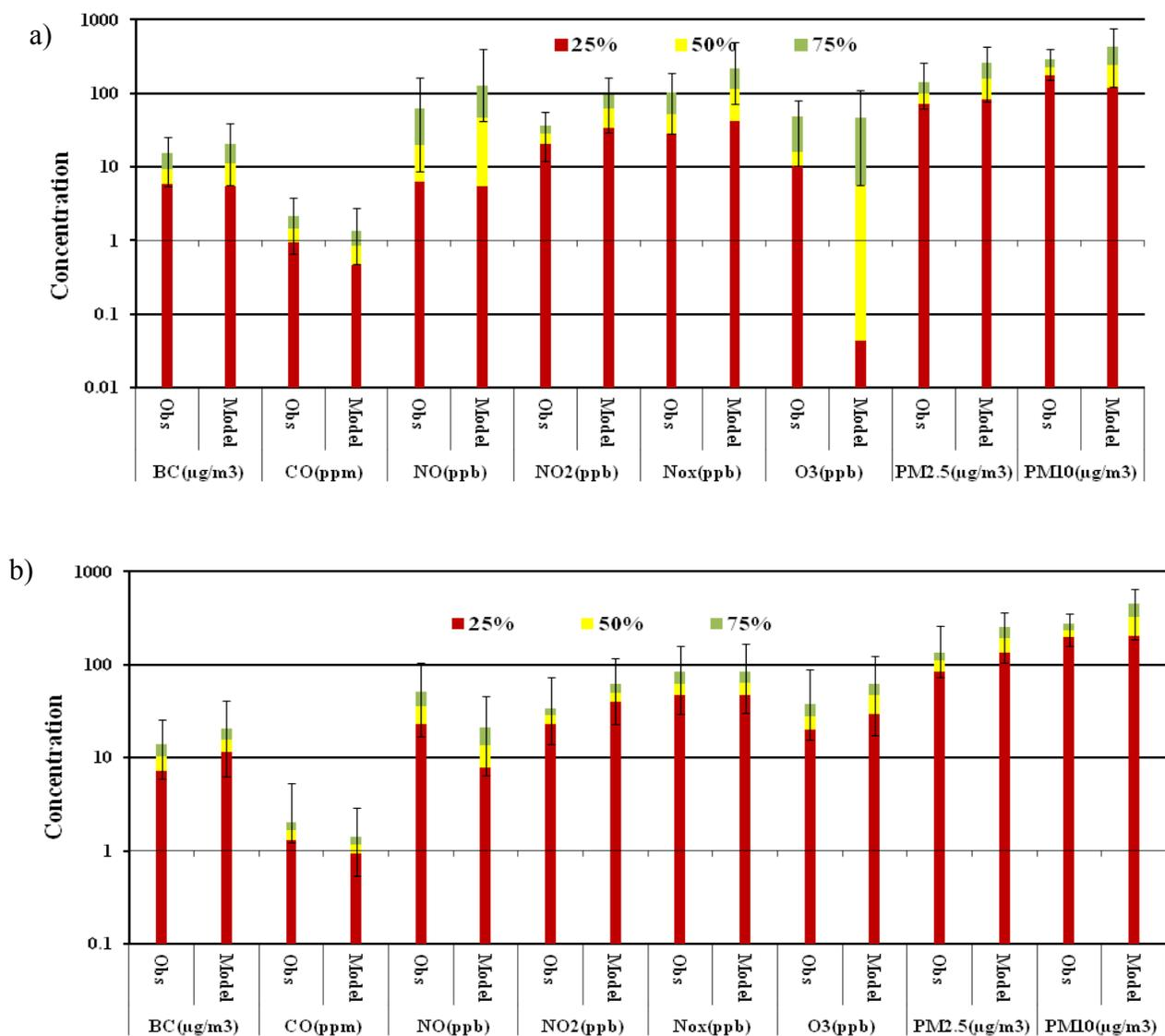


Figure 2.8 Comparison of the distributions of observed and modeled hourly concentrations using data from all sites with lower (25%), median (50%) and upper quartile (75%).

The all data mean value and the minimum and maximum mean values from individual monitoring sites are shown. Red column represents the lower quartile, yellow the median 50% of the data, and green the upper quartile of the data set with minimum

and maximum error bars. The upper panel is for calculations using the emissions shown in Table 1.2 while the lower panel shows results where the NO<sub>x</sub> emissions were reduced by a factor of 3. Some activity data needed to be collected by involving various voluntary or independent service organizations who could practically count the number of various vehicular types passing through different sensitive areas /road /junctions. The second component was to construct the finely gridded emission inventory 1.67\*1.67 km<sup>2</sup> resolution using the above activity data and available emission factors using the GIS based statistical model developed at IITM, Pune.

Table 2.2 Comparison of 20-day mean observed and predicted concentrations of various species at all monitoring sites with NO<sub>x</sub> reduction to one third of its emissions.

<b>NO<sub>x</sub>-Full</b>	<b>BC (µg/m<sup>3</sup>)</b>	<b>CO (ppmv)</b>	<b>NO<sub>x</sub> (ppbv)</b>	<b>O<sub>3</sub> (ppbv)</b>	<b>O<sub>3</sub>- DayTime(ppbv)</b>	<b>PM<sub>2.5</sub> (µg/m<sup>3</sup>)</b>	<b>PM<sub>10</sub> (µg/m<sup>3</sup>)</b>
<b>Mean-obs</b>	<b>9.5</b>	<b>1.7</b>	<b>67.8</b>	<b>30.1</b>	<b>54.5</b>	<b>110.8</b>	<b>237.6</b>
<b>Mean- model</b>	<b>13.8</b>	<b>1.0</b>	<b>150.3</b>	<b>26.3</b>	<b>60.4</b>	<b>181.5</b>	<b>294.3</b>
<b>Bias</b>	<b>10.1</b>	<b>-0.5</b>	<b>91.3</b>	<b>0.3</b>	<b>12.5</b>	<b>83.6</b>	<b>83.5</b>
<b>RMSE(hr avg)</b>	<b>15.7</b>	<b>1.4</b>	<b>170.3</b>	<b>29.2</b>	<b>40.6</b>	<b>162.8</b>	<b>259.5</b>
<b>R(hr avg)</b>	<b>0.6</b>	<b>0.4</b>	<b>0.4</b>	<b>0.7</b>	<b>0.4</b>	<b>0.4</b>	<b>0.4</b>

Table 2.3 Comparison of 20-day mean observed and predicted concentrations of various species at all monitoring sites NO<sub>x</sub> reduced by factor of 3.

<b>NO<sub>x</sub>-one third</b>	<b>BC (µg/m<sup>3</sup>)</b>	<b>CO (ppmv)</b>	<b>NO<sub>x</sub> (ppbv)</b>	<b>O<sub>3</sub> (ppbv)</b>	<b>O<sub>3</sub>-DayTime(ppbv)</b>	<b>PM<sub>2.5</sub> (µg/m<sup>3</sup>)</b>	<b>PM<sub>10</sub> (µg/m<sup>3</sup>)</b>
<b>Mean-obs</b>	<b>9.5</b>	<b>1.7</b>	<b>67.8</b>	<b>30.2</b>	<b>54.5</b>	<b>110.9</b>	<b>237.6</b>
<b>Mean-model</b>	<b>16.9</b>	<b>1.2</b>	<b>64.1</b>	<b>49.1</b>	<b>38.3</b>	<b>193.2</b>	<b>330.1</b>
<b>Bias</b>	<b>7.5</b>	<b>-0.6</b>	<b>-3.7</b>	<b>18.9</b>	<b>-9.7</b>	<b>82.4</b>	<b>92.5</b>
<b>RMSE(hr avg)</b>	<b>13.3</b>	<b>1.3</b>	<b>68.3</b>	<b>43.9</b>	<b>36.9</b>	<b>157.1</b>	<b>254.4</b>
<b>R(hr avg)</b>	<b>0.3</b>	<b>0.4</b>	<b>0.4</b>	<b>0.7</b>	<b>0.1</b>	<b>0.4</b>	<b>0.4</b>

Further insights into the pollutant distributions in Delhi are found by analyzing the time series. The 20 day average diurnal cycle of BC observed at Dhyanchand Stadium is shown in Figure 2. 9 along with the diurnal emission used in the model and the predicted PBL height. The BC observations show a strong diurnal cycle, with minimum in the mid-afternoon when the PBL is the highest and maximum in late evening when the PBL height is at a minimum and emissions are at their highest. The evening and early morning features reflect the cooking and traffic patterns and the trapping of these surface emissions by the shallow mixing layer. These diurnal features are well captured by the model, which suggests that the diurnal pattern used in the emissions accurately capture these activities. The daytime values are accurately captured, while the night time values are biased high. This suggests that the daytime PBL is reasonably well predicted, but the nighttime values may be too low. The diurnal profiles of PM<sub>2.5</sub> and PM<sub>10</sub> show similar diurnal variations as BC, with minima during mid-afternoon and peak values at night, but with less asymmetry between mid-night and 6 am values, reflecting their stronger dependency on traffic patterns.

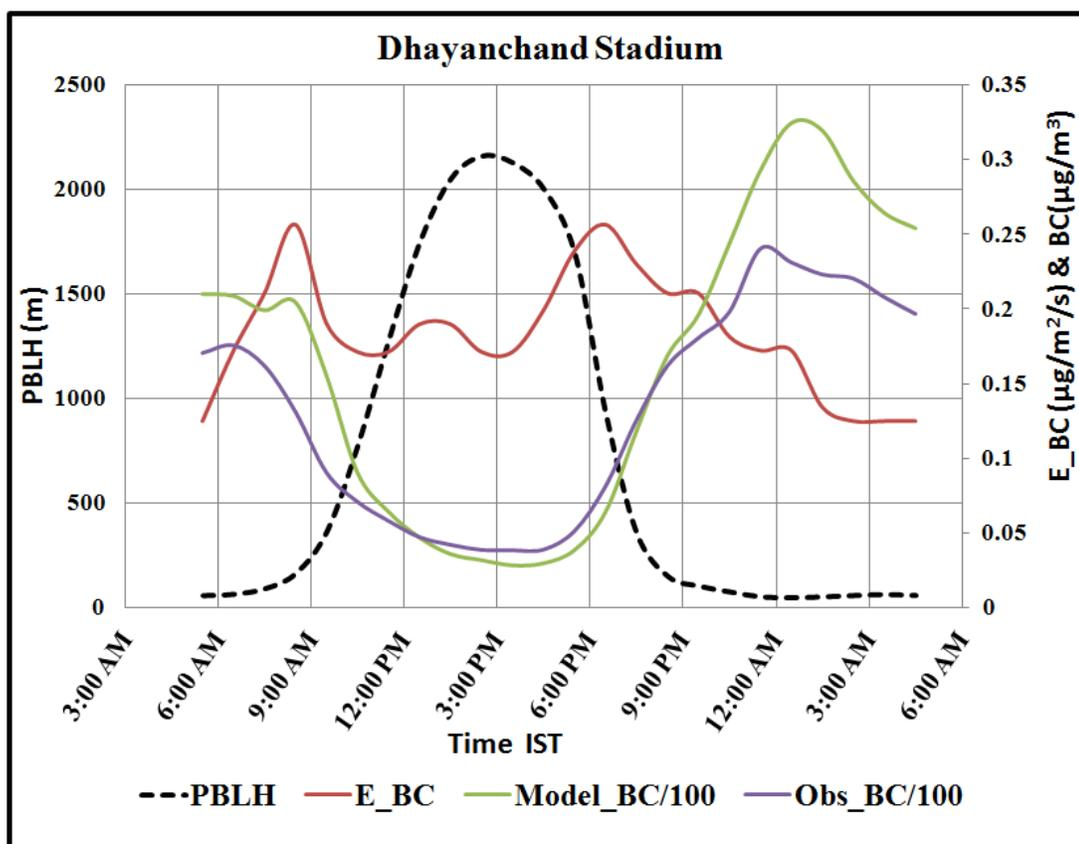


Figure 2. 9 Mean diurnal variation in boundary layer height, emissions and BC concentrations from model and observations at the Dhayanchand Stadium site.

The predicted mean composition of  $PM_{2.5}$  at Dhayanchand stadium is shown in Figure 2.10. (There is very slight variability in the percent contribution at the different monitoring stations.) BC accounts for about 8% of the fine mode mass and is greater than that for sulfate. OC accounts for ~30% and other primary PM accounts for the largest fraction. Nitrate contribution exceeds that of sulfate.

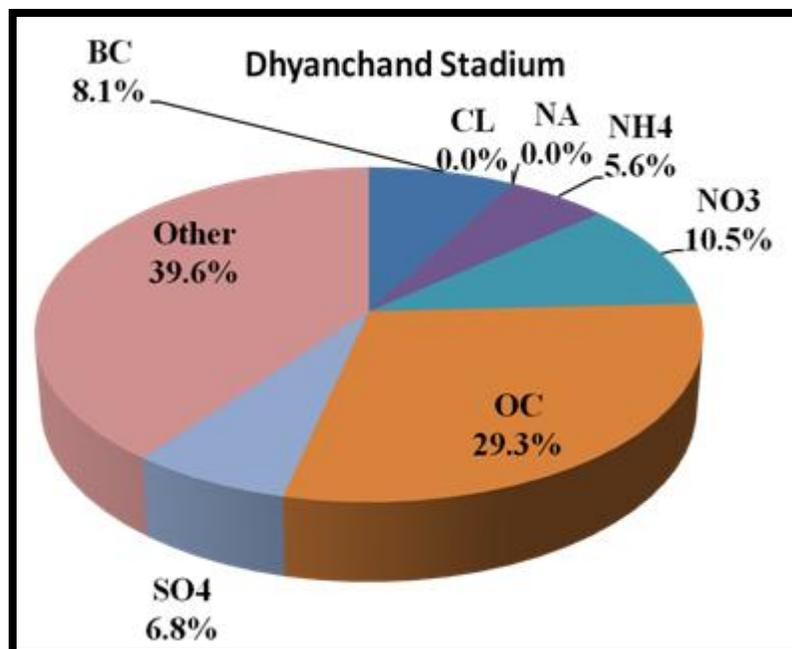


Figure 2.10 Percent contribution of each species to total PM<sub>2.5</sub> at Dhyanchand Stadium.

### 2.3.4 Sector Contribution

The goal of this study is to identify the emission sources making the largest contribution to the pollution levels. Therefore, detailed studies are needed to understand the contribution of each source sector to total pollution levels in Delhi. In order to facilitate this study the emissions from Delhi emission Inventory were categorized into four sectors and used as input into the WRF-Chem model. The model was run for four different cases for the analyses of the sectors. An initial run was carried out to calculate the total pollution from all sources i.e. anthropogenic, biogenic and biomass burning. Then individual runs are carried out to estimate the concentrations from each sector. The

equation below explains the process for how the transportation sector results were determined.

$$\text{Anthropogenic (A)} = \text{Transportation (T)} + \text{Power (P)} + \text{Industry (I)} + \text{Domestic (D)} \quad (1)$$

$$\text{Initial run} = \text{I (A + Biogenic + Biomass Burning + Boundary)} \quad (2)$$

$$\text{Individual run} = \text{S (A - T + Biogenic + Biomass Burning + Boundary) (Transportation)} \quad (3)$$

$$\text{Sector contribution} = \text{I - S, concentrations from transportation sector emissions only} \quad (4)$$

(Transportation)

This process is repeated for all three sectors. In doing so the source sector contribution are estimated.

Figure 2.11 show the spatial distribution of the % contribution to surface concentrations from the Transportation, Power, Industry and Residential sectors for BC, PM<sub>2.5</sub> and O<sub>3</sub>. The sector contributions are similar for CO, NO<sub>x</sub> and PM<sub>10</sub>. In general the largest contributions are from transport and domestic sectors. The area affected by transport is larger, but the peak contributions are larger for domestic sector. The contributions from industry are also significant and are highest in the center of the domain and are responsible for the highest peak values. For the secondary pollutant ozone there is non-linear correlation between the precursor emissions and O<sub>3</sub> concentrations where decreasing one of the precursors somewhere may cause an increase in O<sub>3</sub> concentrations elsewhere and vice versa. There are uncertainties associated with the sector contribution calculations. Elimination of one sector at a time may not affect non-reactive species calculations but for the non-linear reactions such as ozone, this can create some problem because of OH and HO<sub>2</sub> variations.

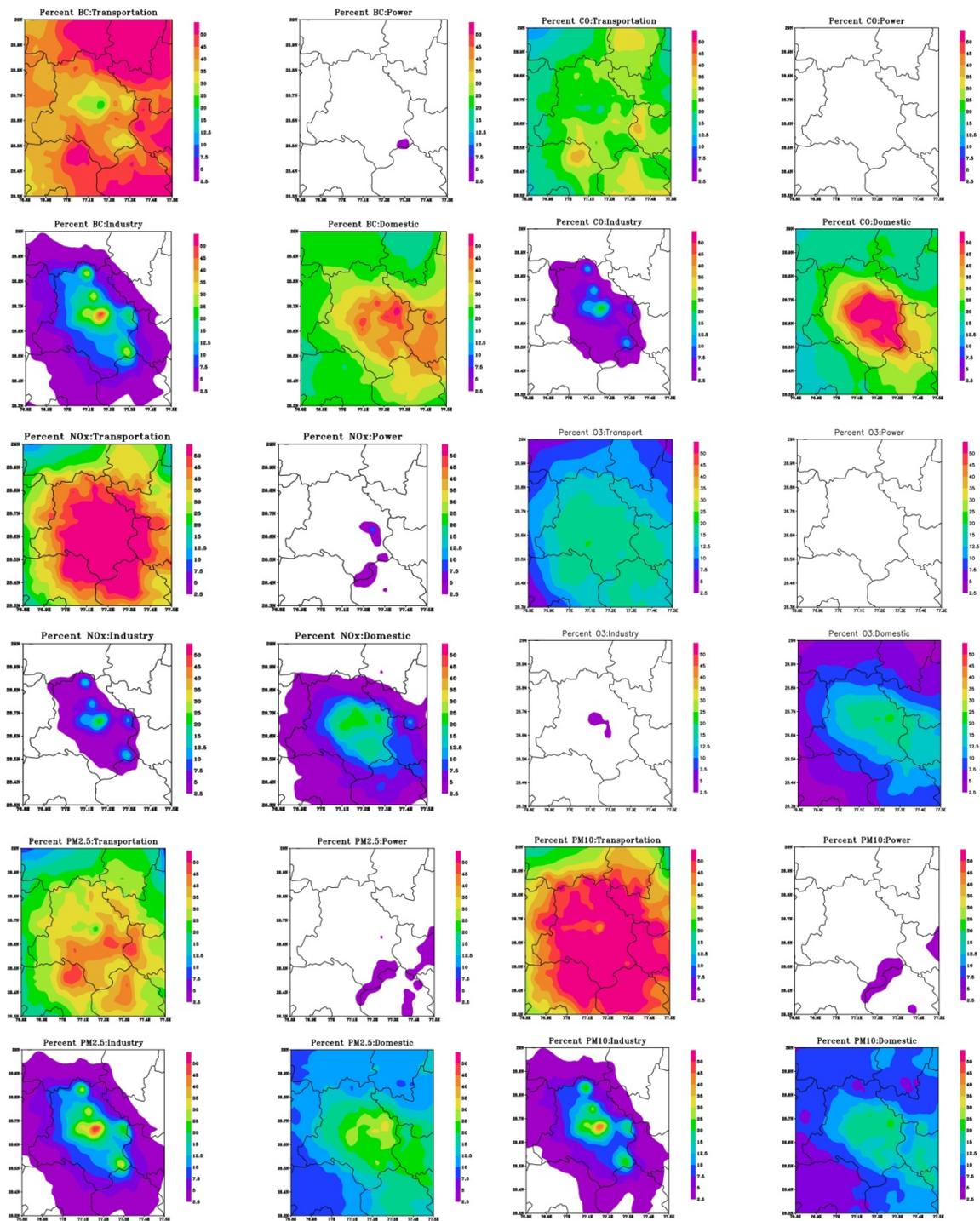


Figure 2.11 Spatial distributions of pollutants from various sectors to period mean surface concentrations.

Further insights into the sector contributions are found by looking at their diurnal variations. Figure 2.12 show the 20-day average diurnal variation of the sectoral contributions to various criteria pollutants at the monitoring station Dhyanchand stadium. The contributions are shown in terms of percentages. In the case of BC residential and transportation sectors are important at all times, but with maximum values in the late evening and early mornings. During the daytime as the mixing layer grows, it entrains air masses from higher altitudes as shown by the black shading, which represents other contributions (not accounted for from these four sectors). These other contributions are from emissions that are outside of the inner most grids, which are transported into this region through the boundaries.  $PM_{2.5}$  and  $PM_{10}$  sector plots are similar to BC, with  $PM_{2.5}$  showing a larger contribution from the residential sector than  $PM_{10}$ , and  $PM_{10}$  showing a larger contribution from transport. CO shows a similar diurnal variation, but with a larger contribution from the domestic sector and much larger daytime contribution from distant sources, which is expected due to the much longer lifetime of CO in the atmosphere with respect to BC. In the case of  $NO_x$ , the transport sector dominates; except for the daytime periods, where other sources become important. During the daytime the power sector also contributes to surface concentrations as the growing mixed layer entrains the  $NO_x$  emissions from nearby power plants. During the nighttime the power plant plumes are above the mixed layer and are decoupled from the surface. Ozone has the largest contributions from outside. The contributions of outside the domain sources to the mean surface concentrations are shown in Figure 2.13. Within Delhi the outside sources are important and contribute from 20 to 50% depending on species. This has important implications for control strategies and indicates the need for regional perspectives.

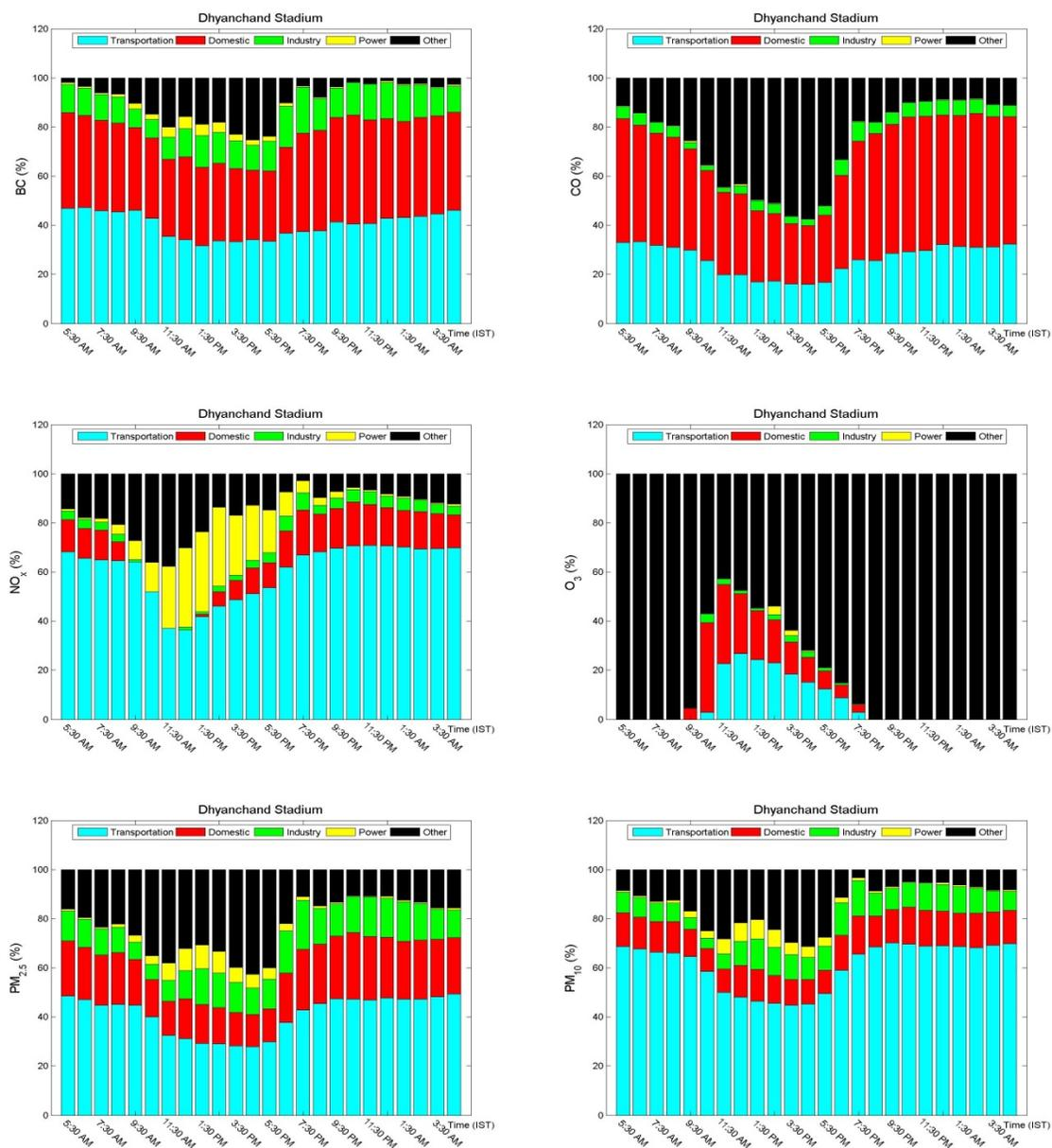


Figure 2.12 Diurnal variation in the sector contribution (in %) to period mean surface concentrations of different pollutants at the Dhyan chand monitoring station.

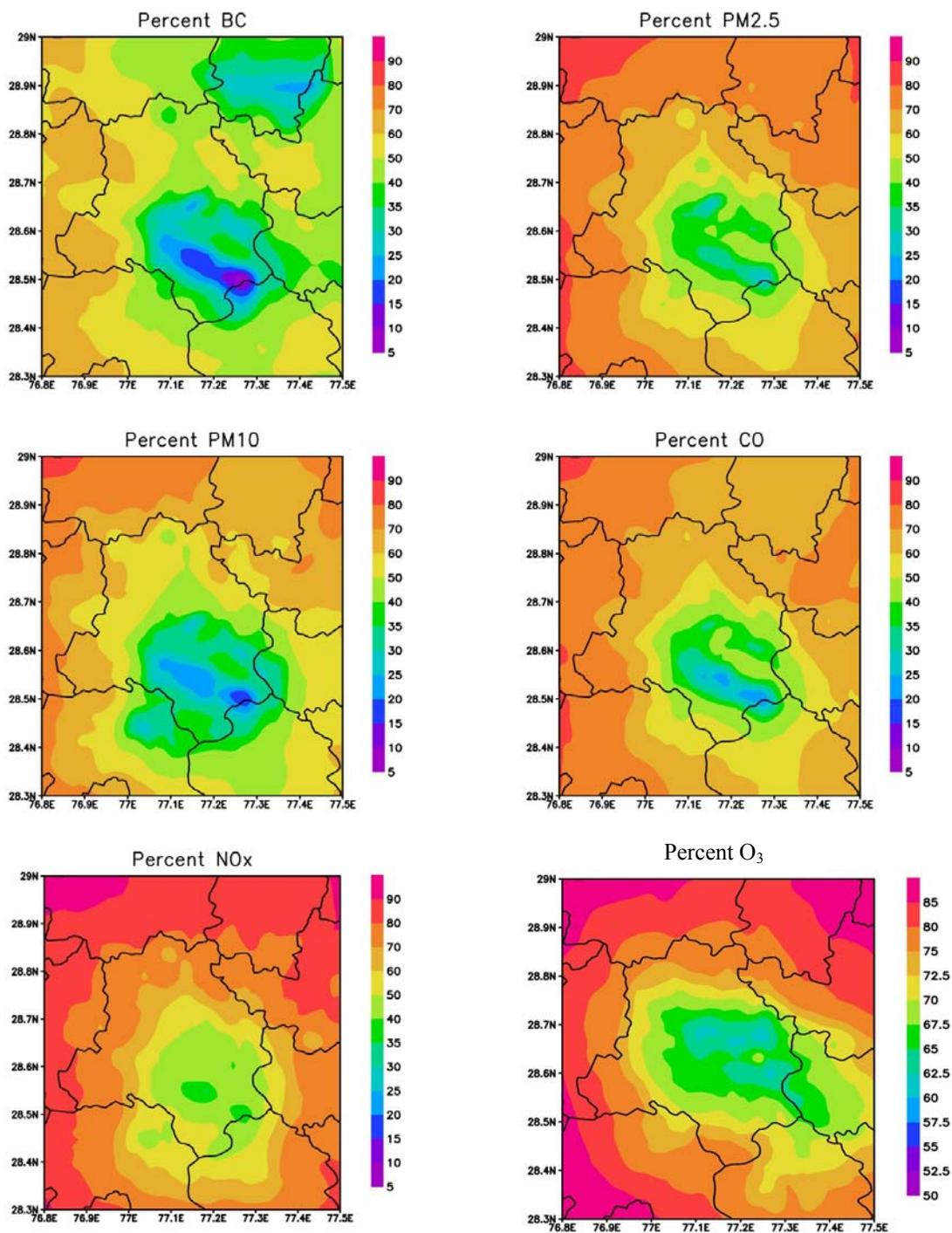


Figure 2.13 20-day mean contributions of pollutants from outside source.

### 2.3.5 Evaluation of Emissions

The comparisons of the observations and predictions for each species were discussed earlier in association with

. Comparison of correlations between different species can provide further insights into the emissions inventory. Illustrative results are shown in Figure 2.14, where various combinations of regressions for the all station observations combined are presented. The observations show good correlations between BC and CO, NO<sub>x</sub> and CO, PM<sub>10</sub> and BC, and PM<sub>2.5</sub> and PM<sub>10</sub>. Also shown are the same correlations based on the modeled surface concentrations. The model values also show strong correlation, with higher correlation coefficients than the observations. The PM<sub>2.5</sub> to PM<sub>10</sub> and the PM<sub>2.5</sub> to BC slopes are similar for the observations and the model values. However absolute concentrations are over predicted. This suggests that the emissions are overestimated. In contrast the NO<sub>x</sub> to CO modeled slope is too high, while the concentrations of NO<sub>x</sub> and CO are over and under predicted, respectively. This suggest that the NO<sub>x</sub> emissions are too high and the CO emissions too low. Assuming that the observations at these sites are representative and that all the errors are associated with the emissions then to make the modeled concentrations and slopes consistent with the observed values the emissions need to be scaled by the following: 0.6 for NO<sub>x</sub>, 2 for CO and 0.7 for BC, PM<sub>2.5</sub> and PM<sub>10</sub>.

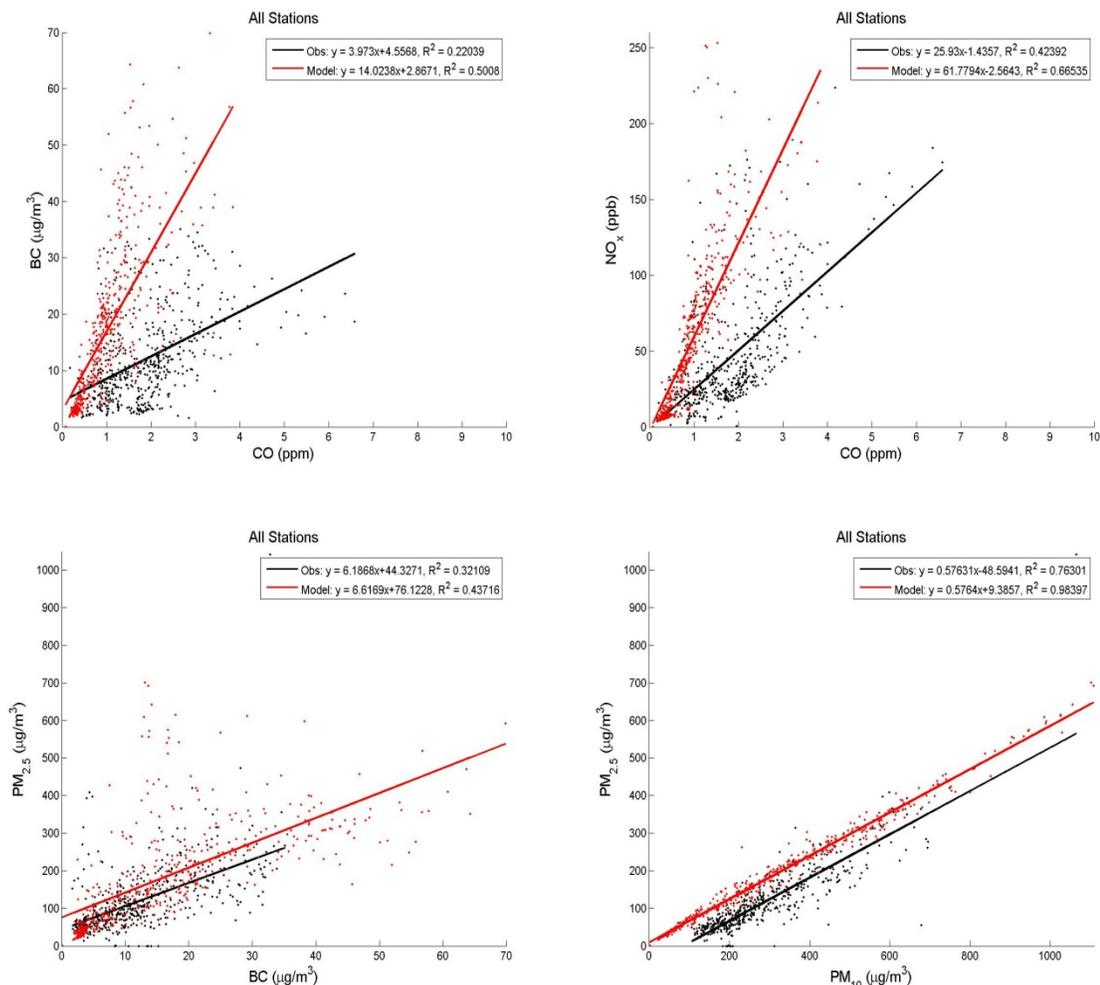


Figure 2.14 Comparison of correlations between different species for all the sites combined based on observations and modeled concentrations.

### 2.3.6 Importance of Feedbacks

**Feedbacks:** WRF-Chem has two different options to work, i.e. with aerosol feedbacks and no feedbacks. Aerosol feedbacks included are the direct aerosol feedbacks and indirect cloud aerosol feedbacks. For direct feedbacks absorption or scattering by aerosols are feed back into the meteorology. The calculated aerosol concentrations are

feed to fast-j photolysis module that calculates radiative forcing that influence the weather. The indirect cloud aerosol feedbacks analysis uses the Lin et.al microphysics scheme. In this process, the calculated aerosol amounts are treated as cloud condensation nuclei, which are used in the cumulus schemes. To evaluate the importance of the feedbacks we performed a series of sensitivity calculations, where the model was run for the 20-day period with and without feedbacks. Since the focus of this project is to look at behavior within Delhi, we analyze in detail the 1.67km domain results. Figure 2.15 show the net change in concentrations levels from with and without feedbacks. The concentrations of primary aerosols in general are lower when feedbacks are included. In contrast CO concentrations are generally higher. The changes in concentrations and spatial distributions are caused by the changes in wind speed, direction and pbl heights as shown in Figure 2.16 to Figure 2.19.

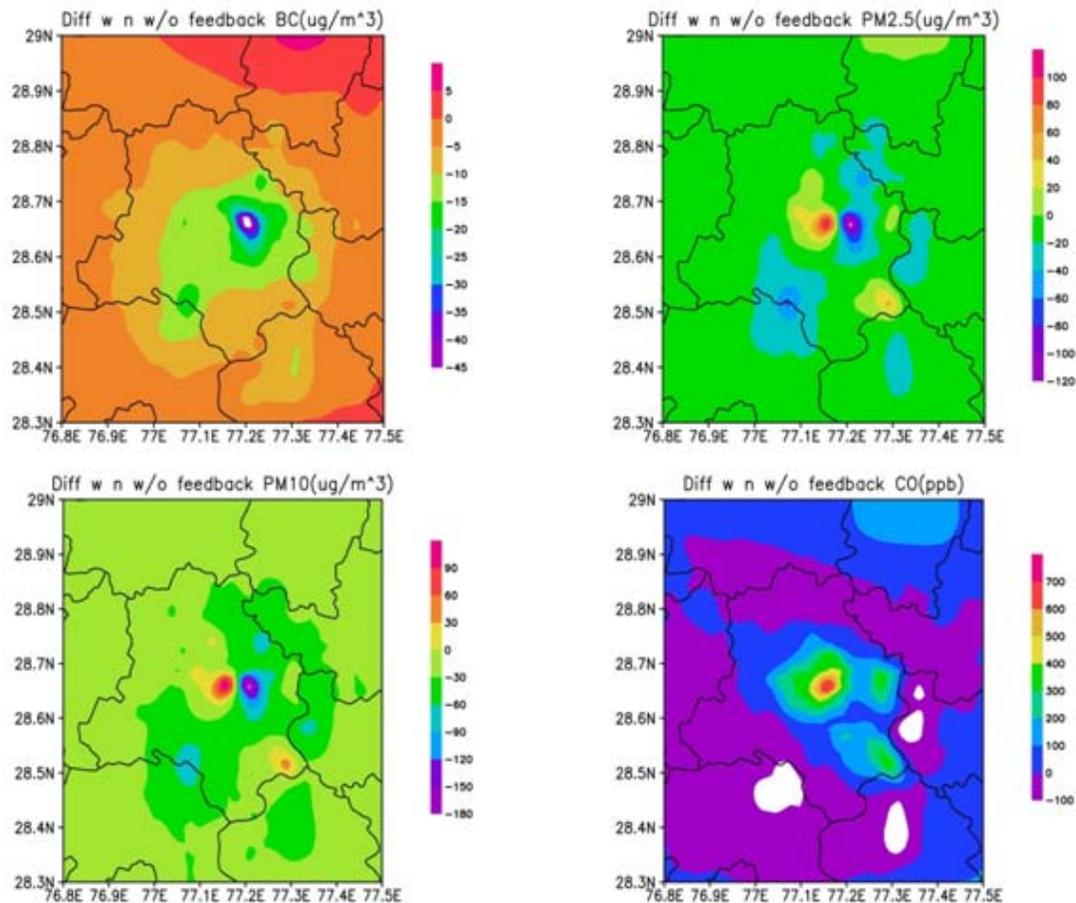


Figure 2.15 Spatial distribution of BC, CO, PM<sub>2.5</sub> and PM<sub>10</sub> over Delhi difference between with and without feedbacks.

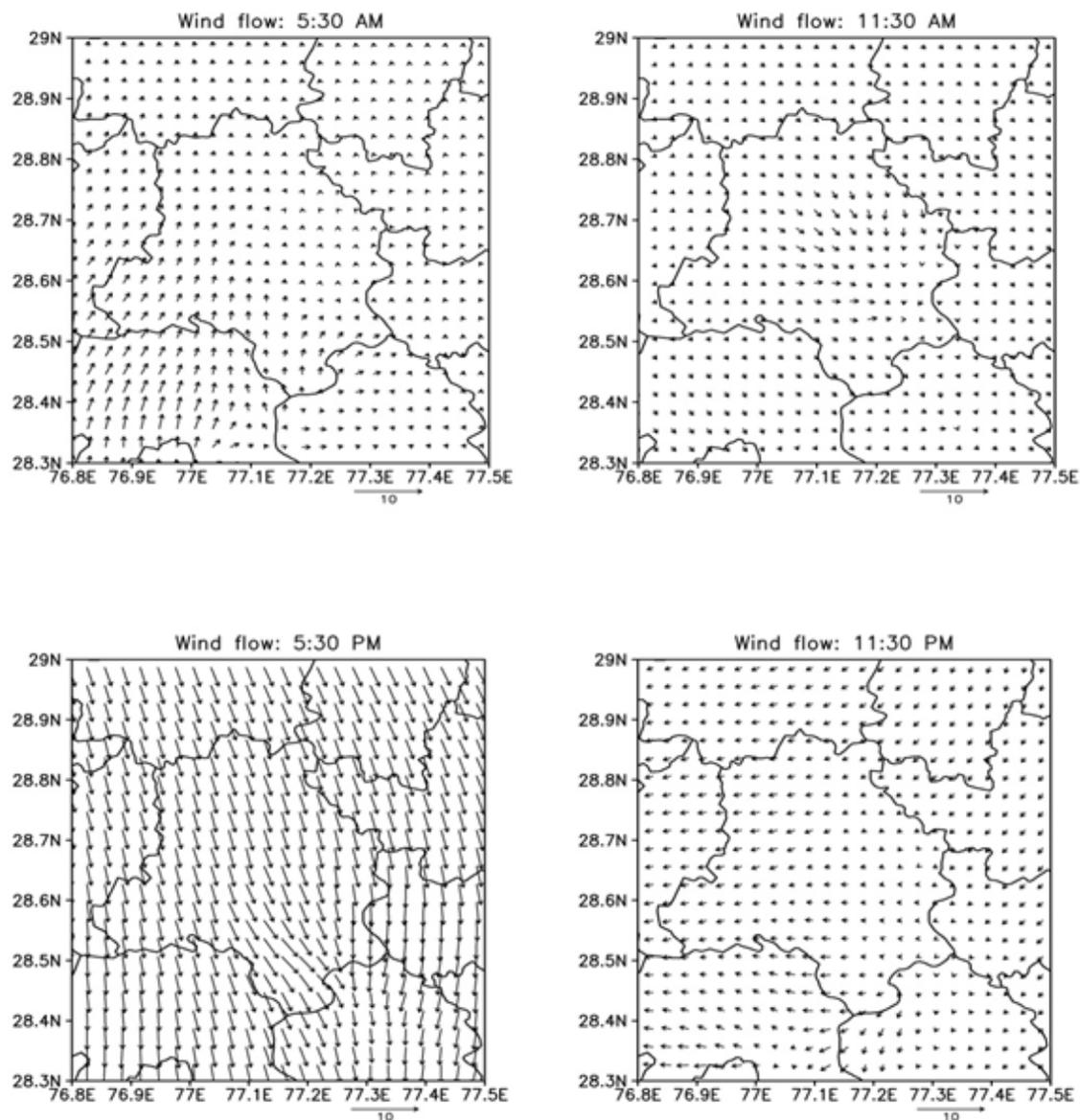


Figure 2.16 Wind profiles over Delhi domain without feedbacks effect at four different time steps of a day.

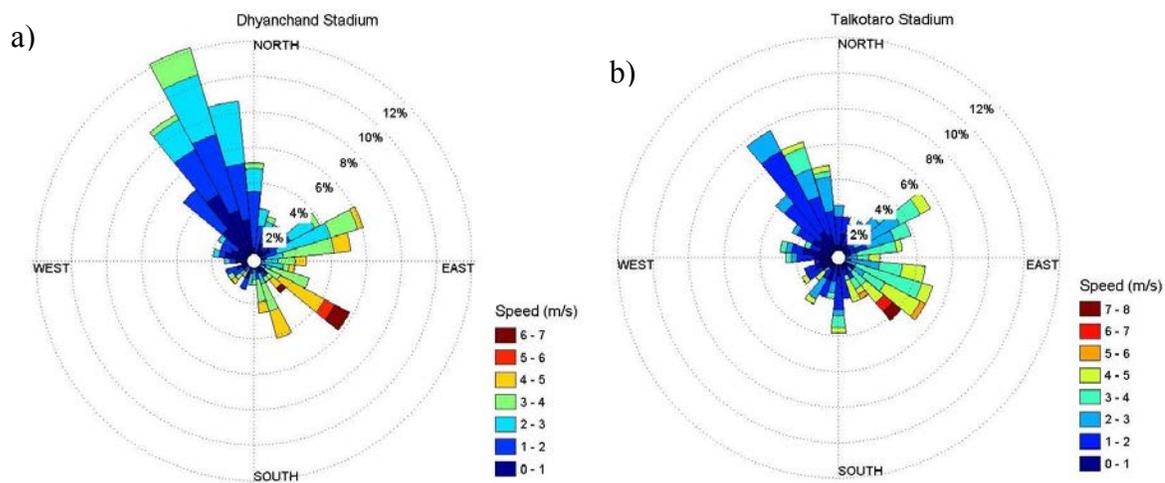


Figure 2.17 Wind rose plot of hourly winds at two monitoring stations a) Dhyanchand Stadium and b) Talkotaro Stadium from the WRF-Chem model for the entire period without feedbacks.

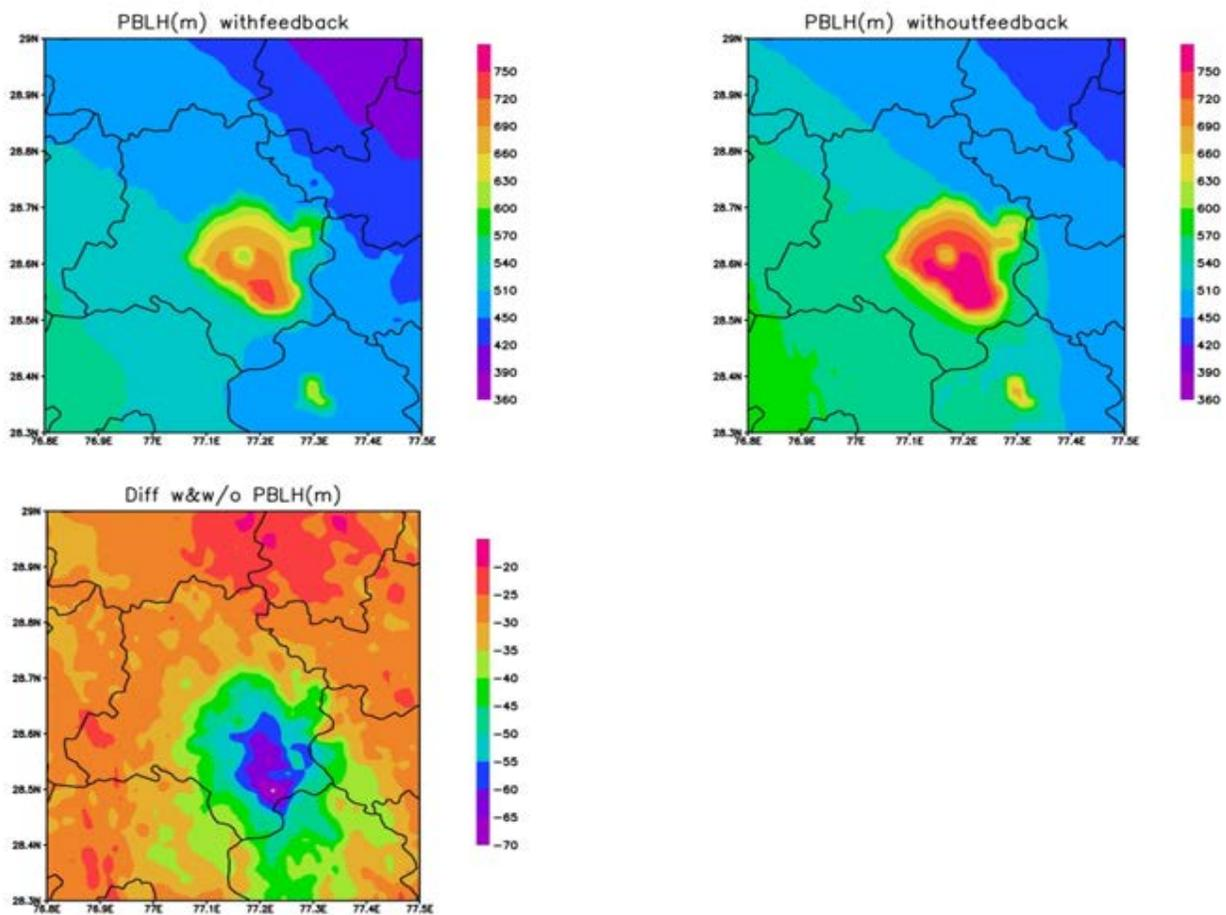


Figure 2.18 Change in PBL height due to the aerosol feedbacks and without feedbacks over Delhi.

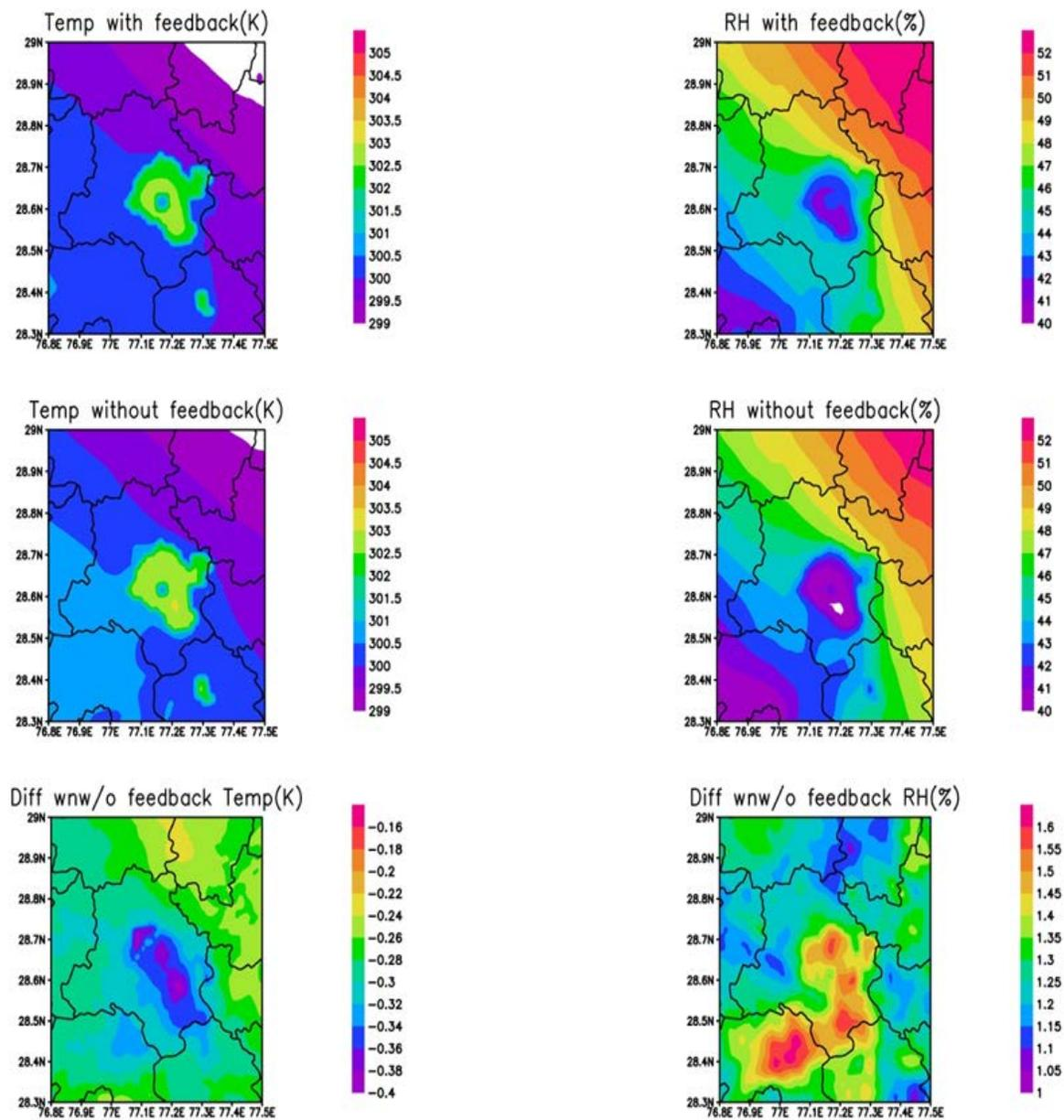


Figure 2.19 Effect of feedbacks and without feedbacks from aerosol on Temperature at 2m from surface, Relative humidity and their net change.

## 2.4 Summary

WRF-Chem system was successfully set up and evaluated for Delhi during the Commonwealth Games period (26<sup>th</sup> Sept to 15<sup>th</sup> Oct, 2010). The predicted concentrations of criteria pollutants and BC had similar distributions and diurnal profiles as the observations, with most exceeding current National Ambient Air Quality Standards. Temporal variability showed that the daytime values are accurately captured, while the night time values are biased high because the daytime PBL is reasonably well predicted, but the nighttime values may be too low. Spatial distributions showed large concentrations in central regions reflecting heavy traffic and high population density. Attributing the over prediction of concentration levels purely to emissions, in order to match the magnitudes and slopes of the observations it was found that emissions estimates would need to be scaled by 0.6 for NO<sub>x</sub>, 2 for CO and 0.7 for BC, PM<sub>2.5</sub> and PM<sub>10</sub>. NO<sub>x</sub> sensitivity studies showed using a lower estimate of the NO<sub>x</sub> emissions yielded ozone predictions closer to the observations.

Sector based studies showed that the transport and domestic sectors were the major contributors to pollution levels in Delhi. Industrial emissions were also large, and the power sector was important for NO<sub>x</sub> and SO<sub>2</sub>. Delhi air quality was found to also be impacted by emissions from outside of Delhi. The contributions from distant sources ranged from 20 – 50% depending on the species. These results have important implications for air quality management, and indicate that regional perspectives to emission reductions are warranted. Finally, the influence of the air pollutants on meteorology was investigated by comparing results from simulations that included

feedbacks with those that did not. The feedbacks impacted boundary heights, temperature and winds, which in turn impacted the pollution concentrations.

## CHAPTER 3 FUTURE EMISSION SCENARIO USING THE GREENHOUSE GAS AND AIR POLLUTION INTERACTIONS AND SYNERGIES (GAINS) MODEL

### 3.1 Introduction

Managing future air pollution levels is a challenge for thriving industrial economy of modern India. Current and future economic growth in India may defeat ongoing efforts to improve air quality through controls of particulate matter emissions from large stationary sources and nitrogen oxide (NO<sub>x</sub>) emissions from vehicles. In a scenario of rapid urbanization, it is expected that between 2005 and 2030, the increase in emissions from point sources and large stationary sources will rise drastically, with SO<sub>2</sub> emissions increasing 5 times and NO<sub>x</sub> multiplying 3 times under business as usual conditions. Increased efforts will be necessary over the coming decades to deal with the continued growth in energy demand.

Advanced emission control technologies are available to help maintain or improve air quality despite the pressure from growing economic activities. Full application of advanced technical end-of-pipe emission control measures in India (e.g., flue gas desulfurization or catalysts for power plants) could lead to a substantial improvement in air quality. A preliminary analysis using the GAINS –Asia computational model estimates that the application of advanced emission control technology to all large sources in India would reduce negative health impacts by half in 2030 (GAINS Report, 2010). But the report also notes that such an undifferentiated application of the controls to all sectors would compound the already existing economic issues, and cost an

additional 0.80% of GDP. Instead of the conventional all-encompassing control-strategy, a cost-effective approach can reduce costs for air pollution control by/in 2030 by up to 50%.

The cost-conscious **Greenhouse Gas and Air Pollution Interactions and Synergies (GAINS)**-Model can identify cost-effective portfolios of emission control measures that achieve improvements in environmental impacts. The GAINS optimization tool selectively allocates specific reduction measures across economic sectors, pollutants and regions, thus reducing air pollution control costs. Such an analysis is very helpful for a developing country such as India. Another advantage of the GAINS model is that it includes controls focused on both indoor and outdoor air pollution, a crucial facet for a village-intensive economy like India where a significant fraction of the population depends on solid fuels for everyday use. Integral elements of air pollution control strategies are the measures directed at eliminating indoor pollution from the combustion of solid fuels. The GAINS model also helps to identify strategies to reduce ozone precursor emissions which would also reduce crop losses, which helps to foster a healthy environment for the generations to come.

The GAINS model also targets the core problem of greenhouse-gas emissions in an economically viable manner. GAINS provide a comprehensive and affordable solution to this foundational problem, building a clean environment and ensuring the health of millions. Besides targeting the greenhouse gas emissions, the GAINS model also adopts certain low carbon measures which reduce air pollution at reasonable costs. GAINS scenarios demonstrate that a strategy employing certain climate-friendly measures, e.g., energy efficiency improvements, fuel substitution, co-generation of heat and power,

integrated coal gasification combined cycle (IGCC) plants, etc., would reduce air pollution at lower costs than a conventional approach that relies on technical end-of-pipe emission control measures. At the same time it would also ensure the lowering of greenhouse gas emissions (GAINS Report, 2010).

This state-of-the-art interdisciplinary model is built on a scientific tool that has already helped European governments reduce air pollution across the continent without compromising economic development (Hordijk and Amann, 2007). The above examination of the various advantages offered by the GAINS model suggests that it would be useful in helping to target air pollution controls in India.

This study employs IIASA's **Greenhouse Gas and Air Pollution Interactions and Synergies (GAINS)**-Model to provide a consistent framework of emission reduction strategies targeted towards air pollution and greenhouse gas co-benefits. To accomplish this goal a scenarios driven by the GAINS model was interfaced with the WRF-Chem simulations. In this chapter we work with the GAINS group to develop a base scenario for Delhi for the year 2030 and a method to interface this scenario with the WRF-Chem model. Results comparing changes in criteria pollutant levels relative to 2010 on a sector and spatial basis are presented and discussed. This work provides a basis for which additional scenarios that target new air quality and/or climate targets can be developed and analyzed using this framework.

### 3.2 Description of the Greenhouse Gas and Air Pollution Interactions and Synergies (GAINS) 2030 Scenario

A study of the Five-Year Plans prepared by the Government of India shows that the GDP is assumed to grow by 8 to 10 percent/year in the 11<sup>th</sup> Five Year plan and then at an average rate of 10 percent/year in the 12th plan in order to double per-capita income by 2016-17 (Planning Commission, 2006a). These increases result from continued population growth (from 1.1 billion people in 2005 to 1.5 billion people in 2030) together with an enhanced economic development that is expected to provide increased economic wealth to the Indian population. As pointed out in the National Energy Map for India such high economic growth will put a heavy demand on the supply of energy (TERI, 2006). Under these plans primary energy consumption is projected to increase by a factor of 3.5 between 2005 and 2030. Moreover, as the growth in the transport sector is expected to further worsen India's oil import dependency (from currently 70 percent to 90 percent in 2030), the maximum utilization of indigenously available energy resources is crucial to safeguard energy security. As shown in Table 3.1, coal is estimated to not only remain the dominant energy-source but is projected to grow by a factor of six by 2030. Other sources of renewable energy (e.g. hydropower and wind) do demonstrate similar growth rates by 2030 in India even though they begin as nominal sources in 2005.

Table 3.1 Baseline projection of fuel consumption for India (PJ/yr).

	1990	2000	2005	2010	2020	2030
Coal	3879	6776	8788	11501	21603	45096
Oil	2606	4314	5538	6843	10726	16846
Gas	593	1294	1627	3107	7153	7873
Renewable	1	9	13	34	41	105
Hydro	260	291	306	774	1258	1693
Nuclear	58	166	165	518	1619	1619
Biomass	4810	5446	6484	6987	6950	6896
Total	12207	18295	22922	29764	49351	80129

Source: GAINS Report, Nov, 2010.

The GAINS model estimates emissions driven by energy projections taking into account fuel types, technologies, and emission control technologies.

Figure 3.1 shows the frame work of the GAINS model. The raw data from different sources regions and or countries are collected and further processed by employing several urban and regional scale models. The Energy model (PRIMES), Transport model (COPERT) and Agriculture model (CAPRI) are used to scale the emissions corresponding to each sector. The modeled GAINS emissions have a single or uniform emission number over a region or province in a country. Here for the present study we used the GAINS-ASIA model baseline emissions which were based on the energy projections in Table 3.1 The baseline scenario diagnoses the possible improvement in air quality levels with emphases on greenhouse gas emissions. The two basic assumptions to fulfill the requirements of cleaner air and lower green house gas

emissions are that existing policies are stringently implemented to the fullest and no additional costs are added to the country budget.

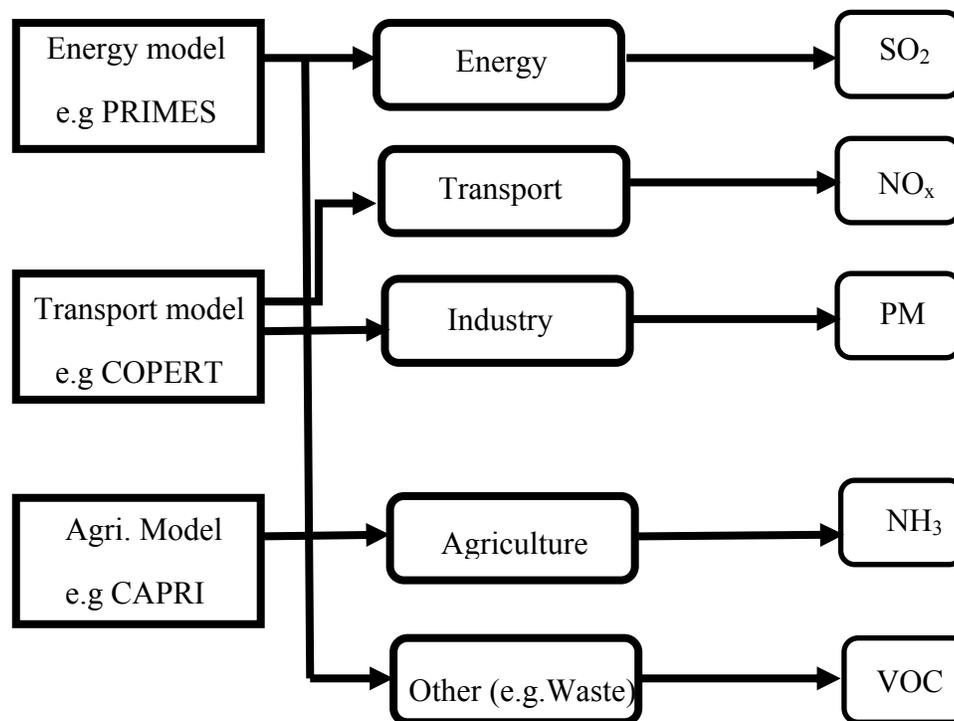


Figure 3.1 GAINS Model Framework adopted to estimate the baseline emission scenario.

The GAINS future emission scenario assumes that various advanced control technologies will be adopted by the year 2030 to reduce the greenhouse gas emissions over India in a cost effective manner. For the current study, year 2030 was adopted as the future emission scenario. Table 3.2 shows the emission control measures adopted in the baseline projection for the year 2030. Certain stringent steps will be taken in the transportation sector such as EURO-II standards are expected to be implemented on two wheeler and EURO –IV on light and heavy duty vehicles. Four wheelers such as cars use CNG fuels and it is anticipated to further expand this to buses and three wheelers in urban

areas. In the case of point sources, equipment with high removal efficiency of particulate matter is projected to be installed in power plants which are built after 2005. In the domestic sector, changes in fuel type and cooking practices are anticipated.

Table 3.2 Emission control measures assumed in the baseline projection.

Stationary Sources	Mobile Sources
<ul style="list-style-type: none"> <li>• Large combustion plants: Electrostatic precipitators (ESP) at large combustion plants to control emissions of particulate matter (TSP and PM2.5), with high removal efficiency (99%) for all plants built after 2005.  Less efficient ESP for large plants built before 2005 and all smaller plants.</li> <li>• Small combustion plants in the power sector and industry:  Cyclones or less efficient ESP for large plants built before 2005 and all smaller plants.</li> <li>• Domestic sector:  Low sulfur medium distillates: 0.25% S from 2000, 0.05% S from 2005, 10 ppm from 2015.  Slow penetration (0.4%/year) of improved cooking stoves</li> </ul>	<ul style="list-style-type: none"> <li>• Two-wheelers: Euro-II (Stage-II) controls after 2005</li> <li>• Light duty and heavy duty vehicles: Euro-1/I after 2000 Euro-2/II after 2004 Euro-3/II after 2006 Euro-4/IV after 2010</li> <li>• Low sulfur gasoline (10 ppm) from 2015</li> <li>• CNG for buses and three-wheelers in urban areas</li> </ul>

Source: GAINS Report, Nov, 2010.

Table 3.3 Emissions Comparison from Delhi 2010 to GAINS 2030.

Delhi -2010 (Kt/year)	SO <sub>2</sub>	NO <sub>x</sub>	CO	PM <sub>10</sub>	PM <sub>2_5</sub>	BC	OC	NMVOC
Industrial	45.3	3.5	39.1	5.4	10.7	1.1	4.3	18.5
Power	57.7	7.2	1.3	5.4	1.5	0.4	1.2	3.3
Residential	21.5	8.8	254.4	1.1	0.01	2.2	15.3	86.3
Transportation	8.48	28.5	106.2	57.6	22.9	1.6	1.8	106.2
<b>Total</b>	<b>132.9</b>	<b>47.9</b>	<b>400.9</b>	<b>69.4</b>	<b>35.2</b>	<b>5.2</b>	<b>22.6</b>	<b>214.3</b>
GAINS- 2030(Kt/year)	SO <sub>2</sub>	NO <sub>x</sub>	CO	PM <sub>10</sub>	PM <sub>2_5</sub>	BC	OC	NMVOC
Industrial	50.8	8.4	8.3	14.4	9.7	3.6	2.9	107.4
Power	185.6	75.3	4.9	15.3	8.9	0.0	0.0	10.9
Residential	0.2	8.5	26.9	5.6	5.6	0.5	1.8	3.2
Transportation	3.5	133.3	288.6	9.1	11.4	6.8	3.3	101.6
<b>Total</b>	<b>240.1</b>	<b>225.5</b>	<b>328.6</b>	<b>44.3</b>	<b>35.6</b>	<b>10.9</b>	<b>8.0</b>	<b>223.1</b>
<b>Times (2030/Delhi)</b>	<b>1.8</b>	<b>4.7</b>	<b>0.8</b>	<b>0.6</b>	<b>1.01</b>	<b>2.1</b>	<b>0.4</b>	<b>1.04</b>

Table 3.3 shows the emission totals from different sectors and species for 2010 and 2030. The 2030 emissions correspond to the GAINS base-line scenario where as 2010 are the Delhi emissions inventory used in the analysis as stated in Chapter2. The distribution patterns are different for all the sectors when compared to year the 2010. There is an increase in emissions for certain species such as SO<sub>2</sub>, NO<sub>x</sub> and BC by factors of 1.8, 4.7, and 2.1, respectively. There is also an increase in NMVOC (~1.04), CO and

particulate matter show a decrease in the emissions in 2030 by 0.8 and 0.6 times, respectively, when compared to 2010.

The Emission Model domain is shown in Figure 3.2 with two grids. The inner grid has the emissions from Delhi city only.

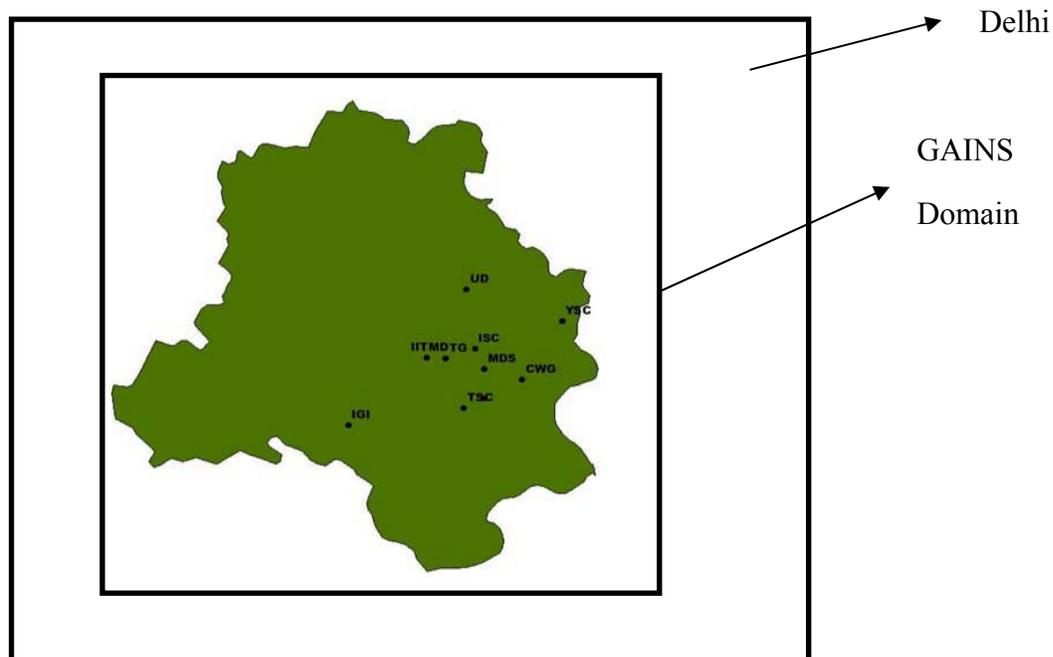


Figure 3.2 GAINS Emissions Model Domain overlapped with total domain choose for research.

The emissions from the GAINS model are outputs at the provincial level i.e., single values for each province. Therefore firstly the raw data has to be gridded onto the chosen domain. To accomplish this job the emission over Delhi at 1.67km from the existing inventory was taken as the base spatial distributions and the following procedure was adapted to re-grid the GAINS raw data. The domain was divided into three regions:

- Case1: Only Delhi
  - Divide the Delhi emissions with the ratios from GAINS baseline to Delhi.

- Case2: Other regions outside Delhi still considered inside the inner grid boundary.
- Case3: Outside Regions
  - Per grid emission = (GAINS emissions x (Area of the Grid))/(State area)

These gridded emissions are further processed to map onto the WRF-Chem readable format. Mapping of raw emissions is supported by emission preprocessor EPRES model. The details of the model are explained in section 2.2. The mapped total GAINS emissions from each species are shown in Figure 3.3. The central regions of Delhi act as hot spots for the emissions. Emissions from point sources i.e. NO<sub>x</sub> and SO<sub>2</sub> are clearly shown the spatial distribution map.

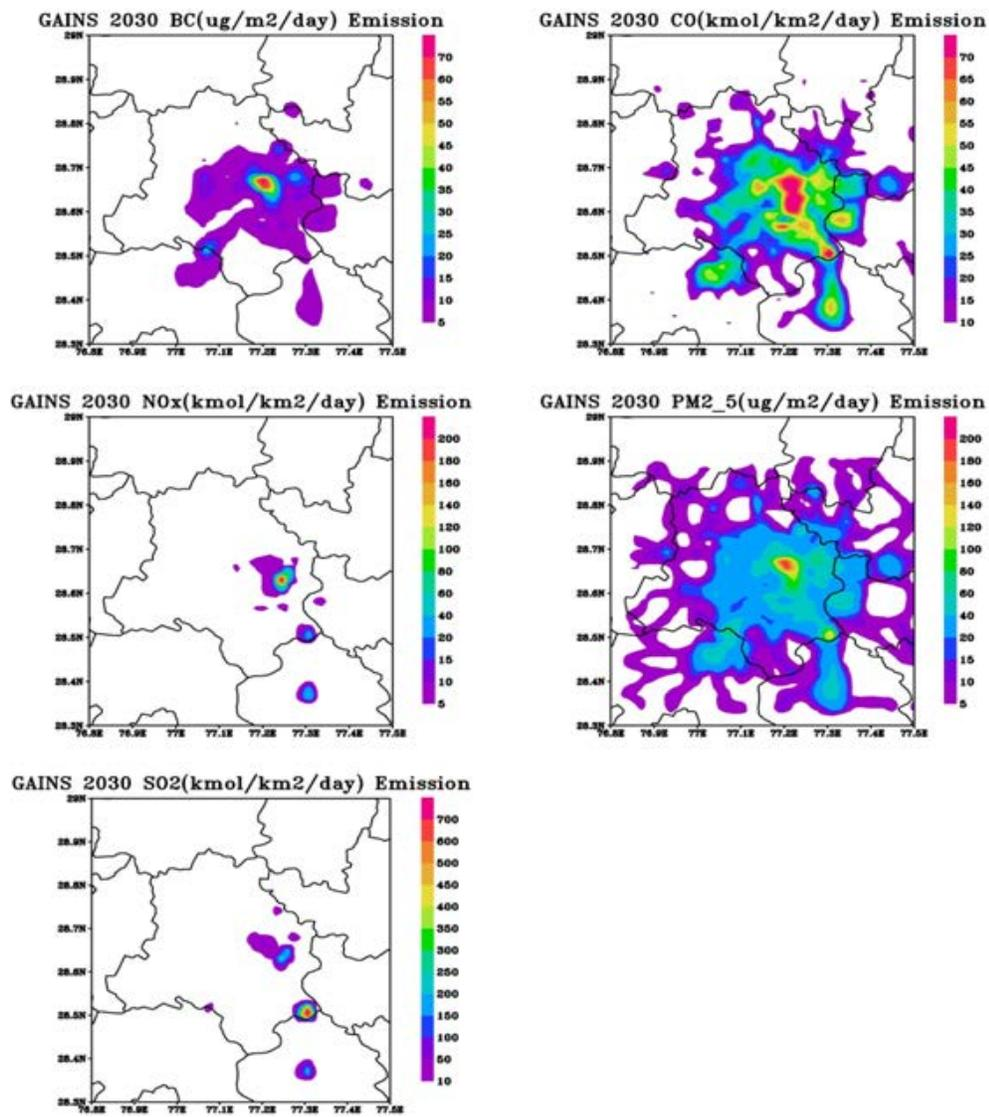


Figure 3.3 Daily average GAINS 2030 emissions from each species over Delhi for the year 2030.

### 3.3 Results and Discussion

Net changes in emissions from 2010 to 2030 were calculated and are shown in Figure 3.4. There is an increase in NO<sub>x</sub> and SO<sub>2</sub> emissions over the domain due to the expected rise in consumption of coal as a primary energy source. Previous analysis for the year 2010 shows that the major source of CO pollution is from the transportation sector, but the baseline scenario 2030 has targeted a huge reduction in CO emissions, as seen in the central regions of Delhi when compared to year 2010. The net increase in BC emissions at certain locations is as high as 50µg/m<sup>2</sup>/day. The reason is the increases in the transport and industrial sectors. This is shown clearly in Figure 3.5 where the net increases in BC emissions from different sectors are presented. Transport and Industry sectors have the largest increase in BC.

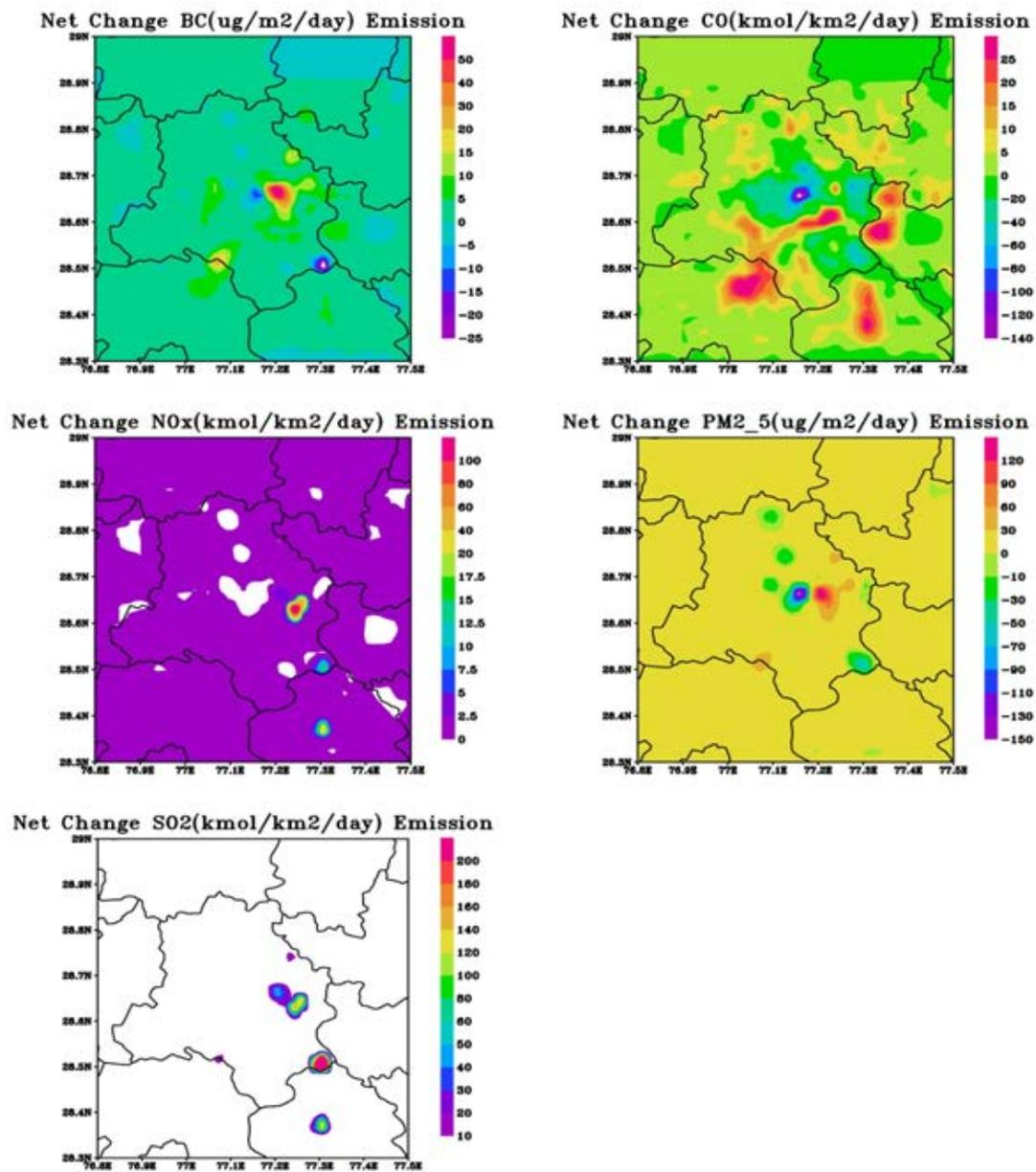


Figure 3.4 Daily average net change in the emissions from 2010 to 2030 over Delhi.

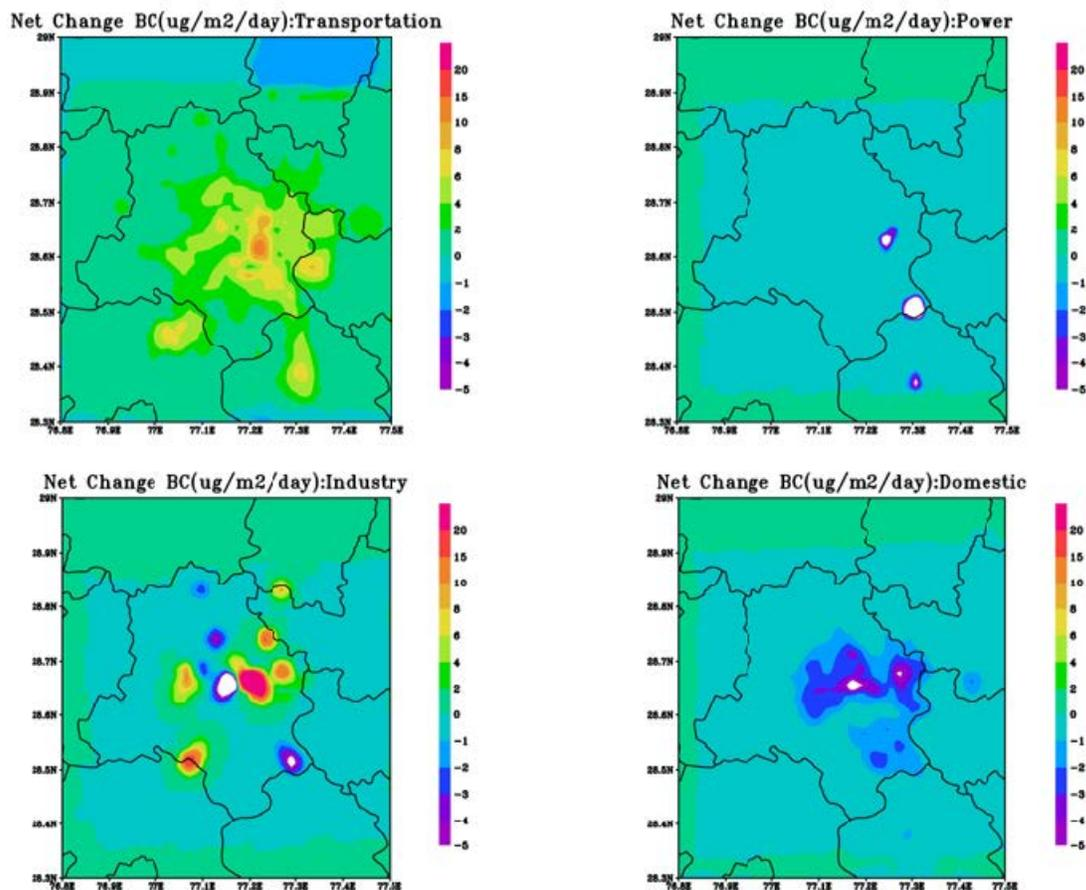


Figure 3.5 Daily average spatial distribution of BC emission from different sectors for the year 2030.

Figure 3.6 shows the 20 day mean spatial distribution of pollutants for the year 2030 with meteorological input conditions of 2010. The flow fields do change between 2010 and 2030 due to feedbacks associated with the pollutant distributions. The hot spots remain similar to the results from 2010 with increase in levels of concentrations as shown in Figure 2.7. Figure 3.7 shows the net percent change in concentration levels. BC has a large increase of 140% over the Delhi city. The increase in emissions levels are reflected in the increasing concentrations. Similar to BC,  $\text{NO}_x$  also has an increase in

concentrations by a 40%. Particulate matter in certain regions has increases and in other regions decreases in concentration levels, due to the differences in emissions via sector (Table 3.3). CO shows large reductions in concentrations (by 50%). O<sub>3</sub> shows large increases in the northern boundary cities.

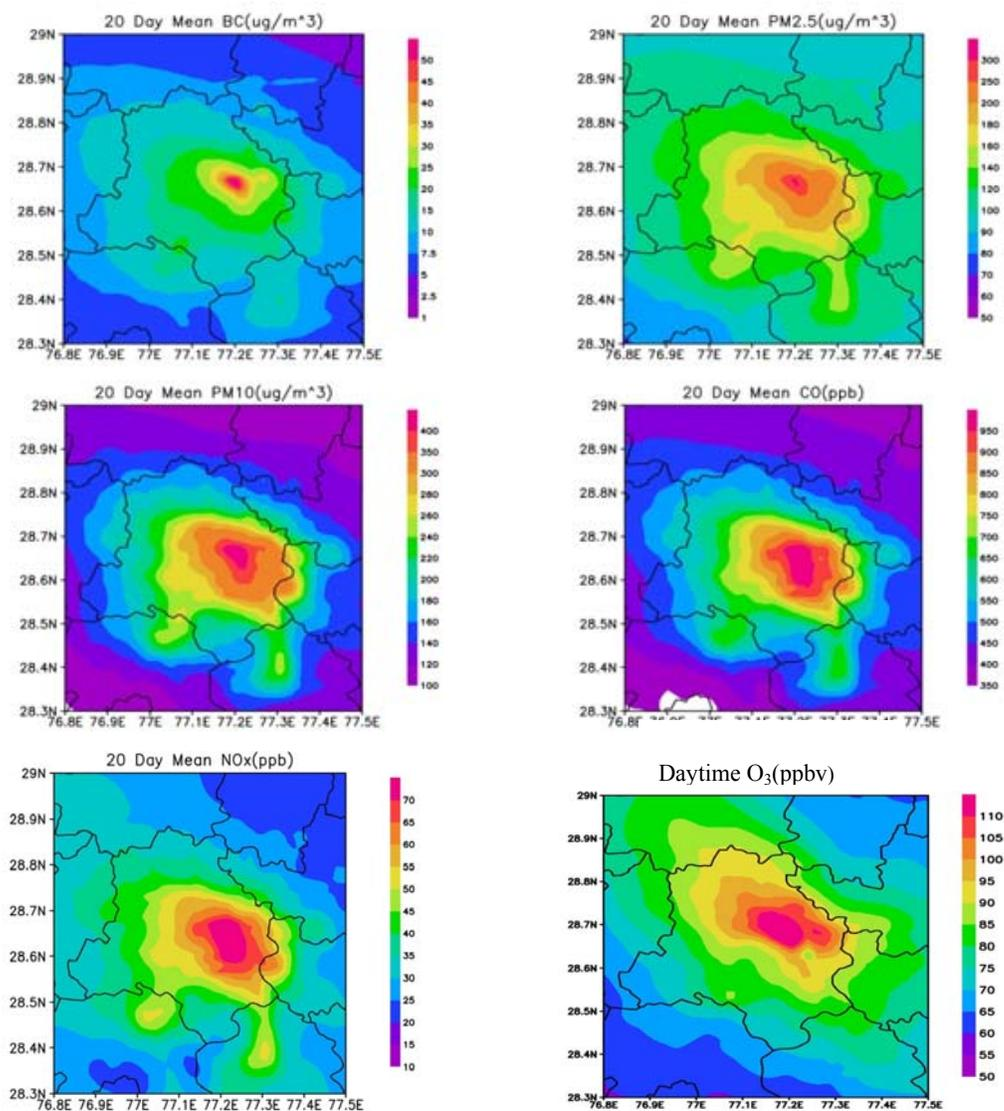


Figure 3.6 20-day Mean spatial distribution of pollutants over Delhi from GAINS 2030 emission scenario.

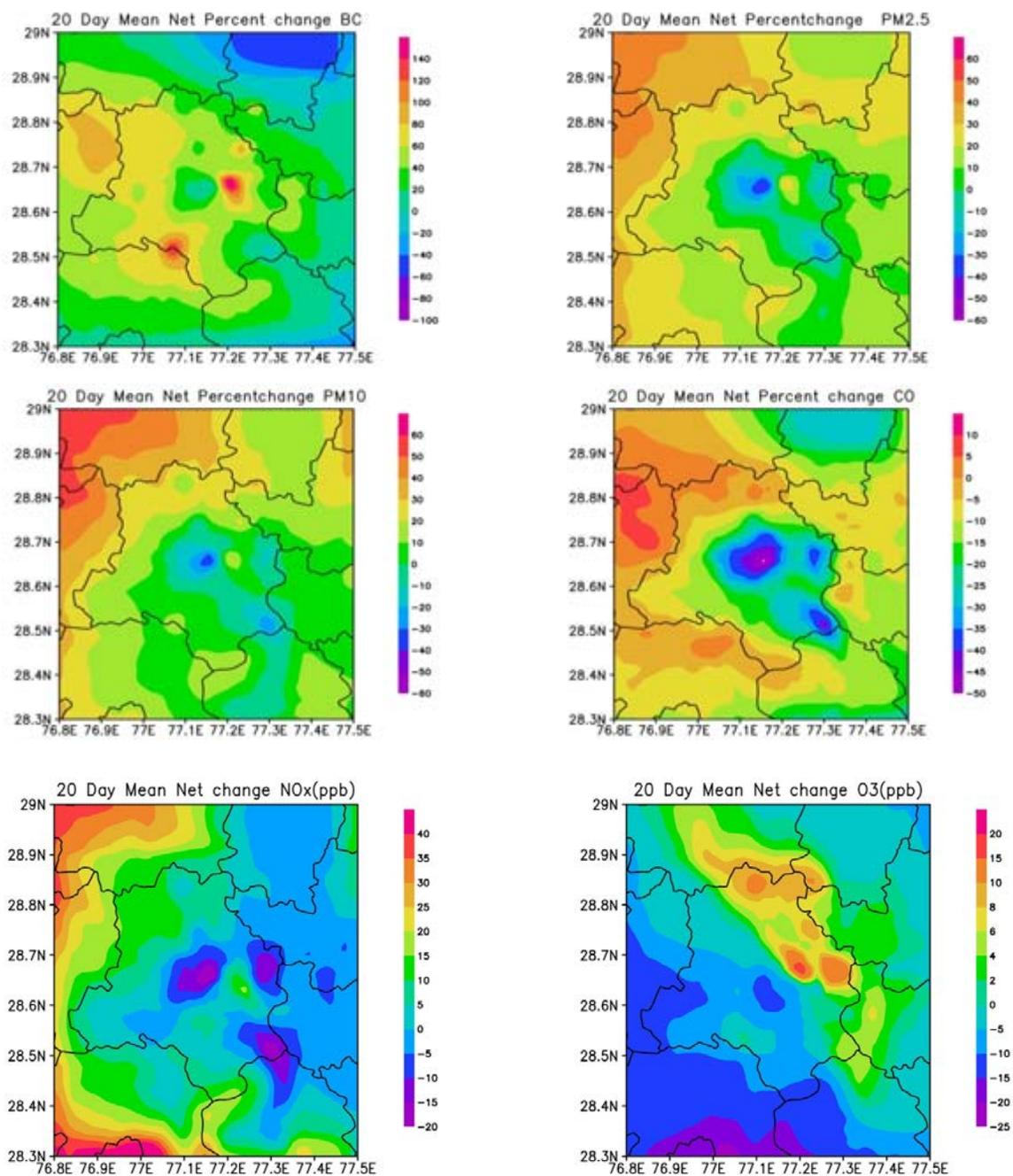


Figure 3.7 20 –day mean net percent change in pollutant concentrations over Delhi from the period 2010 to 2030.

The contributions of each pollutant from different sectors are shown in Figure 3.8. Transportation and Industry sectors act as major source for increases in BC, CO, NO<sub>x</sub> and particulate matter. Increasing levels of emissions trends reflects in the concentration values from that corresponding sector.

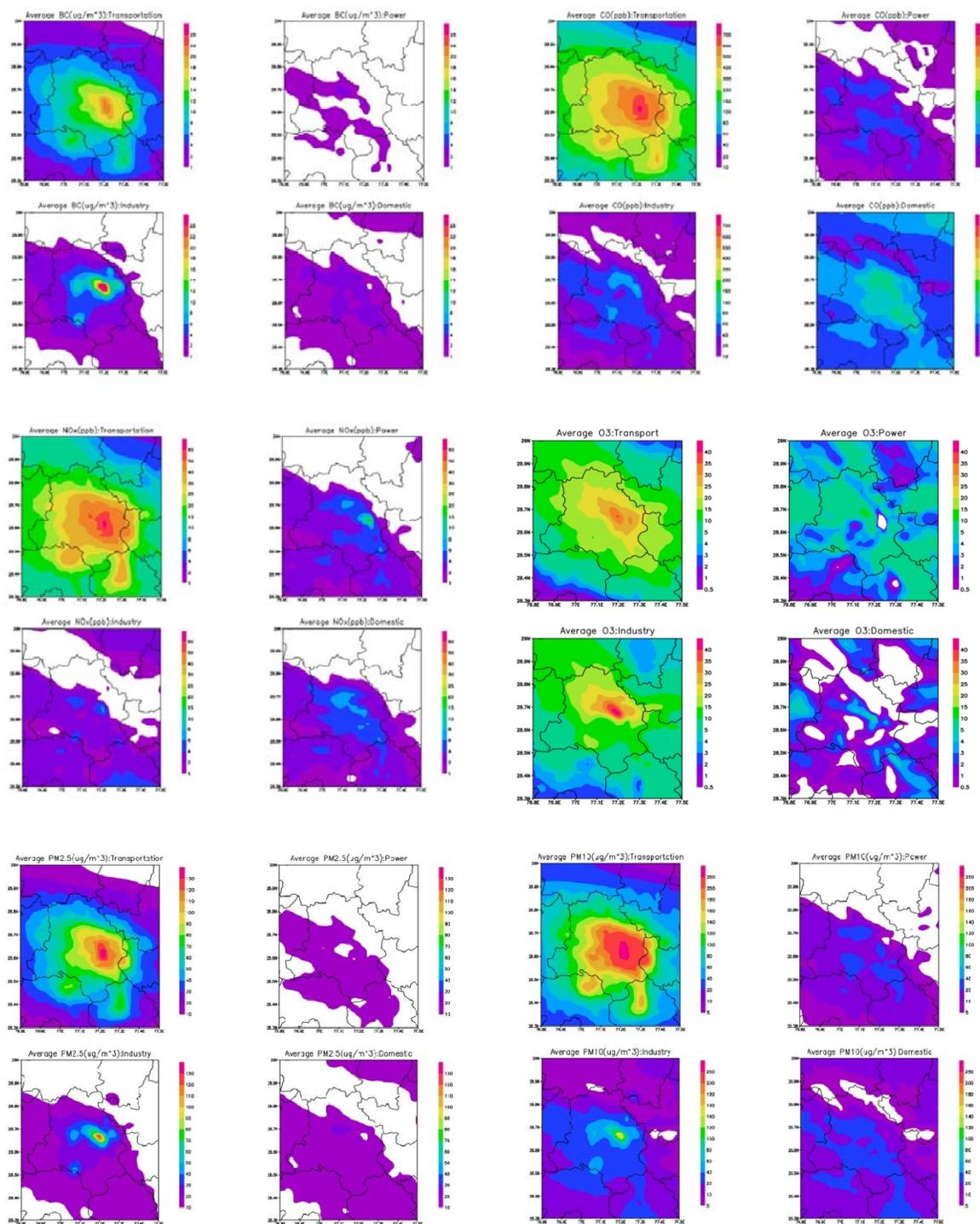


Figure 3.8 Spatial Distribution of pollutants from various sectors from GAINS 2030 emissions.

Figure 3.9 shows the 20 day mean net change in pollutant levels from 2010 to 2030 by sector. There is net increase in BC  $\sim 30\mu\text{g}/\text{m}^3$ . The interesting issue here is that there is a decrease in BC concentrations from residential consumption. This is due to fuel improvements and use of improved cooking gas stoves. From the emissions spatial distribution patterns it is evident that there is decrease in total CO levels over Delhi by the year 2030. These control measures reflected clearly on the concentrations with decrease in levels of CO. The total reduction in CO is  $\sim 900\text{ppbv}$ .

Although preventive measures were incorporated during the emission scenario projections to reduce the particulate matter there is still a significant increase in  $\text{PM}_{2.5}$  and  $\text{PM}_{10}$  concentrations in this scenario. Due to the increases in pollution levels and BC concentrations there is an increase in surface temperatures and anthropogenic radiative forcing. Figure 3.10 shows the increase in surface temperatures over Delhi and the values are as high as 0.65K at the suburban locations. The radiative forcing results are dealt with in Chapter 4.

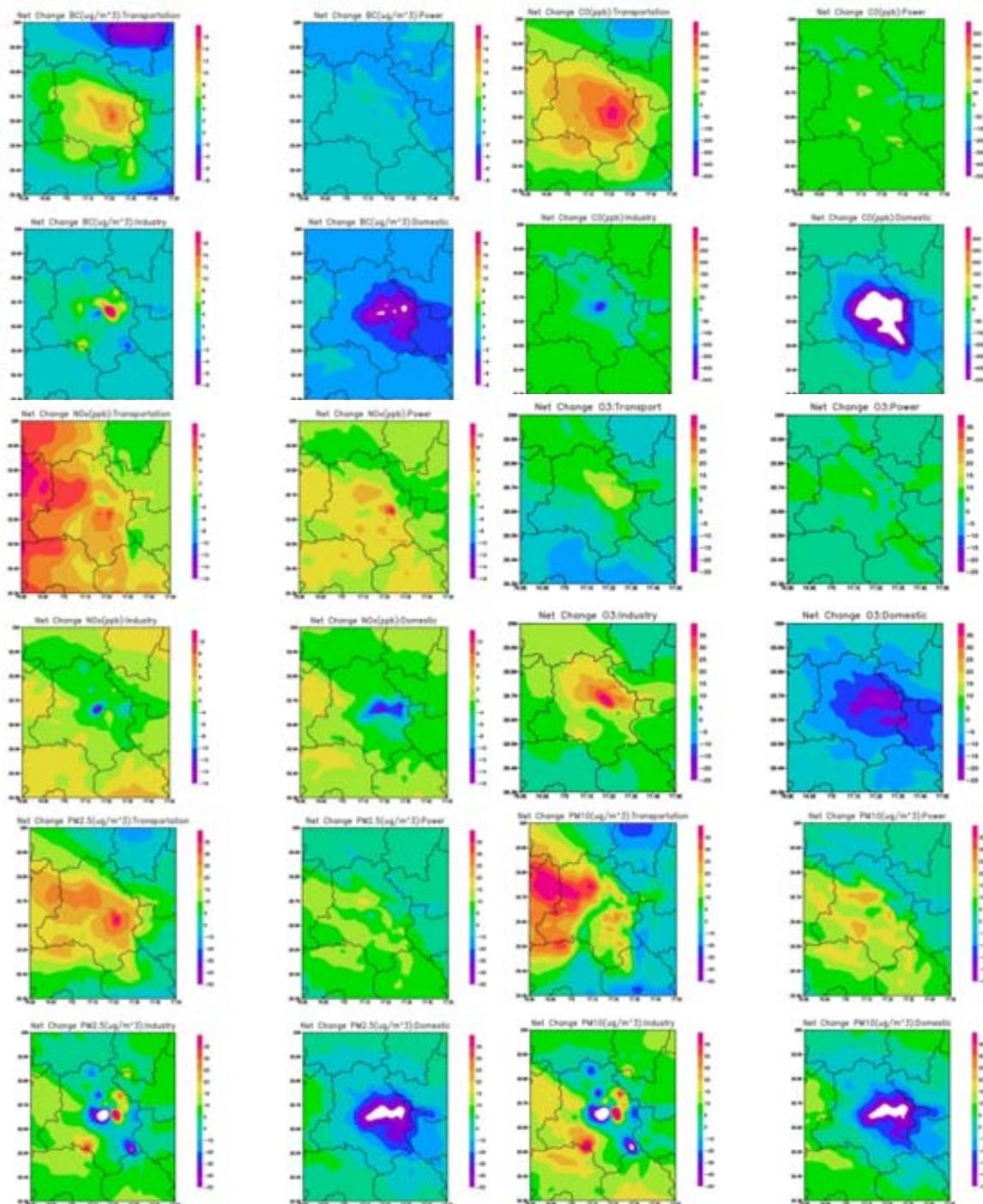


Figure 3.9 20-day mean net change in pollutants concentrations from 2030 to 2010 across various sectors over Delhi.

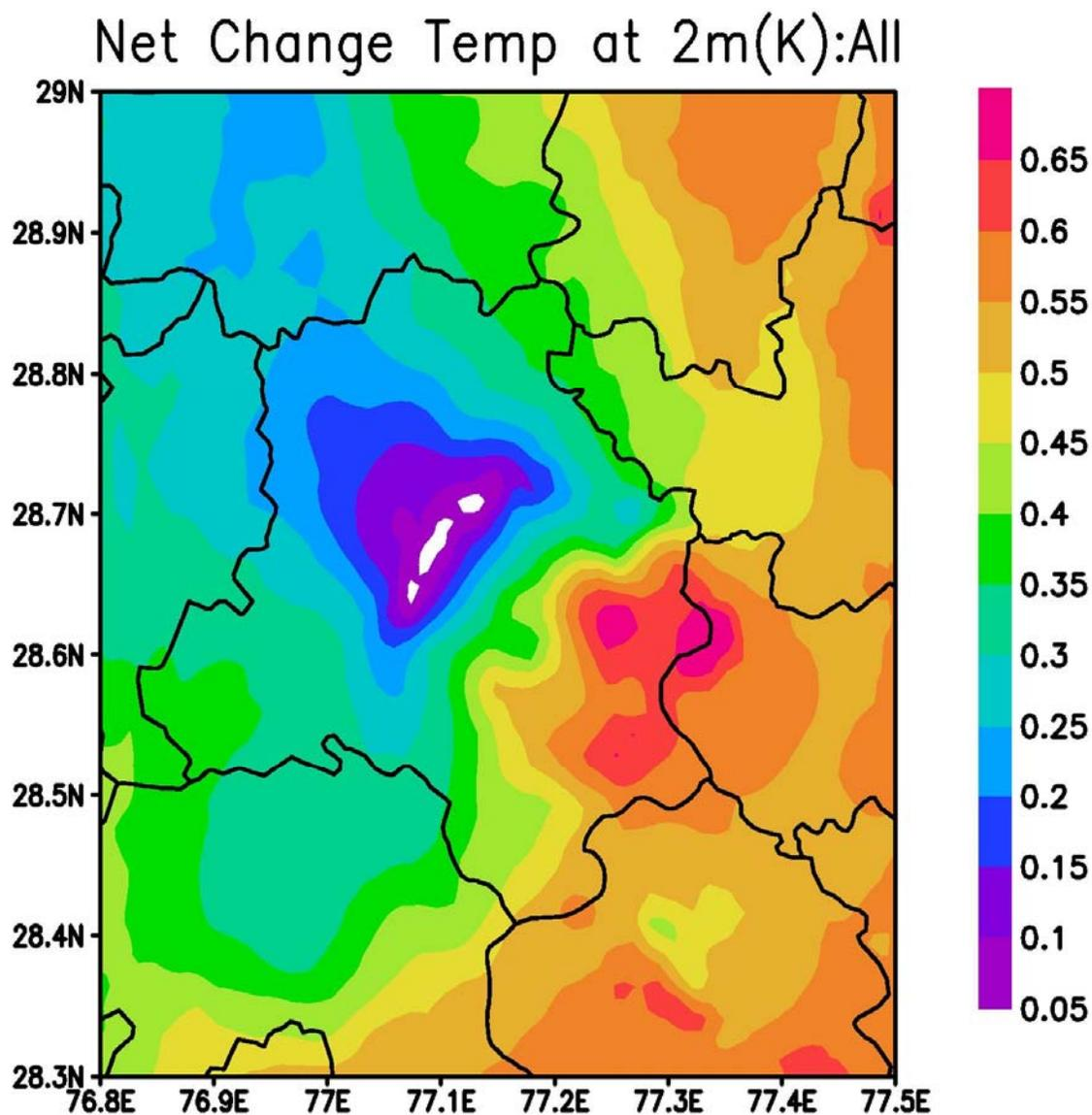


Figure 3.10 Net increase in surface temperature (K) over Delhi from 2010 to 2030.

### 3.4 Summary

GAINS model was used to develop a 2030 advanced control technology emission scenario. The changes in pollution levels in 2030 under this scenario were compared to the baseline 2010 results discussed in Chapter 2. Under this 2030 scenario there was a net increase in emissions of NO<sub>x</sub>, PM<sub>2.5</sub>, BC and a reduction in CO, PM<sub>10</sub>. The net increases were associated in the large increases in net energy use and the large increase in the power and transport sectors. CO emissions went down due to more efficient combustion in the transport, industry and domestic sectors. The emission changes in 2030 differed by sector and this resulted in a change in emissions distribution in 2030 relative to that in 2010. Under this scenario the average air pollution levels in Delhi of ozone, BC and PM<sub>2.5</sub> increased significantly.

## CHAPTER 4 RADIATIVE FORCING OVER DELHI

### 4.1 Introduction

Air pollution impacts human health and climate. Air quality levels and source sector contributions were discussed in Chapter 2 and Chapter 3. This chapter deals with climate influence (as expressed in terms of anthropogenic radiative forcing and changes in meteorology) due to changes in air quality levels over Delhi during the years 2010 and 2030.

As an initial step to understand the influence of air quality on climate, the surface temperatures were modeled for the year 2010 in Figure 2.5 and the net change in temperature levels from 2010 to 2030 were presented in Figure 3.10. The analysis suggests that changes of emission levels from 2010 to 2030 would cause a net increase in total temperature at the surface of up to  $\sim 0.65\text{K}$ . Another effect of the increasing levels of air pollution on climate change is through radiative forcing, short and long wave fluxes, which are discussed in this chapter. Any alterations of the factors that affect climate create energy imbalances in the earth system, and these imbalances are referred to as radiative forcing (IPCC, 2005). The phrase radiative forcing signifies that the factors (such as air pollution) affect the balance between incoming solar radiation and outgoing infrared radiation within the Earth's atmosphere. Positive forcing tends to warm the surface, while negative forcing tends to cool it. Forcing values are expressed in watts per square meter ( $\text{W}\cdot\text{m}^{-2}$ ).

Urban locations tend to have warmer climates when compared to remote places or villages. Urban cities have a profound effect on the climatic conditions and modify it in

various ways like : 1) the surface materials in cities absorb more shortwave radiation; 2) configuration of building increases the absorption of shortwave radiation at low sun angles and reduces the loss of longwave radiation at night; 3) transportation, industry and the heat of buildings artificially warm the air surrounding the cities; 4) precipitation can be higher in cities because increased thermal uplift and because of a greater quantity of condensation nuclei ; and 5) winds are for the most part reduced by the increased friction of the city surface.

The incoming solar radiation is in two forms longwave and shortwave. The radiation emitted from the sun, solar radiation is short wave radiation. Seventy percent of the total shortwave radiation is absorbed and 30% is reflected into the space. The shortwave radiation can have a profound impact on certain biophysical processes, such as canopy photosynthesis and land surface energy budgets, by being absorbed into the soil and canopies. When the solar radiation is absorbed in the earth, a part of it reemitted as longwave radiation. About 70% of the longwave radiation is lost to space and the rest is absorbed in the atmosphere termed, the greenhouse effect.

Figure 4.1 shows the change in radiative forcing in the year 2005 from a baseline of the industrial revolution, from the IPCC report. The net warming due to anthropogenic emissions is  $\sim 1.5 \text{ W m}^{-2}$ . Greenhouse gases like  $\text{CO}_2$ ,  $\text{CH}_4$  and  $\text{N}_2\text{O}$  have a warming effect on the earth's surface, while the direct effects from aerosol cause cooling. The effects of aerosols are complicated and depend on composition. Most aerosols, such as sulfates, nitrates and sea salt scatter solar radiation, while black carbon and brown carbon absorb solar radiation. All aerosols in the atmosphere, due to scattering and absorption, reduce the amount of solar energy reaching the surface (this is called dimming). The

absorbing aerosols heat the atmosphere and act like a greenhouse gas and contribute to global warming. The effect of scattering aerosols is to cool the atmosphere. Currently the net effect of all aerosols is a net cooling.

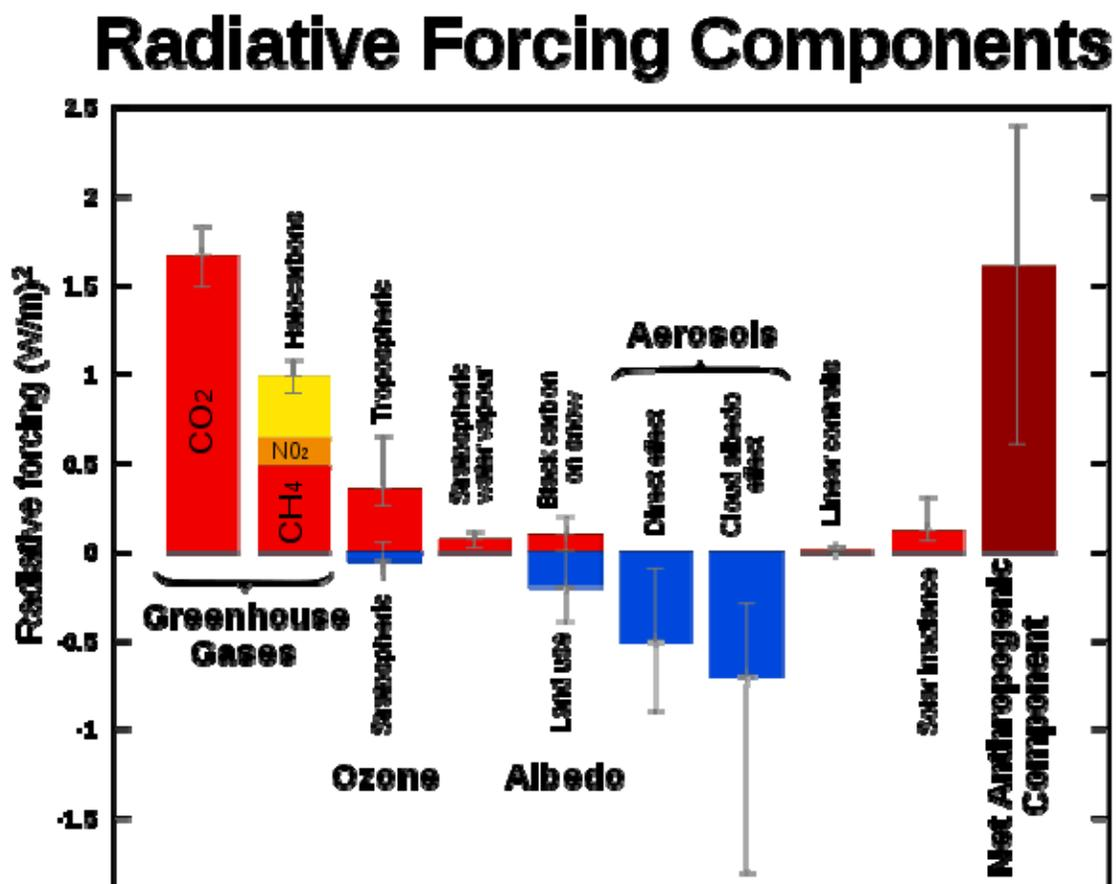


Figure 4.1 Anthropogenic radiative forcing components for the year 2005 from IPCC report (IPCC, 2005).

## 4.2 Results and Discussion

Radiative forcings were calculated for that several WRF-Chem simulations were conducted for the period of 26 Sep to 15 Oct, 2010. Figure 4.2 show the total incoming and outgoing fluxes from the simulation that includes all sources. Part of incoming solar radiation is reflected back to the space and this is termed as outgoing solar radiation (OSR). The outgoing longwave radiation reflects the radiations due to greenhouse gas. OSR is a critical component of the Earth's radiation budget and represents the total radiation going to space emitted by the atmosphere. The earth's radiation balance is nearly balanced since the OSR nearly equals the shortwave absorbed radiation received. The imbalance between sum of the top and bottom is the atmospheric heating.

Figure 4.3 shows the impact of air pollutants from various sectors on radiative forcing. The 20 day mean day time (9:30am to 6:30pm) spatial distribution of the reduction in downward shortwave flux, i.e. radiation reaching the earth's surface for each sector to Delhi city are shown. This reduction is referred to as surface dimming. The total anthropogenic dimming is  $\sim 50\text{Wm}^{-2}$ . The largest dimming of  $16\text{Wm}^{-2}$  is from the transportation and domestic sectors. The central regions of Delhi have high emission contribution sources, like domestic and transportation which are clearly seen in the spatial distribution of air quality levels of Delhi. The reduction in solar radiation has implications for agriculture, as less solar energy means less available energy for photosynthesis.

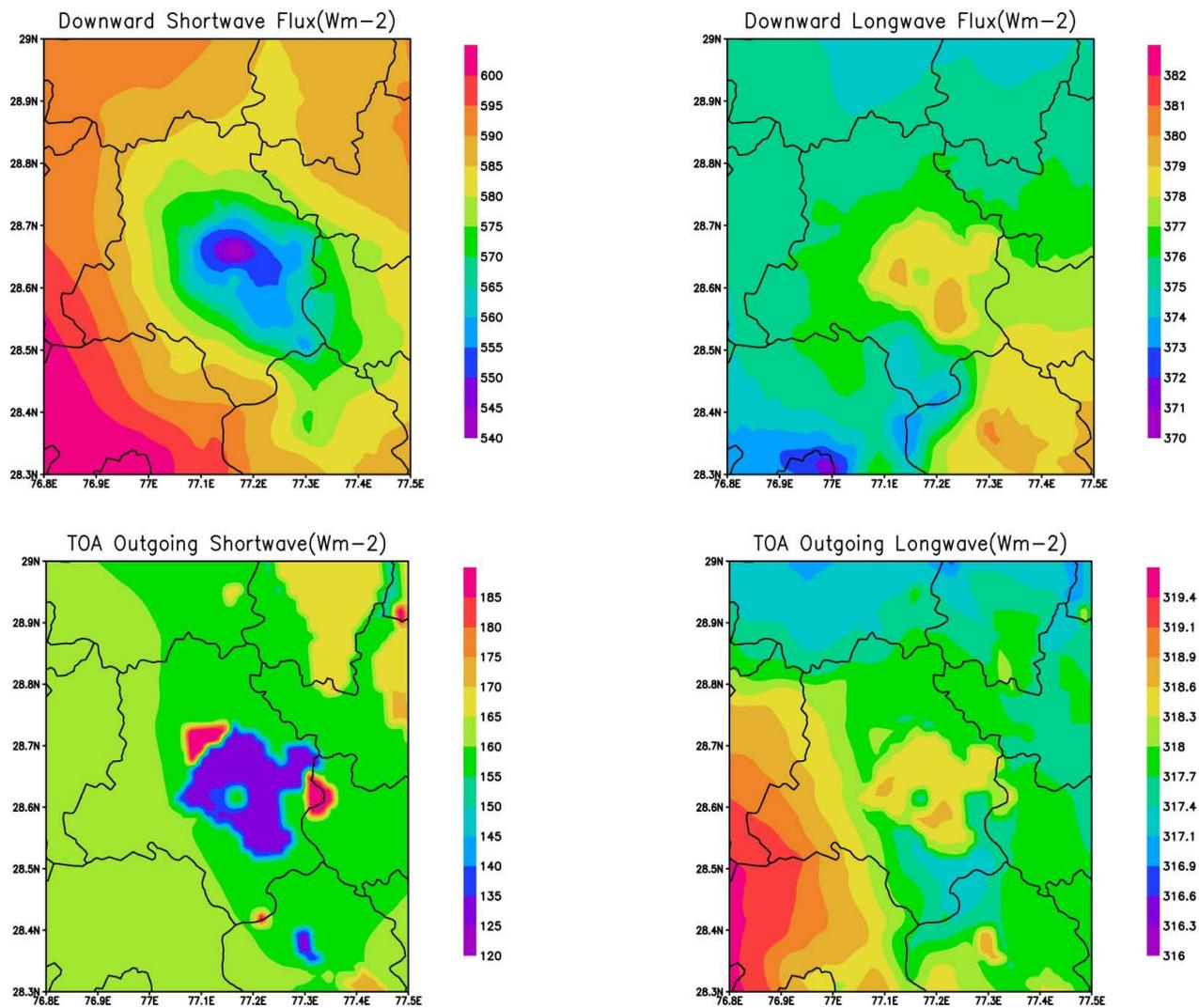


Figure 4.2 20-day mean fluxes over Delhi from 2010 emission inventory. Top left shortwave, top right total longwave reaching the surface. Bottom parts show outgoing shortwave and longwave radiation at the top of the atmosphere.

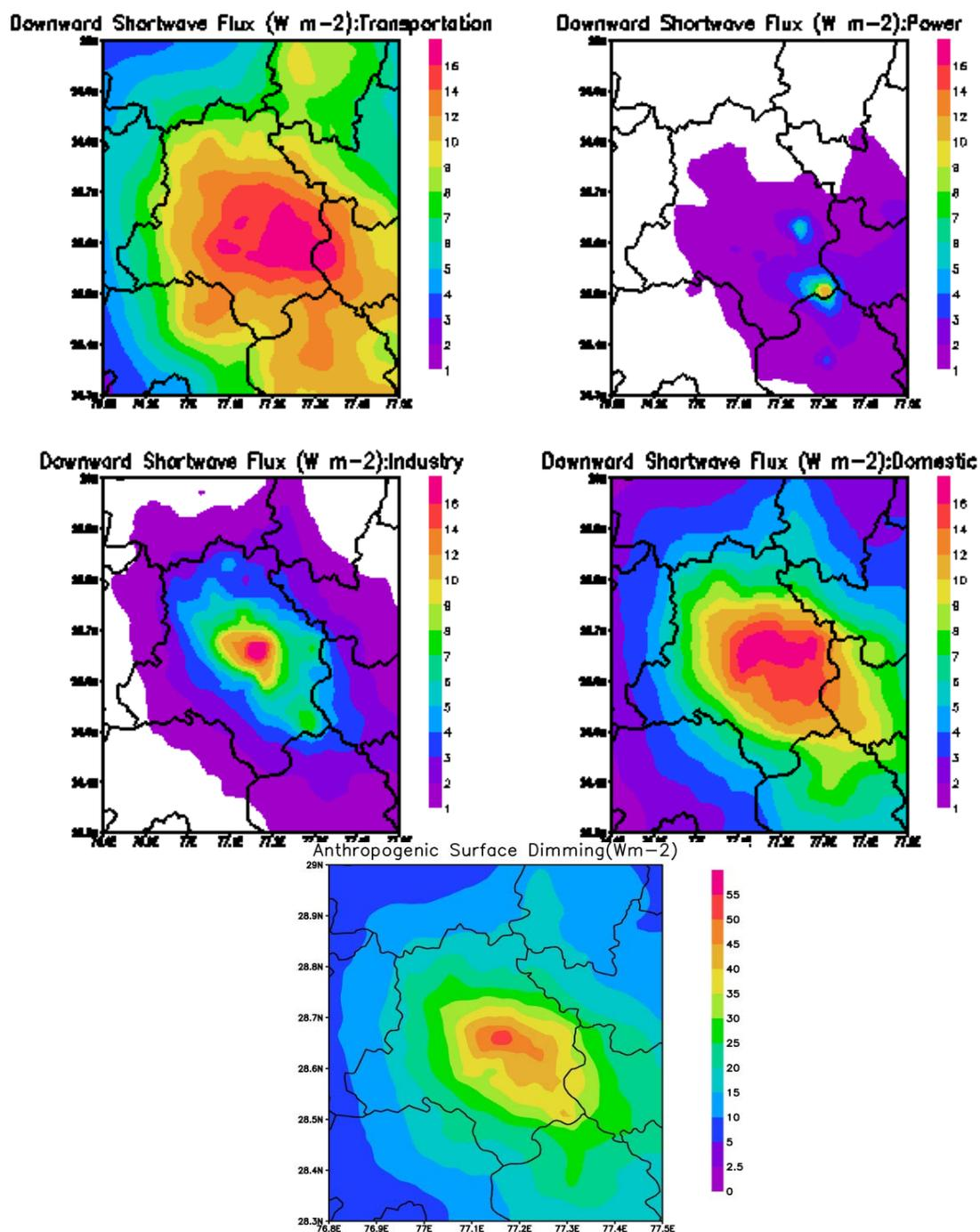


Figure 4.3 20-day mean day time downward shortwave flux ( $W m^{-2}$ ) from various sectors and surface dimming from total anthropogenic emission over Delhi 2010.

The net change in the shortwave radiation i.e. the difference in incoming surface and outgoing top of the atmosphere shortwave radiation is the shortwave atmospheric forcing. Figure 4.4 shows the 20-day mean day time atmospheric forcing from various sectors and the total forcing from anthropogenic emission over Delhi for the year 2010. As mentioned in the definition of radiative forcing positive values show warming effect on the earth's surface. The total anthropogenic atmospheric radiative forcing for the simulated period of 20 days is as high as  $40 - 50 \text{ Wm}^{-2}$ , with the largest contribution from the sectors with high BC emission i.e., transportation and domestic. This atmospheric forcings results in as increase in atmospheric temperature and can impact atmospheric stability and clouds.

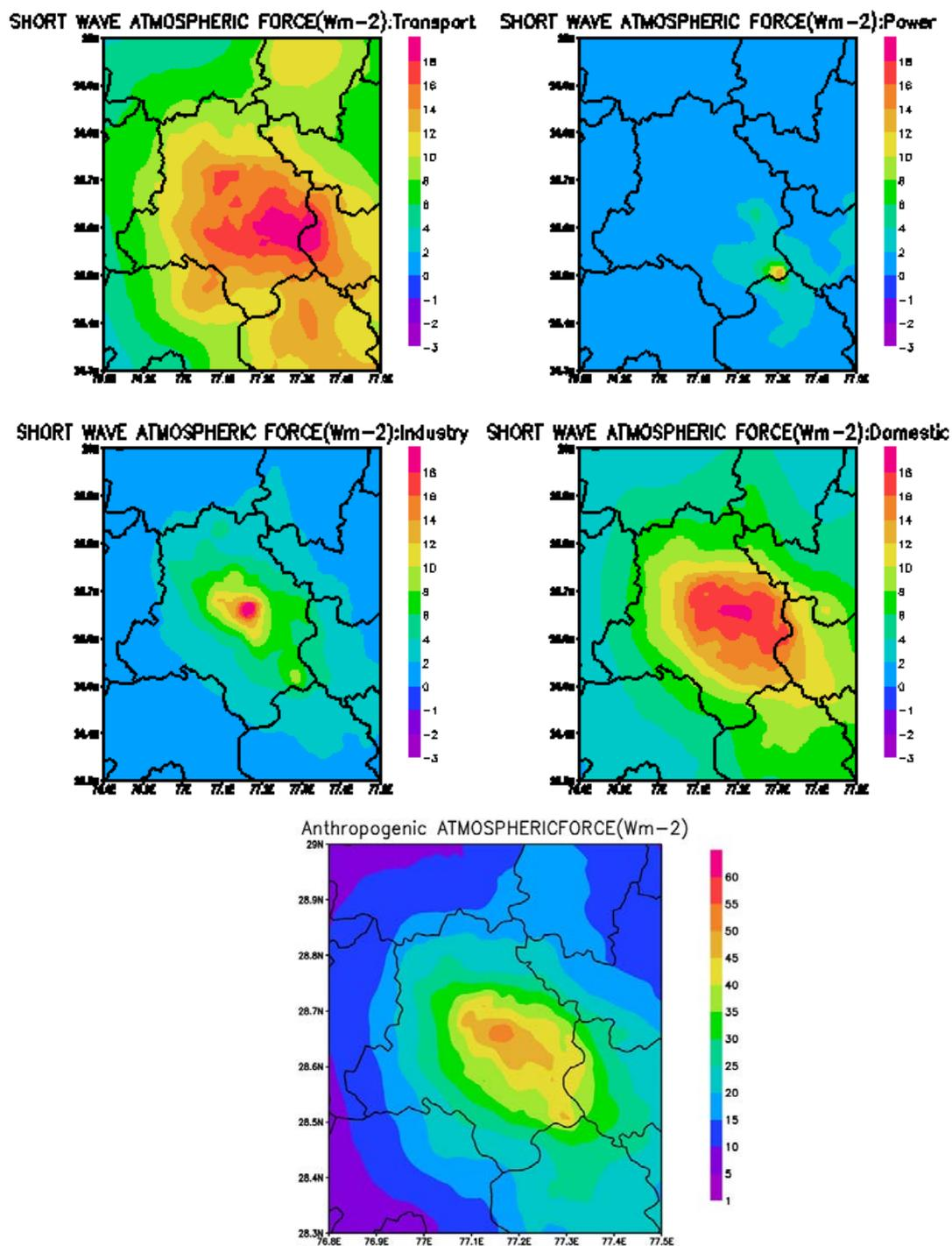


Figure 4.4 20-day mean day time anthropogenic atmospheric radiative forcing from various sectors-2010.

Similar calculations were performed for the year 2030 emission scenario. The sector contributions to surface dimming and atmospheric forcing are shown in Figure 4.5 and Figure 4.6. The net changes in these fluxes are shown in Figure 4.7 and Figure 4.8. Due to the increase in emissions from vehicular traffic there is large increase in surface dimming and atmospheric heating. The forcings due to the domestic sector are significantly reduced in 2030, due to the changes in fuels and improved stoves.

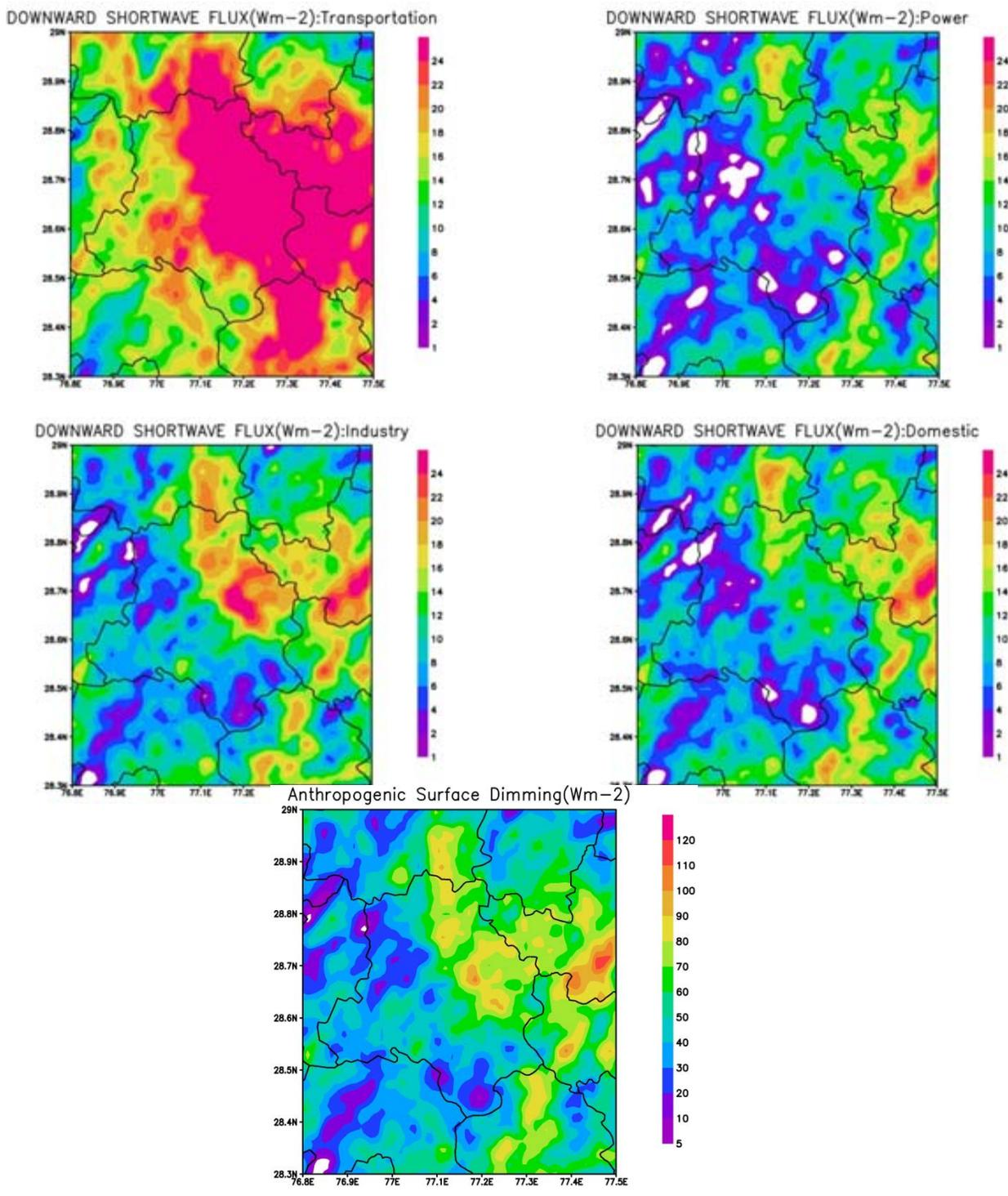


Figure 4.5 20-day mean day time downward shortwave fluxes from various sectors over Delhi-2030.

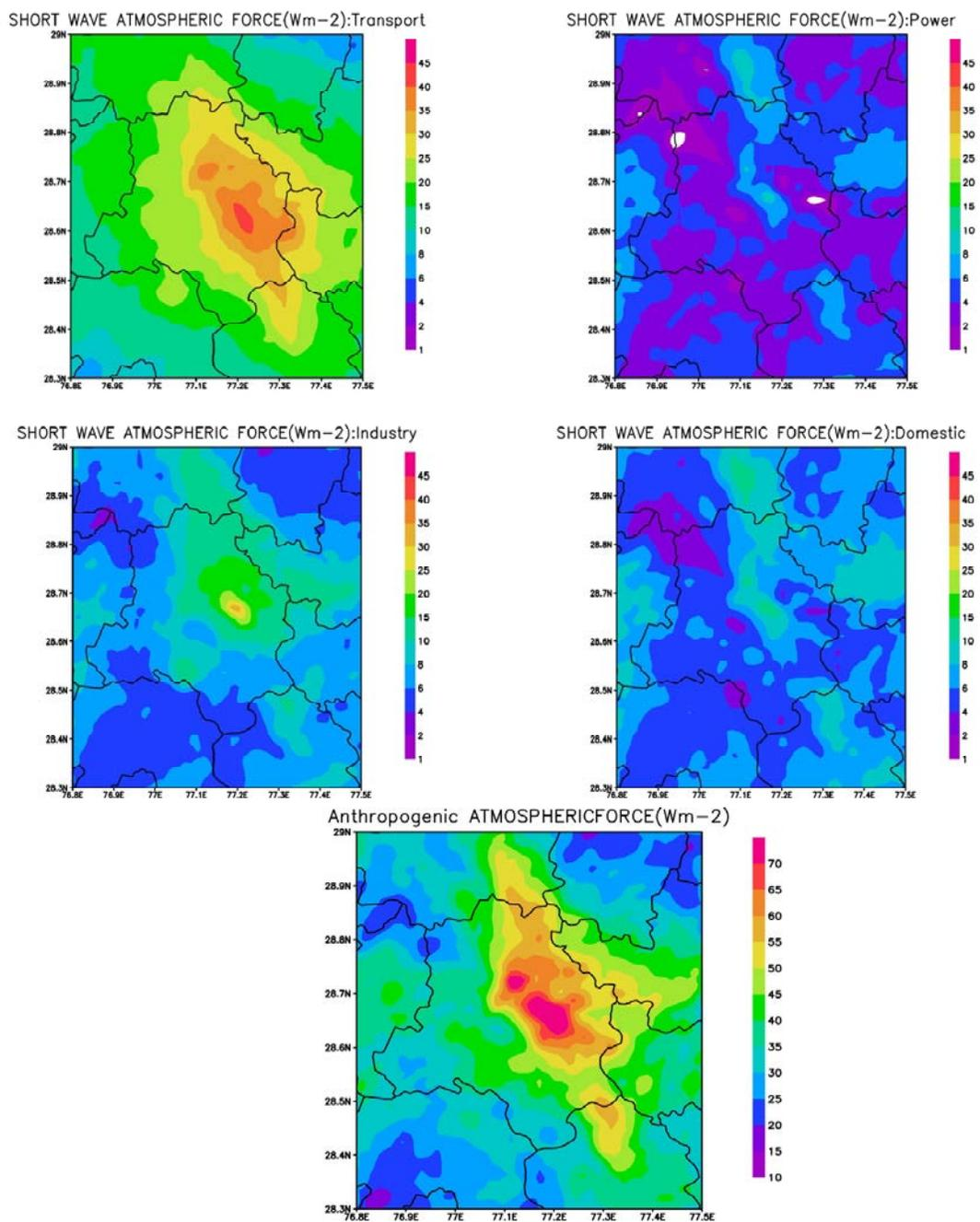


Figure 4.6 20-day mean day time anthropogenic atmospheric radiative forcing from various sectors in the year 2030.

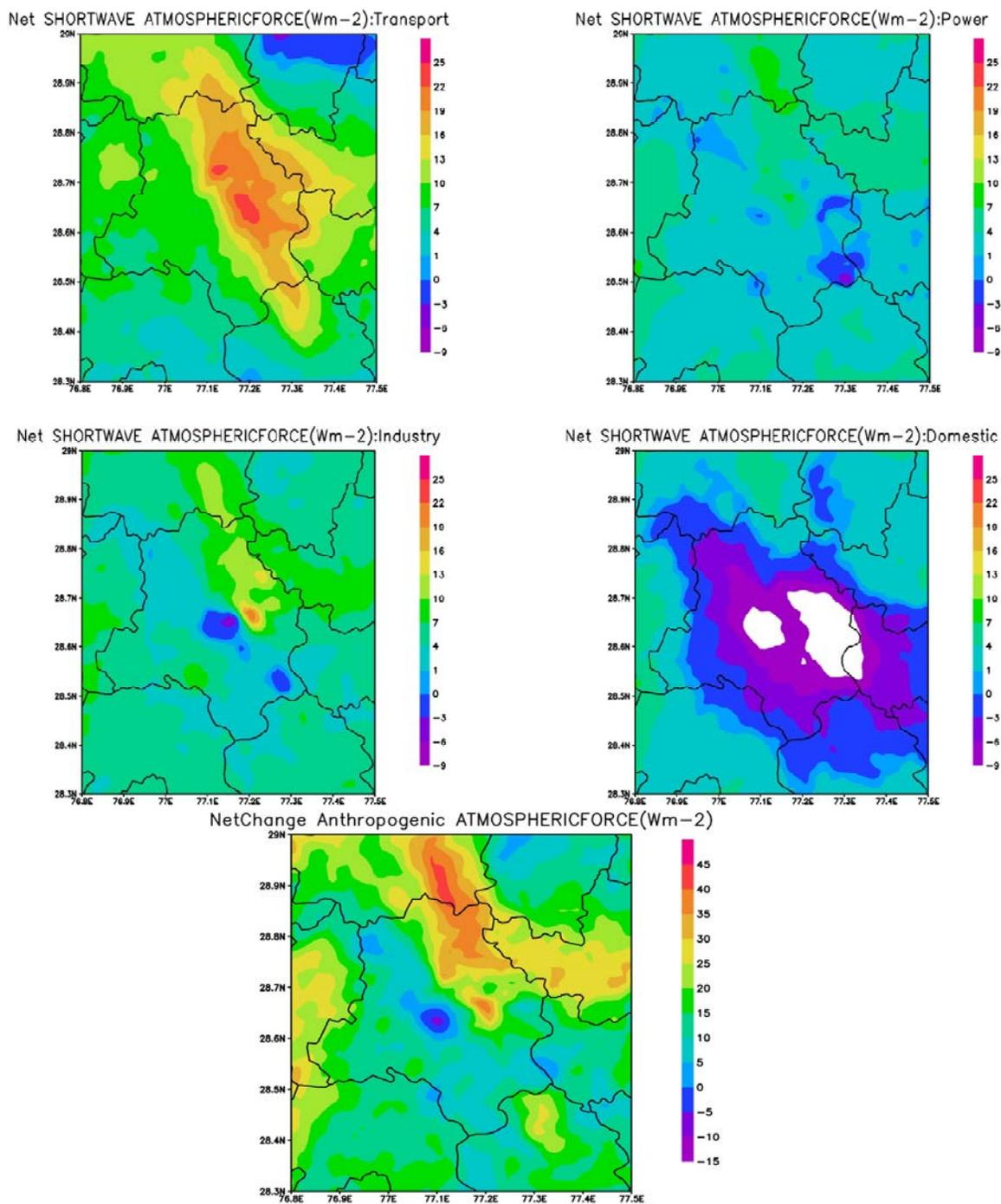


Figure 4.7 20-day mean day time net change in anthropogenic radiative forcing from various sectors year 2010 to 2030.

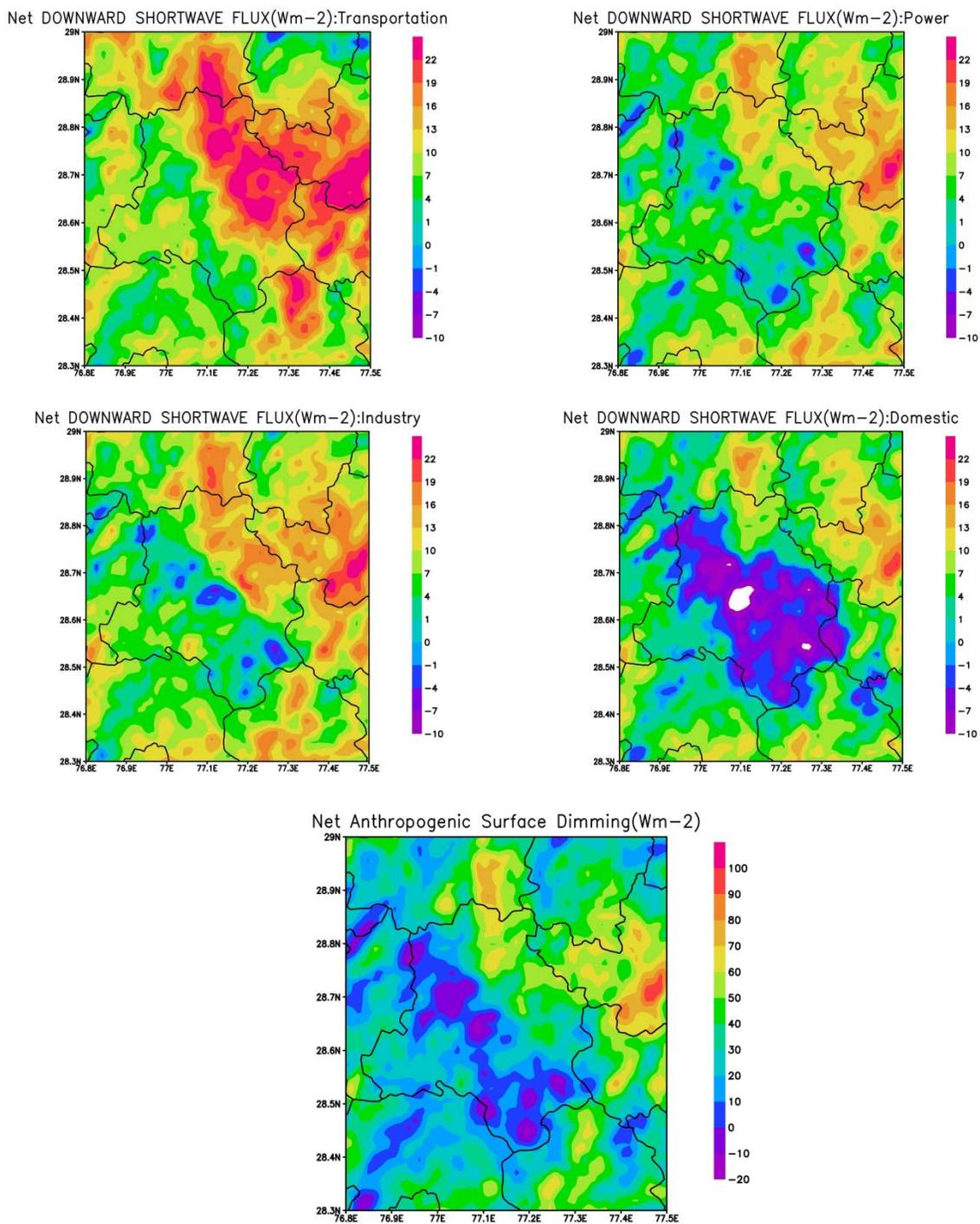


Figure 4.8 20-day mean net surface dimming from different sectors and total dimming from anthropogenic emissions from the year 2010 to 2030.

The spatial mean averages of the anthropogenic forcing in 2010 and 2030 are summarized in Figure 4.9. In 2010 the anthropogenic pollutants in Delhi have a large surface dimming ( $\sim 13 \text{ Wm}^{-2}$ ) and a large atmospheric warming of  $\sim +15 \text{ Wm}^{-2}$ . The net effect is a top of the atmosphere forcing of  $+1.9 \text{ Wm}^{-2}$ , indicating a net warming of the system. This is due to the large emissions of BC from the transport and domestic sectors. In 2030 the surface dimming increases more than atmospheric heating, with a net top of the atmosphere value of  $\sim -20 \text{ Wm}^{-2}$  indicating a net cooling effect of anthropogenic pollution. Scattering aerosols, such as sulfate and nitrate increases faster than absorbing aerosols, leading to a net cooling impact of the air pollution.

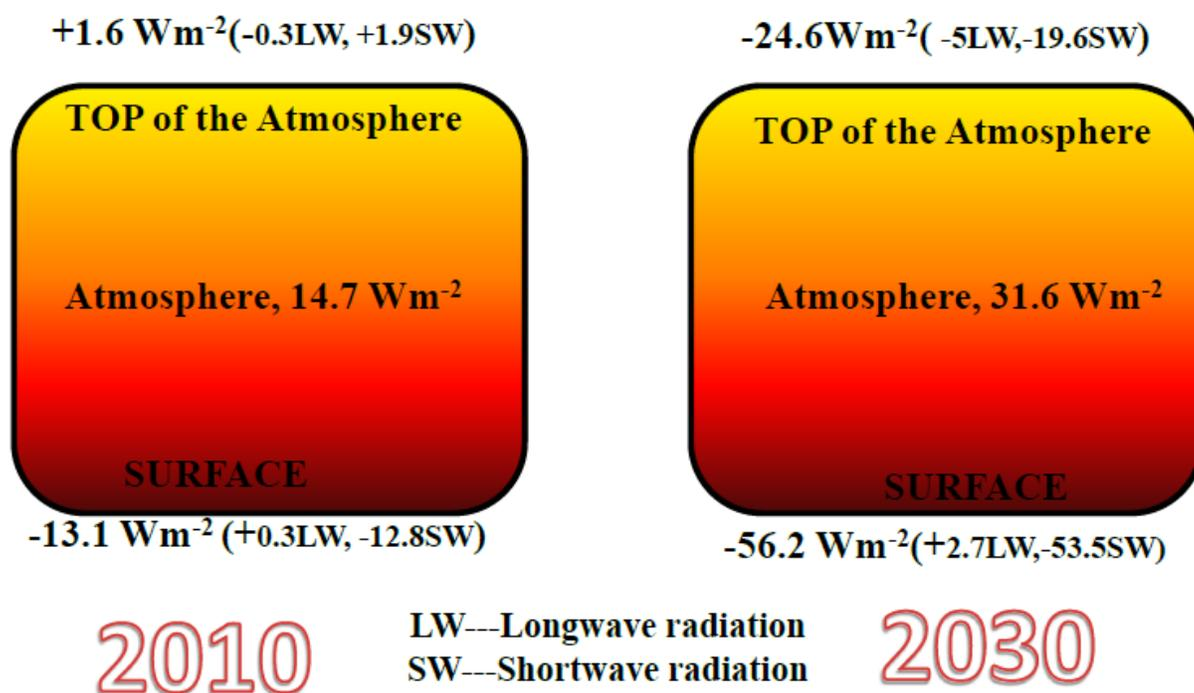


Figure 4.9 20-day spatial mean averages of radiation effects at surface, in and top of the atmosphere for the year 2010 and 2030.

### 4.3 Summary

Atmospheric radiative forcing was evaluated for the year's 2010 and 2030 and their net changes on the forcings were calculated. The spatial mean averages for the year 2010 show that anthropogenic pollutants in Delhi have a large surface dimming  $\sim 50 \text{Wm}^{-2}$ . High levels dimming are due to the high concentrations of primary and secondary aerosols. This reduction in solar energy reaching the surface impacts the vegetation by reducing the photosynthesis processes. These pollution levels also cause a large positive atmosphere forcing due to the large amounts of black carbon. This results in an increase in temperature in the lower atmosphere. The net effect of pollution levels in 2010 is a net warming (top of the atmosphere forcing are positive). Sector based analysis showed that domestic, transportation, and industry all contribute to atmospheric warming due to high levels of BC from corresponding sectors. Future projections of the atmospheric forcing were evaluated for the year 2030. The assumptions used in the 2030 scenario lead to overall increases in many radiative active pollutants, but with significant shifts in emissions by sector. Large increases in forcing occurred in the transport, industry and power sectors. The forcing from the domestic sector were smaller and in some in some regions decreases in the domestic sector due to changes in fuels and improved cook stoves. The net effect of the 2030 emissions was an increase in the surface dimming and in atmospheric forcing, with the dimming larger than the atmospheric forcing, resulting in a top of the atmosphere forcing being negative (cooling). Increase in vehicular traffic reflected on surface dimming and atmospheric heating. Net increase in anthropogenic atmospheric force of  $\sim 40 \text{Wm}^{-2}$  was observed. Contrary to all these there is net cooling effect on the top of the atmosphere but increase in pollution levels. There are large

absorbing aerosols (BC), but relatively very high scattering aerosol like particulate matter (PM<sub>2.5</sub> and PM<sub>10</sub>) leading to net cooling effect.

## CHAPTER 5 CONCLUSION AND FUTURE WORK

### 5.1 Conclusion

The online WRF-Chem model set up with 4 nested grid domains covering South Asia, Northern India and NCR Delhi and Delhi city regions, was run for a 20-day period (26 September to 16 October 2010). This time period corresponds to the Common Wealth Games 2010, held from 4-14 October 2010 in Delhi, India. During this season the winds were more frequent from NNW and generally low (<1m/sec) and pollution levels were generally high. The model performance was evaluated against observations. The model had a dry bias (under predicts RH), slightly under predicted during the peak day time temperatures by 1-2 degrees (~5%), and was biased high in wind speed. The predicted mean surface concentrations of various pollutants showed similar spatial distributions as the observations with peak values in the middle of the domain reflecting the traffic and population patterns in the city. The emissions and criteria pollutants levels exceeded the National Ambient Air Quality standards, with BC levels greater than  $25\mu\text{g}/\text{m}^3$  at residential regions, and  $\text{PM}_{2.5}$  and  $\text{PM}_{10}$  levels of  $220\text{-}350\ \mu\text{g}/\text{m}^3$  and  $350\text{-}550\ \mu\text{g}/\text{m}^3$ , respectively. The day time peak ozone levels were as high as 100ppbv.

The contribution of various emission sectors including transportation, power, domestic and industry were studied through a series of model runs. The sectoral emission runs showed that the transportation and domestic sectors are the largest contributors to CO, BC  $\text{PM}_{2.5}$  and  $\text{PM}_{10}$  concentrations. Within Delhi, the emissions from outside of Delhi were found to contribute from 20% to 50% depending on species. This has

important implications for control strategies and indicates the need for regional perspectives.

Comparison of correlations between different species at various monitoring stations was used to evaluate the emissions inventory. Assuming that the observations at these sites are representative and that all the errors are associated with the emissions then to make the modeled concentrations and slopes consistent with the observed values the emissions would need to be scaled by the following: 0.6 for NO<sub>x</sub>, 2 for CO and 0.7 for BC, PM<sub>2.5</sub> and PM<sub>10</sub>.

The exceeding levels of air pollution in Delhi city for the year 2010, paved an interest to study future projections. 2030 was chosen as the year of study. To accomplish this goal the **Greenhouse Gas and Air Pollution Interactions and Synergies (GAINS)** model was employed and interfaced with WRF-Chem. Under this 2030 scenario there is an increase in emissions for certain species such as SO<sub>2</sub>, NO<sub>x</sub>, BC and PM<sub>2.5</sub> by factors of 1.8, 4.7, 2.1 and 1.01, respectively. There is also a slight increase in NMVOC (~1.04), while CO and PM<sub>10</sub> show a decrease in the emissions in 2030 by 0.8 and 0.6 times, respectively.

Under this scenario, pollution levels generally continue to increase. The net percent changes in concentrations in 2030 relative to 2010 were 140 and 40 for BC and NO<sub>x</sub>, respectively. Large reductions (by 50%) were seen in CO. Similar to the 2010 emissions case, a sector based analysis was conducted with the GAINS inventory so as to understand the major contributing sector to the deteriorating air quality levels of Delhi city. There was a net increase of ~30µg/m<sup>3</sup> BC from all sectors, but interestingly there was a decrease in concentrations from domestic sources. The control measures taken to

reduce the CO emission were reflected in a net decrease of ~900ppb. Although preventive measures were incorporated during the emission scenario projections to reduce the particulate matter, there was still a significant net increase in PM<sub>2.5</sub> and PM<sub>10</sub> concentrations.

The worsening air quality levels have a profound influence on the climate. The simulations conducted for the year 2010 and 2030 suggests that, changes of emission levels from 2010 to 2030 would cause a net increase in mean temperature at the surface by ~ 25%. Another effect of the increasing levels of air pollution was seen on climate change as measured through radiative forcing (IPCC, 2005). The pollution levels in Delhi in 2010 show a large surface dimming. The total anthropogenic radiative forcing for the simulated period of 20 days was as high (40-50Wm<sup>-2</sup>). These high levels have influence not only environment but also the eco-system i.e. effecting the crop production.

The radiative effects for the year 2030 were also studied. The 20day-mean values show an increase in downward shortwave radiative flux at the surface. The total anthropogenic atmospheric forcing is increased to 70W m<sup>-2</sup>. These increasing levels of the radiative forcing have multiple effects such as meteorological, changes in the monsoon period, human health and imbalances in the ecosystem.

## 5.2 Future study

Out of the 26 mega-cities in the world, with population more than 10 million, 13 of them are affected by atmospheric brown clouds and 5 of them are in South Asia. There is very limited information about aerosols in general from this region compared to North America and China. The spatial and temporal variability analysis on Delhi provide

an understanding how much and what time of the day the pollutants effect the air quality levels of the city. This study focusing on Delhi at a finer resolution 1.67km can act as pilot study to further extend to the other mega cities in South Asia and India in particular.

An important extension of this study will be to investigate the source-receptor relationships across the domain at urban, local and regional scales. To facilitate this study similar WRF-Chem sensitivity runs will be carried on the coarse domain (South Asia and Northern India) to understand the long-range transport of pollutants from outside of Delhi and pinpoint sectors that will be critical for air quality management. This sector based analysis will be extended to other regions across the domain and will require validating the model with observations from other regions in the domain. The satellite based products (e.g. AOD) will also be used for model validation. Aerosol Optical Depth (AOD) is the measure of atmospheric extinction through a vertical column of atmosphere. The main composition of AOD includes sulfate, black carbon, and dust. AOD gives the generic representation of the visibility and air quality from aerosols in the city. The AOD data is available globally from NASA satellites and ground based measurements network (e.g. AERONET). The online WRF-Chem also produces the AOD output at 300nm, 400nm, 600nm, and 999nm wavelengths.

Black carbon (soot) has been receiving increased attention due to its important role in global warming. The major sources of BC emissions are biomass burning and bio fuel cooking and these estimates are highly uncertain. This research will build upon the Common Wealth Games forecasting experience and focus on BC and study the sources and remedial measures necessary to reduce the adverse impacts of BC on the aerosol radiative forcing and health.

## APPENDIX

Table A1 Statistical analysis of various air quality species for the period of 20 days at different monitoring stations with NO<sub>x</sub> one third emissions.

BC	CWG	ID	IGI	ISC	JSC	MDS	TG	TSC	UD	YSC
Mean-obs ( $\mu\text{g}/\text{m}^3$ )		6.7			10.6	13.1	12.5		4.4	
Mean- model( $\mu\text{g}/\text{m}^3$ )		17.1			12.0	16.0	17.2		22.4	
Bias( $\mu\text{g}/\text{m}^3$ )		10.3			1.4	2.9	4.7		18.0	
RMSE(hr avg)( $\mu\text{g}/\text{m}^3$ )		15.0			9.4	9.8	12.1		20.4	
R		0.6			0.6	0.7	0.6		0.7	
CO	CWG	ID	IGI	ISC	JSC	MDS	TG	TSC	UD	YSC
Mean-obs(Ppmv)	1.5	1.4	1.8	1.8	1.1	2.1	1.4	1.4	2.8	2.1
Mean- model(ppmv)	1.1	1.3	0.8	1.3	1.0	1.2	1.3	1.3	1.4	1.0
Bias(ppmv)	-0.4	-0.1	-1.0	-0.5	-0.1	-0.9	-0.1	-0.1	-1.4	-1.2
RMSE(hr avg)(ppmv)	0.8	0.8	1.3	1.2	1.0	2.0	1.1	0.9	2.3	1.5
R	0.5	0.5	0.5	0.4	0.4	0.5	0.3	0.5	0.2	0.3
NO <sub>2</sub>	CWG	ID	IGI	ISC	JSC	MDS	TG	TSC	UD	YSC
Mean-obs(Ppbv)	37.3	14.1	37.1	33.3	32.7	32.3	14.7	22.4	41.8	30.8
Mean- model(ppbv)	49.9	50.3	40.5	55.7	40.2	53.8	50.5	50.0	51.4	46.9
Bias(ppbv)	12.5	36.2	3.3	22.4	7.5	21.5	35.8	27.5	9.6	16.1
RMSE(hr avg)(ppbv)	28.6	50.2	39.8	44.9	31.8	44.8	52.9	43.4	41.0	33.1
R	0.7	0.4	0.3	0.3	0.5	0.1	0.1	0.5	0.2	0.4
NO <sub>x</sub>	CWG	ID	IGI	ISC	JSC	MDS	TG	TSC	UD	YSC
Mean-obs(Ppbv)	80.5	28.2	51.9	79.5	72.9	123.9	33.2	67.4	90.9	49.6
Mean- model(ppbv)	65.4	63.8	47.5	77.7	49.0	73.3	67.5	65.6	67.6	63.4
Bias(ppbv)	-15.1	35.6	-4.4	-1.9	-23.9	-50.6	34.3	-1.8	-23.3	13.9
RMSE(hr avg)(ppbv)	61.7	60.9	48.3	77.3	67.2	109.5	63.4	57.4	76.7	61.0
R	0.5	0.4	0.4	0.4	0.5	0.5	0.5	0.5	0.4	0.2
O <sub>3</sub> -daytime	CWG	ID	IGI	ISC	JSC	MDS	TG	TSC	UD	YSC

Table A1 Continued...

Mean-obs(ppbv)	60.9	46.5	56.7	55.8	61.0	48.2	67.2	56.9	46.9	44.8
Mean-model(ppbv)	35.4	38.5	39.4	36.4	38.7	36.9	39.0	39.9	39.2	39.1
Bias(ppbv)	-21.8	-3.8	-9.9	-16.1	-7.0	-9.8	-24.5	-15.8	10.3	1.6
RMSE(hr avg)(ppbv)	38.6	29.4	34.0	37.9	39.2	34.4	46.3	38.4	43.1	27.6
R	0.2	0.2	0.1	0.0	0.1	0.0	0.1	0.0	0.1	0.1
PM <sub>2.5</sub>	CWG	ID	IGI	ISC	JSC	MDS	TG	TSC	UD	YSC
Mean-obs( $\mu\text{g}/\text{m}^3$ )	115.5	114.1	143.5	107.8	123.3	76.8	88.3	91.5	119.6	128.2
Mean-model( $\mu\text{g}/\text{m}^3$ )	187.4	208.9	141.8	211.0	157.0	201.9	210.4	192.6	220.3	201.0
Bias( $\mu\text{g}/\text{m}^3$ )	71.9	94.8	-1.7	103.2	33.7	125.1	122.0	101.1	100.7	72.8
RMSE(hr avg)( $\mu\text{g}/\text{m}^3$ )	138.2	161.0	87.1	171.3	131.0	180.9	189.9	166.8	179.6	165.6
R	0.4	0.4	0.6	0.5	0.3	0.4	0.4	0.4	0.4	0.2
PM <sub>10</sub>	CWG	ID	IGI	ISC	JSC	MDS	TG	TSC	UD	YSC
Mean-obs( $\mu\text{g}/\text{m}^3$ )	258.8	209.9	212.3	249.9	221.7	217.7	200.1	232.7	267.2	305.7
Mean-model( $\mu\text{g}/\text{m}^3$ )	321.1	346.3	243.1	375.4	265.2	362.3	365.6	334.5	358.4	329.5
Bias( $\mu\text{g}/\text{m}^3$ )	62.4	136.4	30.8	125.4	43.5	144.6	165.5	101.7	91.2	23.8
RMSE(hr avg)( $\mu\text{g}/\text{m}^3$ )	208.5	263.5	151.8	286.8	219.0	291.3	333.4	264.8	276.5	247.9
R	0.5	0.5	0.6	0.5	0.4	0.4	0.1	0.4	0.4	0.2

Table A2 Statistical analysis of various air quality species for the period of 20 days at different monitoring stations with full NO<sub>x</sub> emissions.

BC	CWG	ID	IGI	ISC	JSC	MDS	TG	TSC	UD	YSC
Mean-obs ( $\mu\text{g}/\text{m}^3$ )		6.7			10.6	13.1	12.5		4.4	
Mean-model( $\mu\text{g}/\text{m}^3$ )		13.8			14.5	14.3	14.2		16.4	
Bias( $\mu\text{g}/\text{m}^3$ )		7.3			8.9	1.9	1.7		16.3	
RMSE(hr avg)( $\mu\text{g}/\text{m}^3$ )		12.5			16.7	11.4	11.5		22.3	
R		0.5			0.6	0.7	0.6		0.7	
CO	CWG	ID	IGI	ISC	JSC	MDS	TG	TSC	UD	YSC
Mean-obs(PPmv)	1.5	1.4	1.8	1.8	1.1	2.1	1.4	1.4	2.8	2.1
Mean-model(ppmv)	0.9	1.0	0.7	1.1	1.1	1.0	1.0	1.1	1.2	0.9
Bias(ppmv)	-0.5	-0.3	-1.1	-0.7	0.5	-1.1	-0.2	-0.3	-0.7	-0.5
RMSE(hr avg)(PPmv)	1.0	0.8	1.4	1.4	1.4	2.3	1.2	0.9	2.3	1.8
R	0.5	0.5	0.5	0.4	0.4	0.5	0.3	0.5	0.2	0.3
NO <sub>2</sub>	CWG	ID	IGI	ISC	JSC	MDS	TG	TSC	UD	YSC
Mean-obs(PPbv)	37.3	14.1	37.1	33.3	32.7	32.3	14.7	22.4	41.8	30.8
Mean-model(PPbv)	67.0	64.4	53.4	73.3	69.0	71.1	66.9	66.0	69.7	61.0
Bias(PPbv)	29.9	50.6	17.5	42.6	50.8	39.9	52.8	44.4	42.4	38.0
RMSE(hr avg)(PPbv)	46.6	61.2	40.6	59.7	66.5	54.9	65.2	57.1	65.5	55.8
R	0.7	0.4	0.3	0.3	0.5	0.1	0.1	0.5	0.2	0.4
NO <sub>x</sub>	CWG	ID	IGI	ISC	JSC	MDS	TG	TSC	UD	YSC
Mean-obs(PPbv)	80.5	28.2	51.9	79.5	72.9	123.9	33.2	67.4	90.9	49.6
Mean-model(PPbv)	149.9	143.7	96.5	176.4	162.6	168.3	156.5	153.1	163.9	132.4
Bias(PPbv)	70.1	116.3	46.4	103.3	122.0	47.0	124.7	88.2	104.5	90.7
RMSE(hr avg)(PPbv)	148.8	167.5	96.8	192.5	201.9	164.6	184.9	162.7	211.8	171.7
R	0.5	0.4	0.4	0.4	0.5	0.5	0.5	0.5	0.4	0.2
O <sub>3</sub> -daytime	CWG	ID	IGI	ISC	JSC	MDS	TG	TSC	UD	YSC
Mean-obs(ppbv)	60.9	46.5	56.7	55.8	61.0	48.2	67.2	56.9	46.9	44.8
Mean-model(ppbv)	58.5	60.5	58.6	56.1	62.6	59.0	62.1	63.3	62.0	61.6
Bias(ppbv)	1.3	18.1	9.3	3.6	16.9	12.3	-1.4	7.6	33.1	24.1

Table A2 Continued...

RMSE(hr	38.1	34.6	33.9	37.4	44.9	36.7	39.4	35.3	62.7	43.5
---------	------	------	------	------	------	------	------	------	------	------

avg)(ppbv)										
R	0.5	0.6	0.2	0.5	0.4	0.4	0.4	0.5	0.1	0.4
PM <sub>2.5</sub>	CWG	ID	IGI	ISC	JSC	MDS	TG	TSC	UD	YSC
Mean-model( $\mu\text{g}/\text{m}^3$ )	179.4	180.3	132.0	195.6	187.8	188.9	185.3	178.9	207.4	179.6
Bias( $\mu\text{g}/\text{m}^3$ )	63.8	70.9	-7.9	92.8	118.7	112.5	97.1	90.3	128.4	69.8
RMSE(hr avg)( $\mu\text{g}/\text{m}^3$ )	137.1	142.3	86.3	169.8	203.2	169.9	162.9	156.2	228.3	172.2
R	0.4	.4	0.6	0.5	0.3	0.4	0.4	0.4	0.4	0.2
PM <sub>10</sub>	CWG	ID	IGI	ISC	JSC	MDS	TG	TSC	UD	YSC
Mean-obs( $\mu\text{g}/\text{m}^3$ )	258.8	209.9	212.3	249.9	221.7	217.7	200.1	232.7	267.2	305.7
Mean-model( $\mu\text{g}/\text{m}^3$ )	294.3	288.9	209.2	326.0	308.8	318.1	304.0	294.5	319.9	279.1
Bias( $\mu\text{g}/\text{m}^3$ )	35.5	86.3	6.2	87.5	184.5	101.3	104.3	68.6	143.4	17.3
RMSE(hr avg)( $\mu\text{g}/\text{m}^3$ )	207.8	224.3	148.8	271.0	345.4	256.0	265.5	245.7	359.3	271.4
R	0.5	0.5	0.6	0.5	0.4	0.4	0.1	0.4	0.4	0.2

Table A3 Statistical analysis of various meteorological parameters for the period of 20 days at different monitoring stations.

Temp	IITMD	YSC	ISC	MDS	JNS	TSC	CWG	UD	IGI	TG	NCM
Mean-Obs(°C)	28.5	29.4	29.0	28.9	30.5	28.5	28.9	28.8	28.9	28.3	29.0
Mean-Model(°C)	28.9	28.1	29.0	28.9	29.0	29.2	28.2	28.8	28.6	29.2	27.7
Bias Error(°C)	7.2	6.2	7.7	7.4	8.3	9.4	7.7	7.4	7.0	9.5	6.5
RMSE(hr avg)(°C)	12.8	12.5	13.5	13.1	14.8	15.0	13.6	13.3	13.0	15.1	12.8
R	0.9	0.9	0.9	0.9	0.9	0.8	0.9	0.9	0.9	0.8	0.9
Wind speed	IITMD	YSC	ISC	MDS	JNS	TSC	CWG	UD	IGI	TG	NCM
Mean-Obs(m sec <sup>-1</sup> )	3.1	0.2	0.4	0.6	0.6	0.7	0.8	0.2	0.3	0.5	7.1
Mean-Model(m sec <sup>-1</sup> )	2.3	2.1	2.1	2.1	2.1	2.1	2.2	2.1	2.6	2.2	2.2
Bias Error(m sec <sup>-1</sup> )	0.0	2.0	1.9	1.7	1.8	1.6	1.7	1.9	2.3	1.9	-3.0
RMSE(hr avg)(m sec <sup>-1</sup> )	3.0	2.3	2.2	2.0	2.0	2.0	2.2	2.2	2.7	2.2	8.6
R	0.6	0.6	0.4	0.6	0.5	0.6	0.4	0.4	0.4	0.4	0.4
RH	IITMD	YSC	ISC	MDS	JNS	TSC	CWG	UD	IGI	TG	NCM
Mean-Obs(%)	50.8	53.0	52.8	56.4	47.2	55.2	53.6	57.8	51.6	57.5	53.0
Mean-Model(%)	43.9	49.5	44.3	44.8	44.2	43.1	48.5	45.2	45.1	43.1	51.5
Bias Error(%)	6.4	9.9	5.4	2.8	13.0	4.8	10.7	2.1	6.6	3.2	12.6
RMSE(hr avg)(%)	30.6	34.3	32.3	33.9	35.4	34.4	36.4	33.6	30.9	35.8	35.2
R	0.8	0.7	0.7	0.8	0.7	0.6	0.7	0.7	0.8	0.6	0.8

## REFERENCES

Agarwal Rachna, Girija Jayaram, Sneha Anand and P.Marimuthu , “Assessing Respiratory Morbidity through pollution status and meteorological conditions for Delhi”, *Environmental Monitoring and Assessment*, 114,2006,489-504.

Aneja P.Viney , A.Agarwal, Paul A. Roelle, Sharon B. Phillips , Quansong Tong, Neilson Watkins, Richard Yablonsky , “ Measurements and analysis of criteria air pollutants in New delhi, India”, *Environmental International*, 27,2001,35-42.

Arteta .J, Cautenet.S, Taghavi.M, Audiffren.N, “Impact of two chemistry mechanisms fully coupled with mesoscale model on the atmospheric pollutants distribution”, *Atmospheric Environment*, 40, 7983-8001, 2006.

Badami .G. Madhav, “Transport and Urban Air pollution in India”, *Environmental Management Vol 36, No.2, 2005, 195-204.*

Badarinath K.V.S, Shailesh Kumar Kharol, Anu Rani Sharma and V. Krishna Prasad, “Analysis of aerosol and carbon monoxide characteristics over Arabian Sea during crop residue burning period in the Indo-Gangetic Plains using multi-satellite remote sensing datasets”, *Journal of Atmospheric and Solar-Terrestrial Physics*,71, 1267-1276, August 2009.

Buka Irena,S.Koranteng.AR Osornio-Vargas, “The effects of air pollution of the health of children”, *Paediatr Child Health*, Vol 11,8,2006,513-516.

Carmichael R.Gregory, Bhupesh Adhikary, Sarika Kulkarni, Alessio D’Allura, Youhua Tang, David Street, Qiang Zhang, Tami C.Bond, Veerabhadran Ramanathan, Aditsuda jamroensan, Pallavi Marrapu, “Asia Aerosol: Current and Year 2030 Distributions and Implications to Human Health and Regional Climate Change”, *Environmental Science and Technology*, Vol.43., No15,2009, 5811-5817.

Davies, D.K., Ilavajhala, S., Wong, M.M., and Justice, C.O. (2009). “Fire Information for Resource Management System: Archiving and Distributing MODIS Active Fire Data”. *IEEE Transactions on Geoscience and Remote Sensing* 47 (1):72-79.

Chapman, E. G., Gustafson Jr., W. I., Easter, R. C., Barnard, J. C., Ghan, S. J., Pekour, M. S., and Fast, J. D.: “Coupling aerosol-cloud-radiative processes in the WRF-Chem model: Investigating the radiative impact of elevated point sources”, *Atmos. Chem. Phys.*, 9, 2009,945-964.

Chung C.E, V.Ramanathan, G.Carmicheal, S.Kulkarni, Y.Tang, B.Adhikary, L.R.Leung and Y.Qian, “Anthropogenic aerosol radiative forcing in Asia derived from regional models with atmospheric and aerosol data assimilation”, *Atmospheric chemistry and Physics Discussions*, 10, 2010, 821-862.

Darby S.Lisa, MckeenA.Stuart, SenffJ.Christoph, White B.Allen, BantaM.Robert, Post J.Madison, Brewer Alan.W, Marchbanks Richard,Alvarez J. Raul II, Peckham E.Steven ,Mao huiting and Talbot Robert, “ Ozone differences between near –coastal and offshore sites in New England :Role of Meteorology”,*J. Geophys. Res.*, 112,D16S91,doi:10.1029/2007JD008446,2007.

Drimal M,Lewis C,FABianova, “Health Risk Assessment to Environmental Exposure to Malodorous sulfur Coumpounds in Central Slovakia”, *Carpathian Journal of Earth and Environmental Sciences*, Vol5,Issue1,2010, 119-126.

Emmons L.K, S.Walters, P.G.Hess, J.-F.Lamarque, G.G,Pfister, D.Fillmore, C.Granier, A.Guenther, D.Kinnison, T.Laepfle, J.Orlondo, X.Tie, G.Tyndall, C.Wiedienmyer, S.L.Baughcum, and S.Kloster, “Description and evaluation of the Model for Ozone and Related chemical Tracers,version 4 (MOZART-4)”,*Geosci.MOdelDev.Discuss.*,2,2009,1157-1213.

Erisman, J.W., van Pul, A., Wyers, P., 1994: Parameterization of surface resistance for the quantification of atmospheric deposition of acidifying pollutants and ozone. *Atmos. Environ.*, 28, 2595–2607.

Fast, J. D., W. I. Gustafson Jr., R. C. Easter, R. A. Zaveri, J. C. Barnard, E. G. Chapman, G. A. Grell, and S. E. Peckham(2006), “Evolution of ozone, particulates, and aerosol direct radiative forcing in the vicinity of Houston using a fully coupled meteorology-chemistry-aerosol model”, *J. Geophys. Res.*, 111, D21305, doi:10.1029/2005JD006721.

GAINS –ASIA Pallav Purohit, Markus Amann, Ritu Mathur, Ila Gupta, Sakshi Marwah, Vishal Verma, Imrich Bertok, Jens Borken, Adam Chambers, Janusz Cofala, Chris Heyes, Lena Hoglund, Zbigniew Klimont, Peter Rafaj, Robert Sandler, Wolfgang Schöpp, Geza Toth, Fabian Wagner, Wilfried Winiwarter, “Scenarios for cost-effective control of air pollution and greenhouse gases in India”, November 2010.

Geng Fuhai, Zhao Chunsheng, Tang Xu, Lu Guoliang, Tie Xuexi, “ Analysis of ozone and VOCs measured in Shanghai: A case study”, *Atmospheric Environemnt*,41,(2007) 989-1001.

Ghude D.Sachin, S.L.Jain, B.C.Arya,G.Beig,Y.N.Ahammaed,Arun Kumar,B.Tyagi, “ Ozone in ambient air at a tropical megacity Delhi: Characteristics trends and cumulative ozone exposure indices”, *Journal of Atmospheric Chemistry* ,60, 2008,237-252.

Goyal P, T.V.B.P.S Rama Krishna and Sankalp Anand , “ Assimilative capacity and Dispersion of Pollutants in Delhi”, *India National Science Academy* ,69,A,No.6,November 2003,775-784.

Grell A.Georg, Knoche Richard, Peckham E. Steven , McKeen A. Stuart (2004), “ Online versus offline air quality modeling on cloud –resolving scales”, *Geophys. Res. Lett.*, 31, L16117, doi:10.1029/2004GL020175.

Grell A. Georg , Peckham E. Steven , Schmitz Rainer ,McKeen A.Stuart, Frost Gregory Skamarock C. William ,Eder Brain, “Fully coupled online chemistry within the WRF model”, *Atmospheric Environment*, 39, 2005,6957-6975.

Guttikunda K.Sarath, Gregory R. Carmichael,Giuseppe Calori,Christina Eck,Jung-Hun Woo, “The contribution of megacities to regional sulfur pollution in Asia”, *Atmospheric Environment*, 37, 2003, 11-22.

Gustafson I.William Jr., Chapman G. Elaine, Ghan J.Steven, Easter C. Richard , “Impact on modeled cloud characteristics due to simplified treatment of uniform cloud condensation nuclei during NEAQS 2004,” *Geophys,Res,Lett.*,34,L19809,doi:10.1029/2007GL030021.

Hordijk, L. and M. Amann (2007). How Science and Policy Combined to Combat Air Pollution Problems. *Environmental Policy and Law* 37(4): 336-340.

IPCC, 2007: *Climate Change 2007:The Physical Science Basis. Contribution of Working Group I to the Fourth Assessment Report of the Intergovernmental Panel on Climate Change* [Solomon et al., (eds.)]. Cambridge University Press, Cambridge, United Kingdom, and New York, NY, USA, 996pp.

Kandlikar .Milind, “Air pollution at a hotspot location in Delhi: Detecting trends, seasonal cycles and oscillations”, *Atmospheric Environment*, 41, 2007, 5934-5947.

Kim Dongchul and Stockwell R.William, “An online coupled meteorological and air quality modeling study of the effect of complex terrain on the regional transport and transformation of air pollutants over the Western United States”, *Atmospheric Environemnt*, 41 ,2319-2334,2007.

Lau .-M, Kim-M.K, “Observational relationships between aerosol and Asian monsoon rainfall, and circulation”, *Geophysical Research Letters*, Vol.,33, L21810, doi:10.1029/2006GL027546, 2006. Madronich, S., 1987: Photodissociation in the atmosphere, 1, actinic flux and the effects of ground reflections and clouds. *J. of Geophys. Res.*, 92, 9740–9752.

Mohan Manju, Anurag Kandya, “An Analysis of the Annual and Seasonal Trends of Air Quality Index of Delhi”, *Environmental Monitoring and Assessment*, 131: 2007,267-277.

Mohan Manju, Lalit Dagar and B.R.Gurjar, "Preparation and Validation of Gridded Emission Inventory of Criteria Air Pollutants and Identification of Emission Hotspots for Megacity Delhi", *Environmental Monitoring and Assessment*, 130, 323-339, 2006.

Naseema Beegum.S, K. Krishna Moorthy, S. Suresh Babu, S.K. Satheesh, V. Vinoj, K.V.S. Badarinath, P.D. Safai, P.C.S. Devara, Sacchidanand Singh, Vinod, U.C. Dumka

and P. Pant, "Spatial distribution of aerosol black carbon over India during pre-monsoon season", *Atmospheric Environment*, 43,2009,1071-1078.

Novaes, Priscila, Saldiva, Paulo Hilario do Nascimento, Matsuda, Monique, Macchione, Mariangela, Rangel, Maristela Peres, Kara-Jose, Newton, Berra, Alejandro, "The effect of chronic exposure to traffic derived air pollution on the ocular surface", *Environmental Research*, Vol110, Issue 4, 2010,372-374.

Planning Commission. (2006). *Integrated Energy Policy: Report of the Expert Committee*. Government of India, New Delhi.

Planning Commission (2006a) *Towards Faster and More Inclusive Growth: An Approach to the 11th Five Year Plan (2007-2012)*. Government of India, New Delhi, India.

Planning Commission (2006b). *Integrated Energy Policy: Report of the Expert Committee*. Government of India, New Delhi.

Ravindra Khaiwal, Suman Mor, Ameena, J.S. Kamyotra and C.P. Kaushik, "Variation in Spatial Pattern of Criteria Air pollutants before and during Initial rain of monsoon", *Environmental Monitoring and Assessment*, 87: 2003,145-153.

Sahu, S. K., G. Beig, and C. Sharma (2008), "Decadal growth of black carbon emissions in India", *Geophys. Res. Lett.*, 35, L02807, doi:10.1029/2007GL032333.

Shekar Reddy M, Venkataraman Chandra, "Inventory of aerosol and sulfur dioxide emissions from India: I-Fossil fuel combustion", *Atmospheric Environment*, 36, 2002, 677-697.

Shekar Reddy M, Venkataraman Chandra, "Inventory of aerosol and sulfur dioxide emissions from India: II-biomass combustion", *Atmospheric Environment*, 36, 2002, 699-712.

TERI (2006). *National Energy Map for India. Technology Vision 2030: Summary for Policy Makers*. Office of the Principal Scientific Adviser to the Government of India, New Delhi, India.

Tie Xuexi, Madronich Sasha, Li GuoHui, Ying Zhuming, Zhang Renyi, Garcia R. Agustin, Taylor Julia Lee, Liu Yubao, "Characterization of chemical oxidants in Mexico City: A regional chemical dynamical model (WRF-CHEM) study", *Atmospheric Environment*, 41,2007,1989-2008.

Sjaak Slanina (Lead Author); Wayne Davis (Topic Editor);. 2010. "Aerosols." In: *Encyclopedia of Earth*. Eds. Cutler J. Cleveland (Washington, D.C.: Environmental Information Coalition, National Council for Science and the Environment). [First published in the *Encyclopedia of Earth* October 18, 2006; Last revised January 2, 2010; Retrieved May 5, 2010.

Suresh Babu. S , S. K. Satheesh, K. Krishna Moorthy, C. B. S. Dutt, Vijayakumar S. Nair, Denny P. Alappattu and P. K. Kunhikrishnan, "Aircraft measurements of aerosol black carbon from a coastal location in the north-east part of peninsular India during ICARB", *Journal of Earth System Science*, 117, S1, July 2008, pp263-271.

Tulet, P., V. Crassier, F. Cousin, K. Suhre, and R. Rosset , "ORILAM, a three- moment lognormal aerosol scheme for mesoscale atmospheric model: Online coupling into the Meso-NH-C model and validation on the Escompte campaign," *J. Geophys. Res.*, 110, D18201, doi:10.1029/2004JD005716,2005.

Yiwen Xu and Gregory R. Carmichael, "Modelling the dry Deposition Velocity of Sulfur Dioxide and Sulfate in Asia", *Journal of Applied Meteorology*, 37, 1998, 1084-1099.  
 Warneke C, Mckeen S.A, J.A.de Gouw, Goldan P.D, Kuster W.C, Holloway J.S, Williams E.J, Lerner B.M, Parrish D.D, Trainer M, Fehsenfeld F.C, Kato S, Atlas E.L, Baker A, Blake D.R, "Determination of urban volatile organic compound emission ratios and comparison with an emission database", *J.Geophys,Res*,112,D10S47,doi10.1029/2006JD007930.

Wesley, M.L., 1989: Parameterization of surface resistance to gaseous dry deposition in regional numerical models. *Atmos. Environ.*, 16, 1293–1304.

Zhang Q, D.G.Streets, G.R.Carmichael, K.He,H.Huo, A.Kannari, Z.Klimont, I.park, S.Reddy, J.S.Fu, D.Chen, L.Duan,Y.Lei, L.Wang,and Z.Yao, "Asian emissions in 2006 for the NASA INTEX –B mission", *Atmospheric chemistry and Physics Discussions*,9,2009,4081-4139.

Zhang Y, "Online coupled meteorology and chemistry models: history, current status, and outlook", *Atmospheric chemistry and Physics Discussions*, 2, 2008, 1833-1912.